The Abdus Salam International Centre for Theoretical Physics

United Nations Educational, Scientific and Cultural Organization

IAEA International Atomic Energy Agency

2168-4

Joint ICTP-IAEA Workshop on Dense Magnetized Plasma and Plasma Diagnostics

15 - 26 November 2010

Summary of results from POSEJDON Plasma-Focus

H. Schmidt
Herrenberg
Germany

Diagnostics and Scaling of Fusion-Produced Neutrons in PF Experiments

Hellmut Schmidt

International Centre for
Dense Magnetized Plasmas, Warsaw
and
University of Stuttgart, Germany

Outline

- Introduction
- Neutron Detection
  - Activation
  - Scintillation
  - TLDs and Bubble detectors
- Neutron Diagnostics
  - Fusion Reaction Models
  - Gyrating Particle Model
- Scaling of Neutron Yield
  - Beam Target and Thermal Production of Neutrons

Introduction

Radial Compression (Pinch) Phase of the Plasma Focus

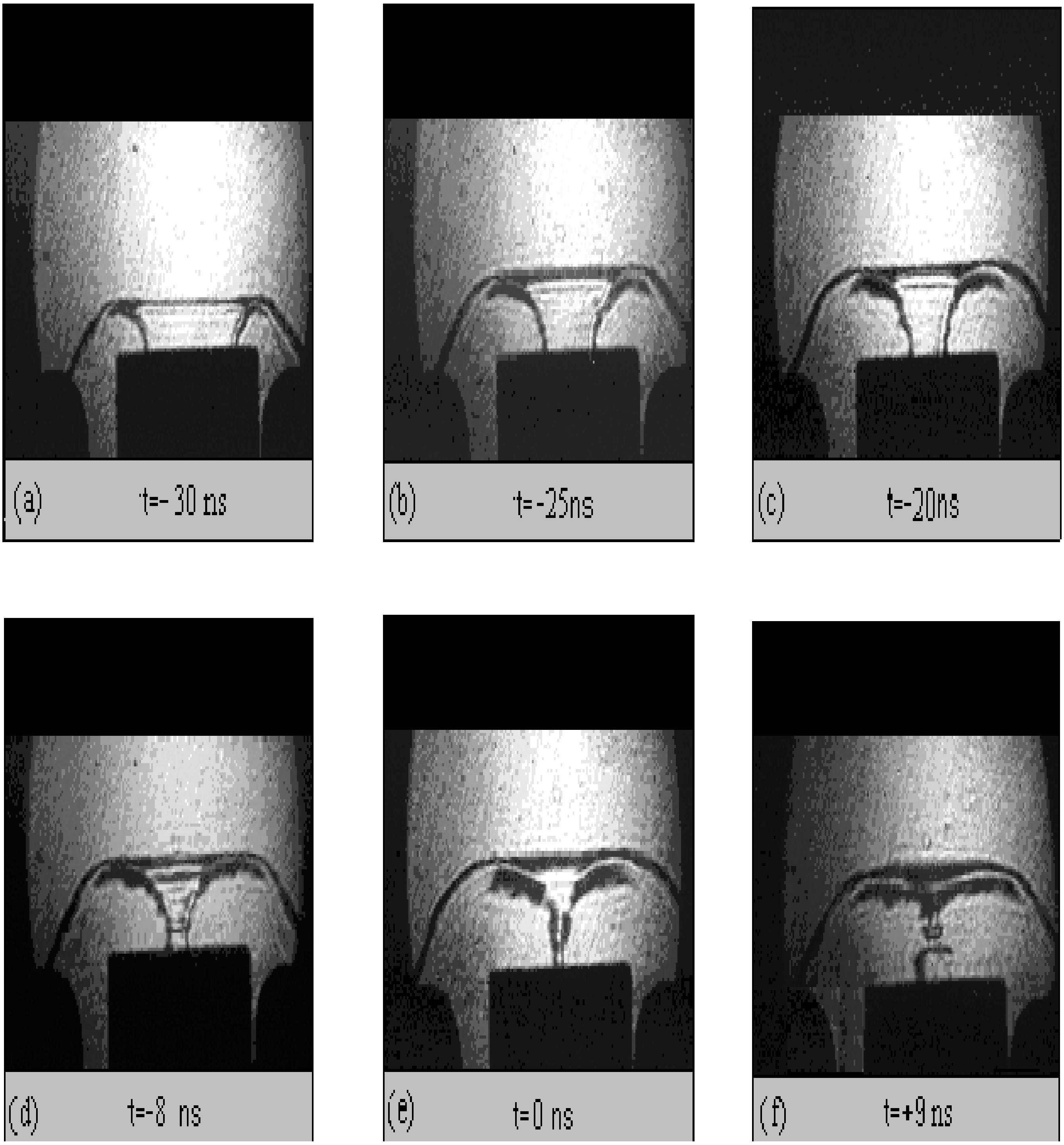

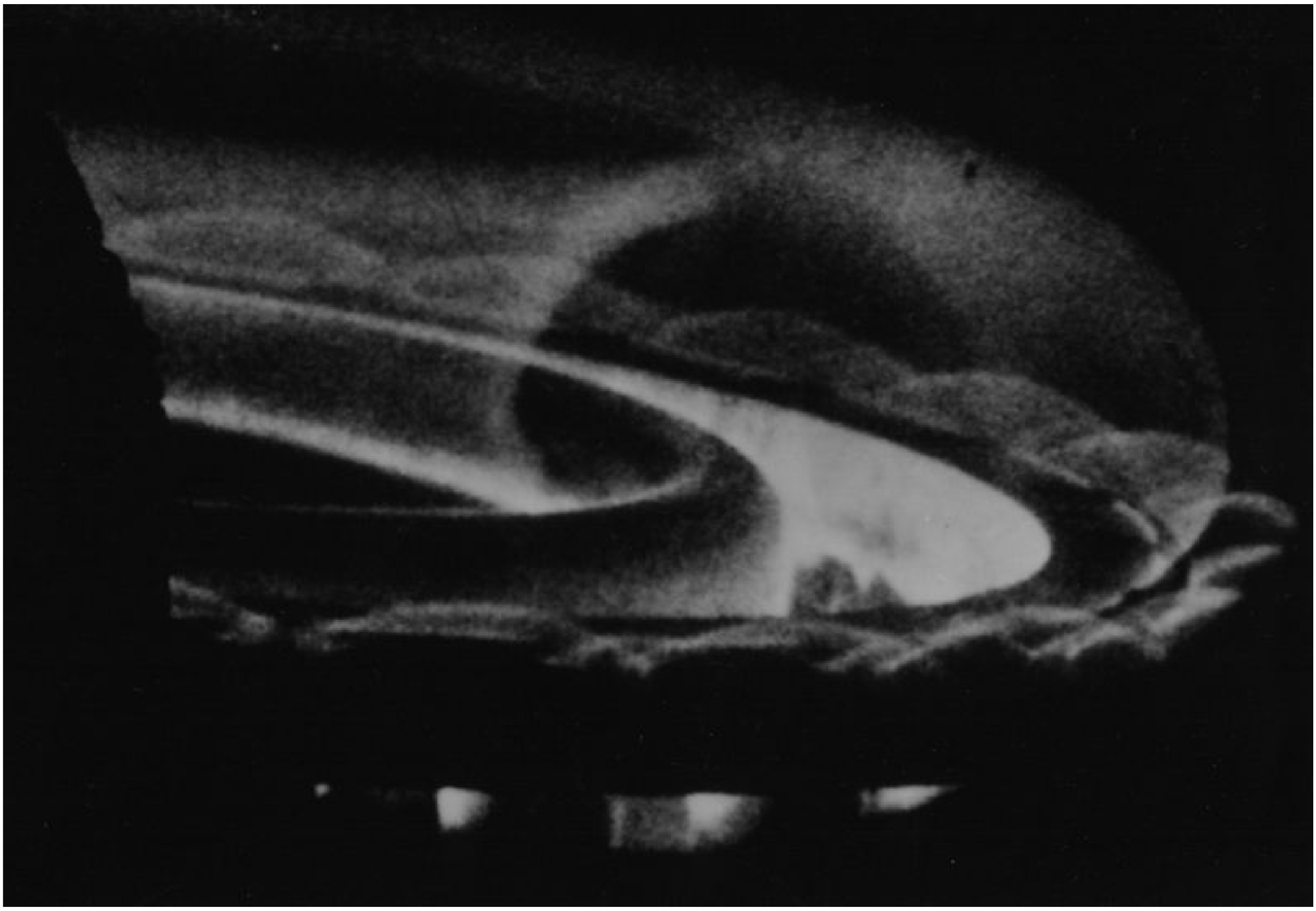

Density sheath of POSEIDON PF
Before maximal compression

Current and Density Sheaths In a Mather type Plasma Focus

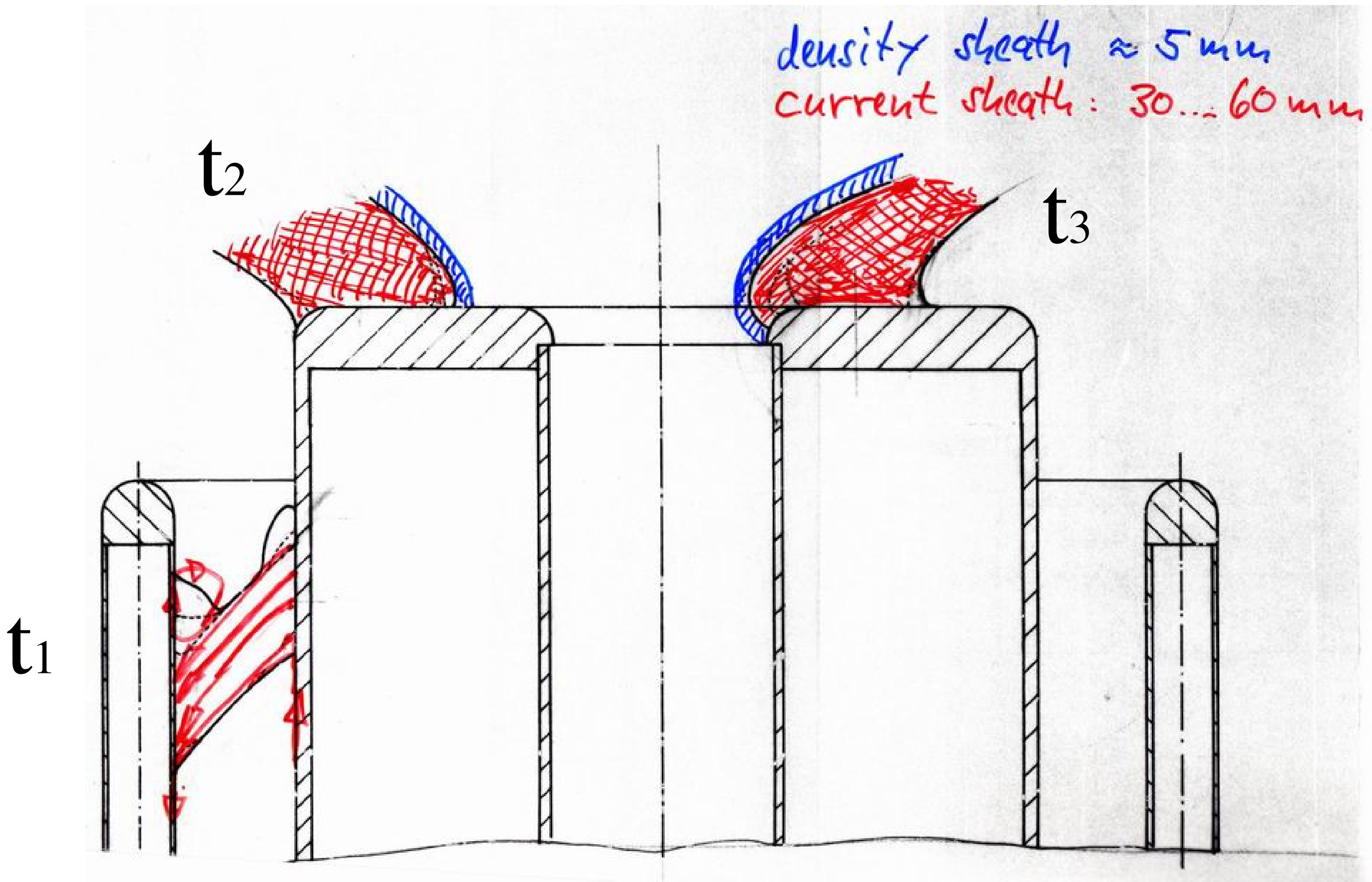

cathode anode

Radial Streak Picture, shot 5055 of PF1000

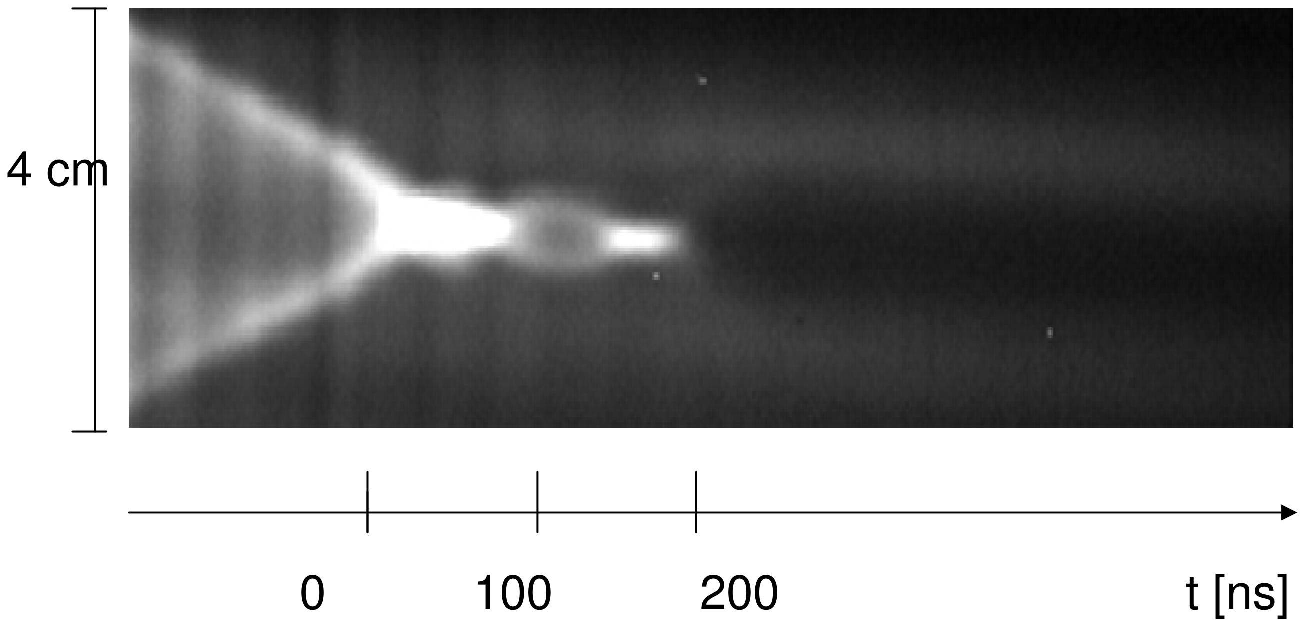

Radial Streak Picture of PF1000 (shot 5055)

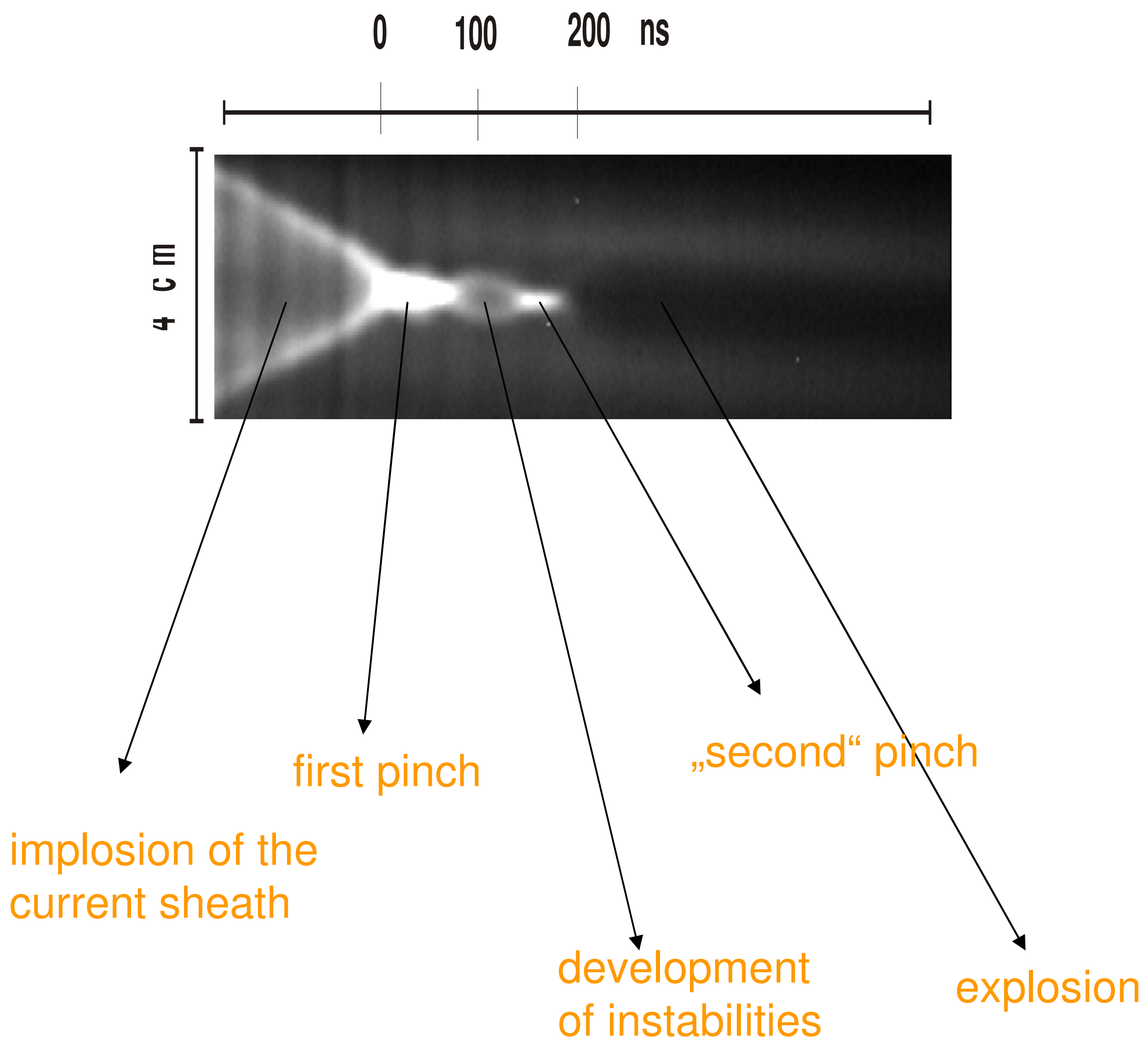

Typical Behaviour

Radial Streak Pictures of POSEIDON (280 kJ)

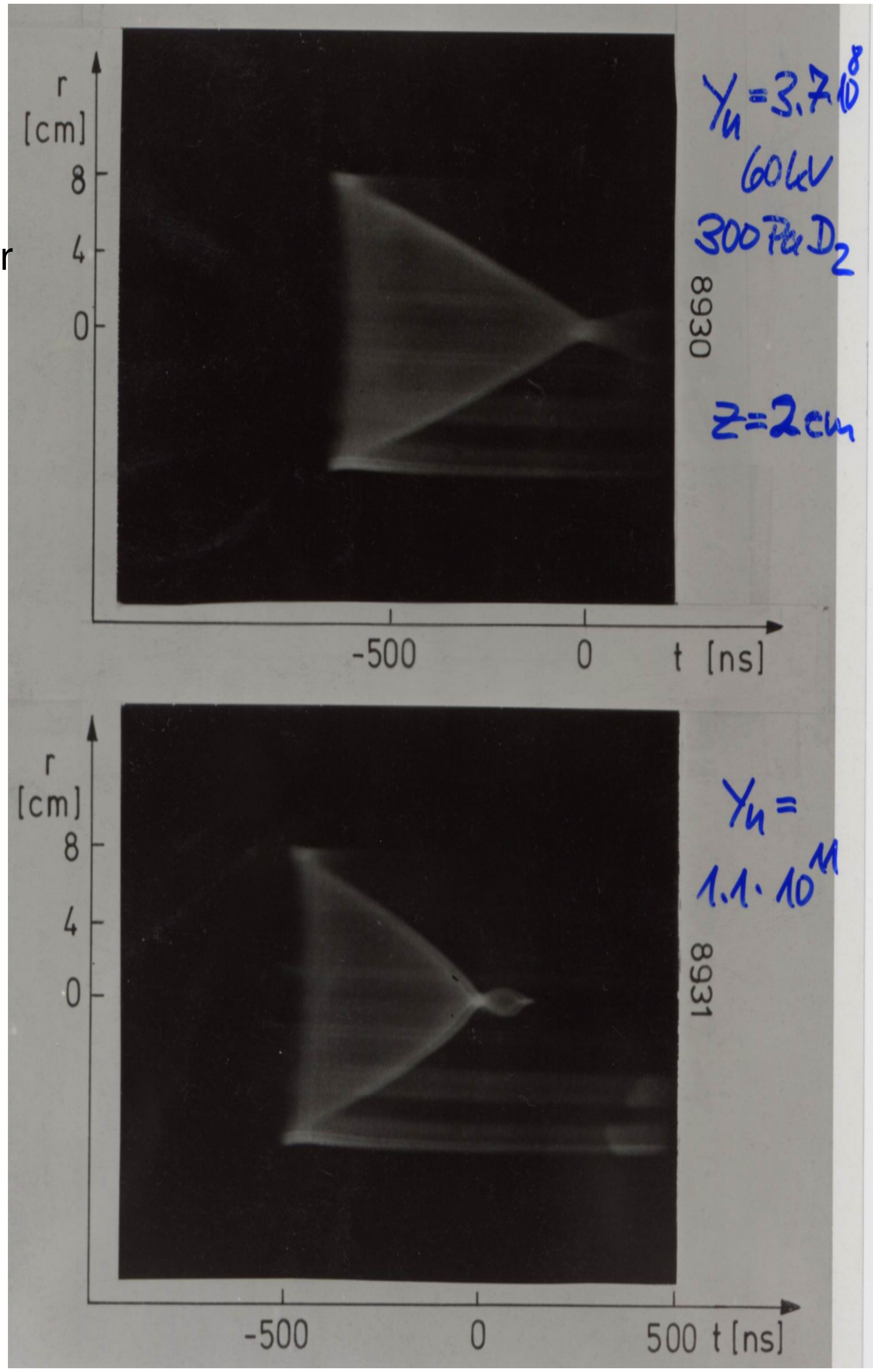

Bad Behaviour

Typical Behaviour

Trieste
November 2010

Plasma Focus Phases

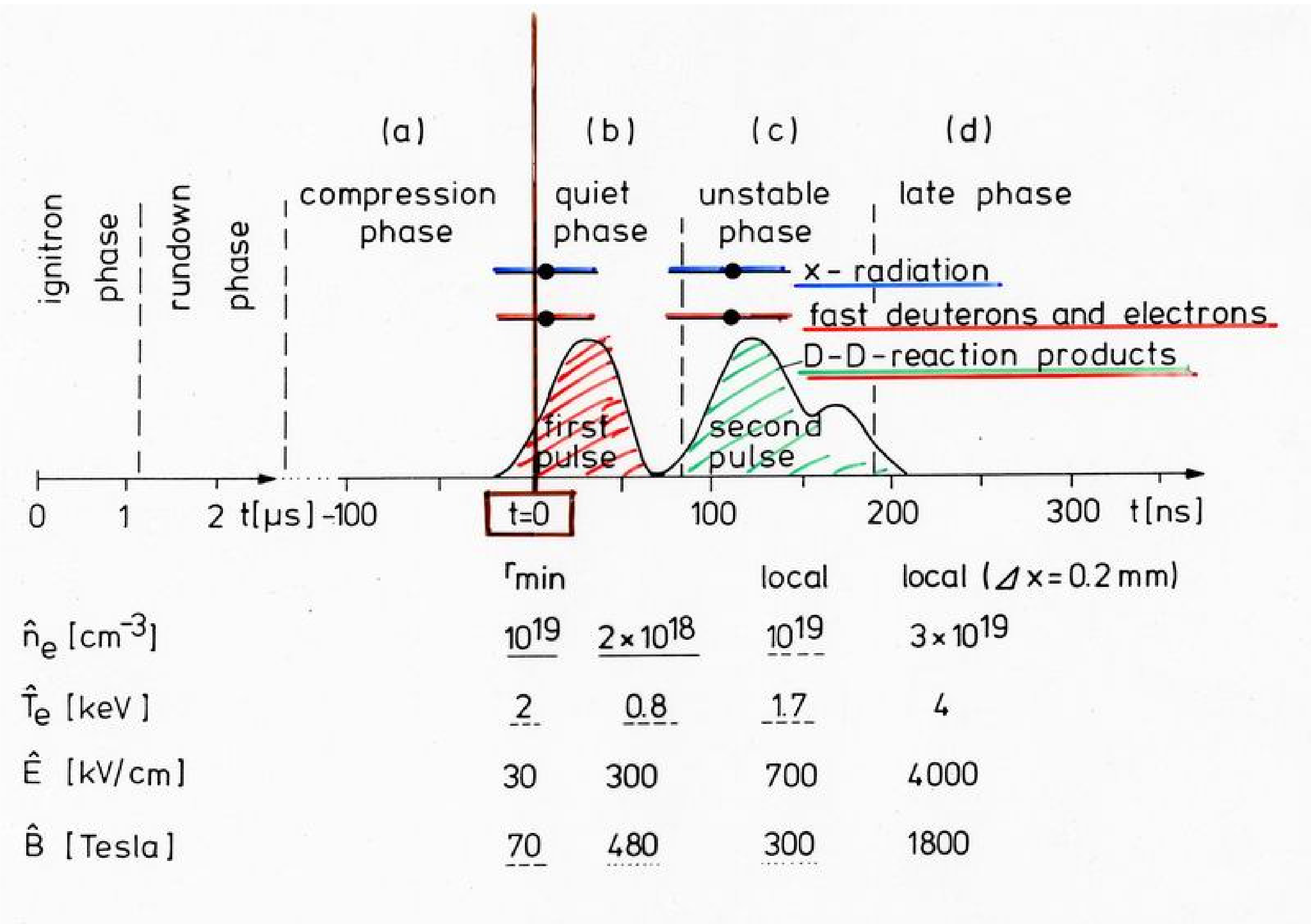

Fig. 3: Plasma focus phases with emission periods of D-D-reaction products (neutrons, protons), X-radiation, electrons and deuterons. Data for electron density and temperature, electric and magnetic fields, as obtained experimentally (underlined) or theoretically, are also given for the two fusion phases.

5 Schlieren pictures

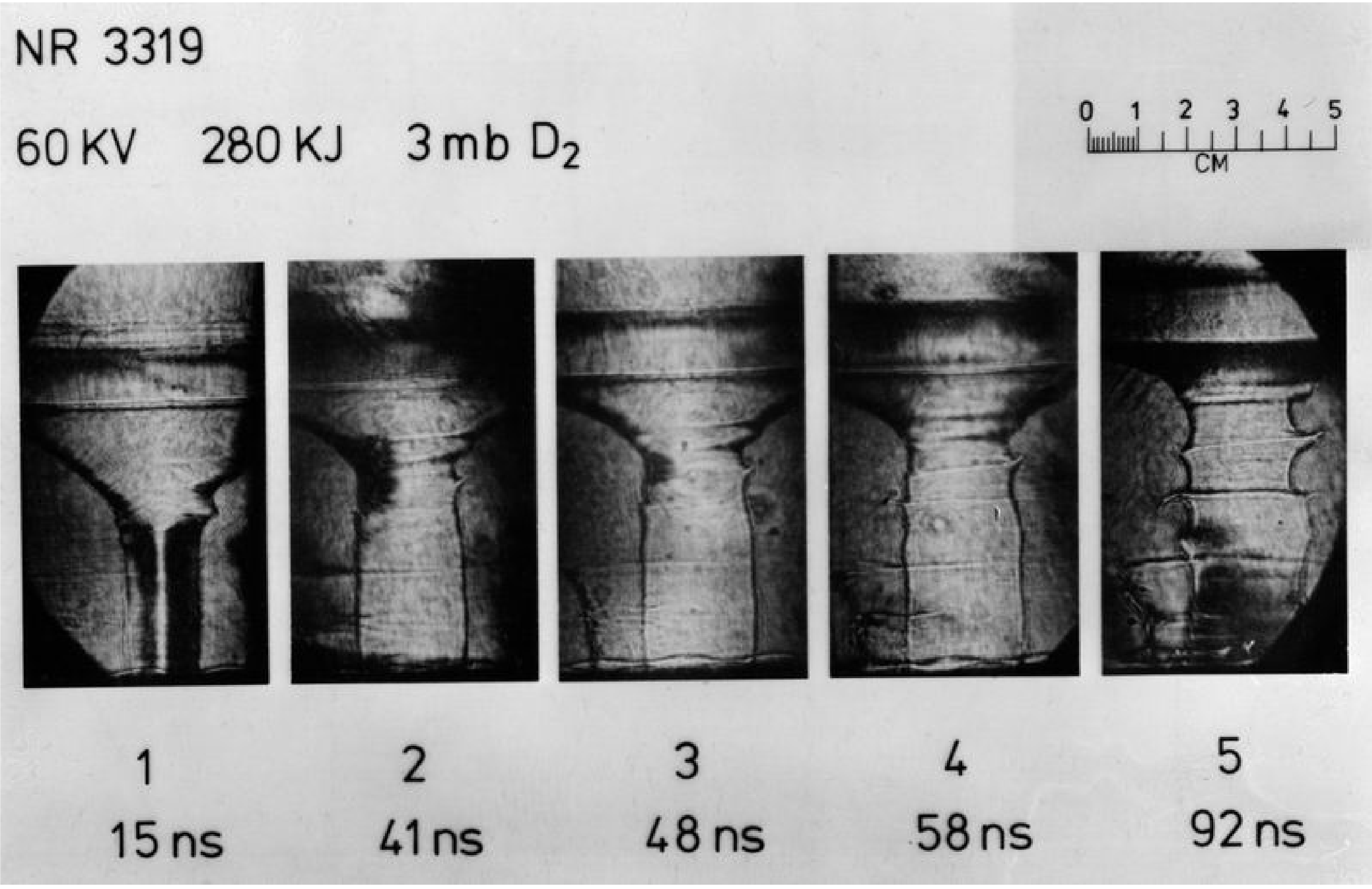

First neutron pulse

5 Schlieren pictures

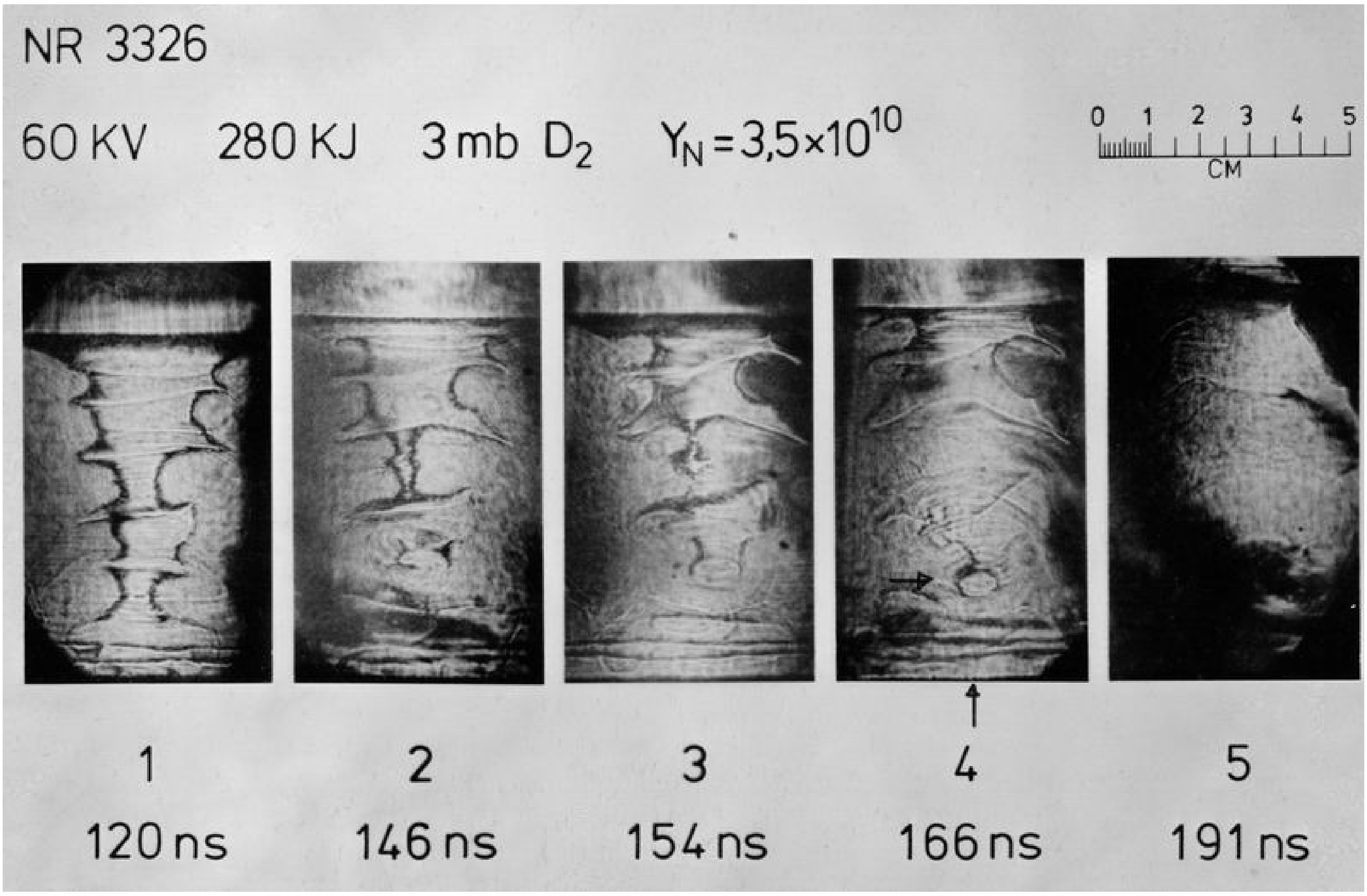

Second neutron pulse

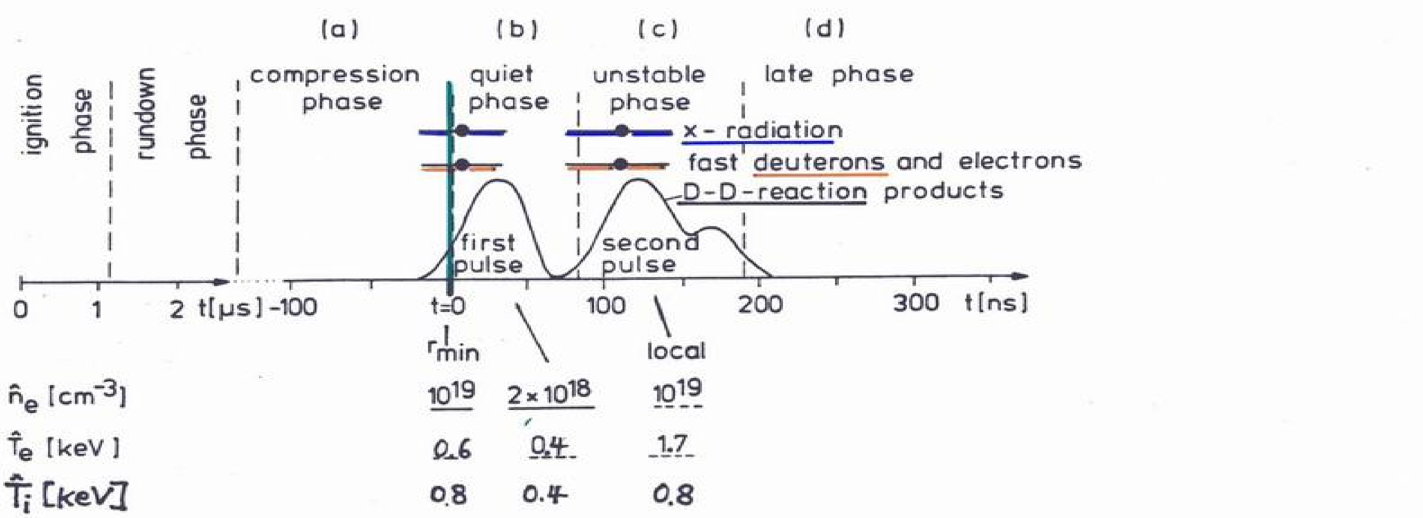

Examples of emissions

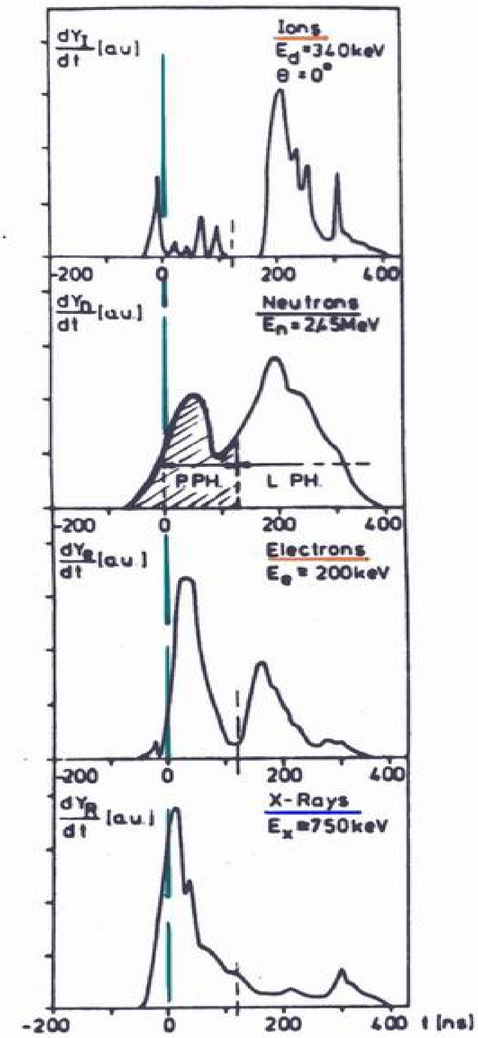

deuterons (340 keV) ↑ +z

neutrons

electrons (200 keV) ↓ −z

hard X-rays (750 keV)

Neutron Detection

Neutron Activation

TABLE I. Comparison of various elements employed for pulsed neutron detection.

Element	Half-life $\tau_{1/2}$ (s)	Reaction	Neutron energy	Operation mode	Particle detected
Arsenic	0.017	$^{75}As(n,n')\,^{75m}As$	Fast	Repetitive	γ
Beryllium	0.807	$^{9}Be(n,\alpha)\,^{6}He$	Fast	Repetitive	β
Boron tri fluoride	⋯	$^{9}B(n,\alpha)\,^{7}Li$	Thermal	Repetitive	α
Helium-3	⋯	$^{6}He(n,p)\,^{3}H$	Thermal	Repetitive	p
Indium	14.1	$^{115}In(n,\gamma)\,^{116}In$	Thermal	Single	β
Rhodium	42.3	$^{103}Rh(n,\gamma)\,^{104}Rh$	Thermal	Single	β
Silver	24.6	$^{109}Ag(n,\gamma)\,^{110}Ag$	Thermal	Single	β
	142	$^{107}Ag(n,\gamma)\,^{118}Ag$			

Be-detector

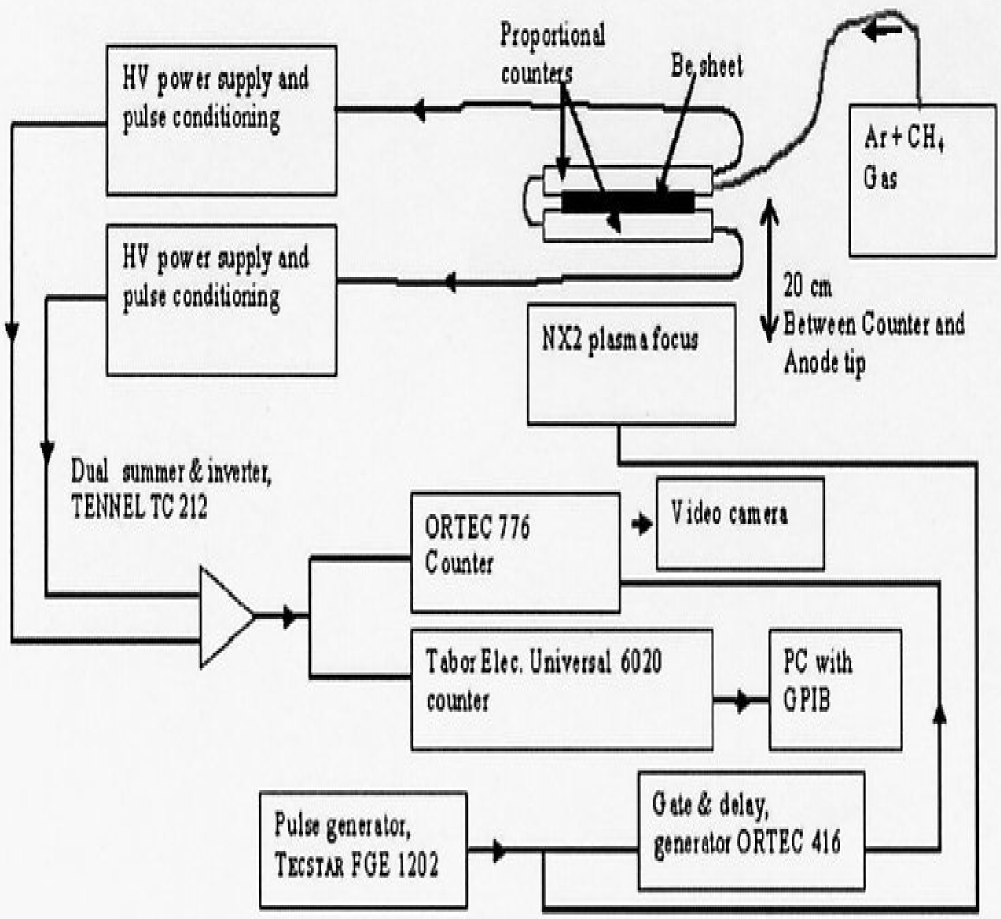

FIG. 1. Schematic diagram of the beryllium counter, DPF, triggering, and data acquisition system.

Silver activation counter

Example of a specific design

When used with fast neutrons, the counter is normally placed within a polyethylene moderator

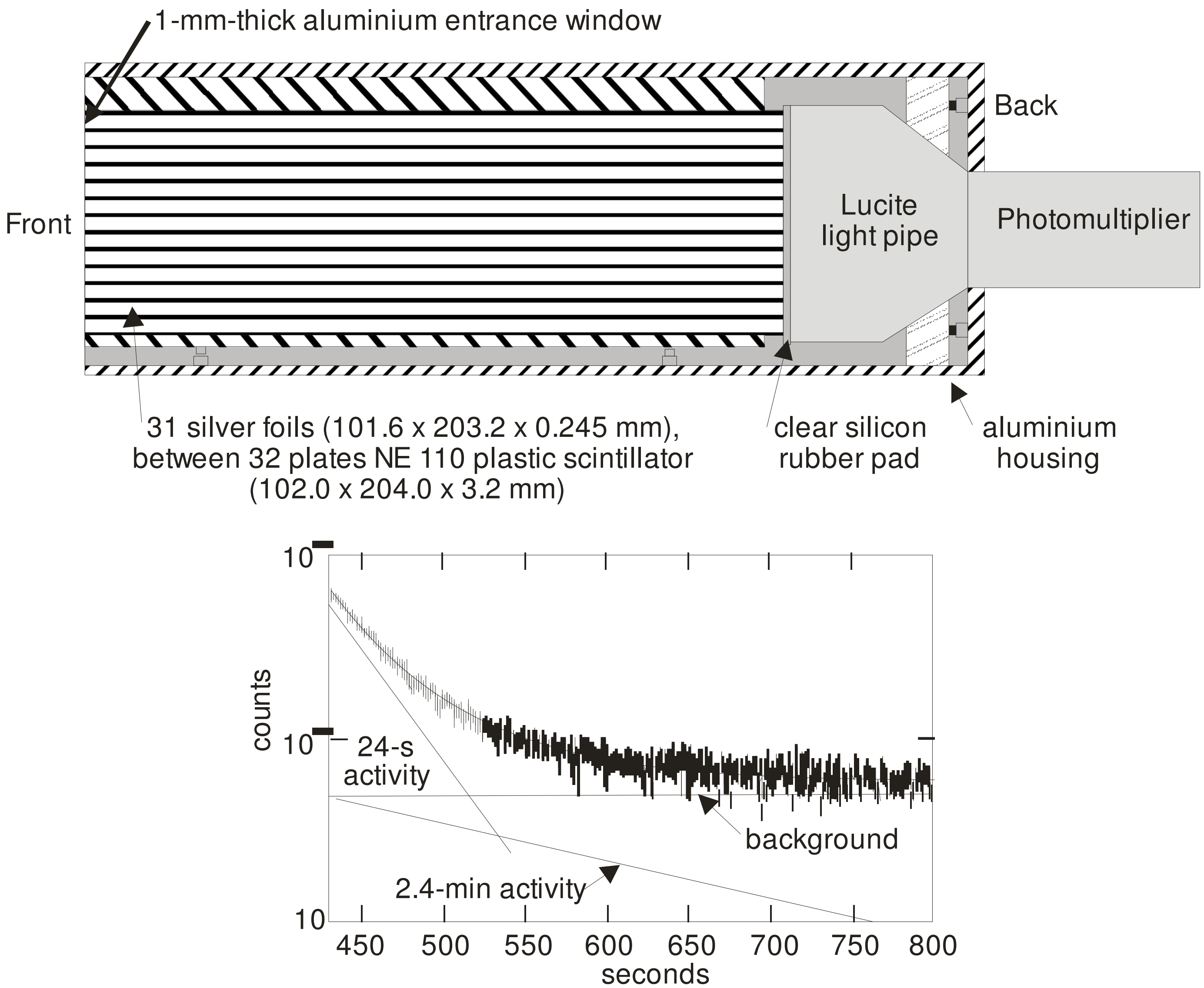

Activity after insertion in a constant neutron flux

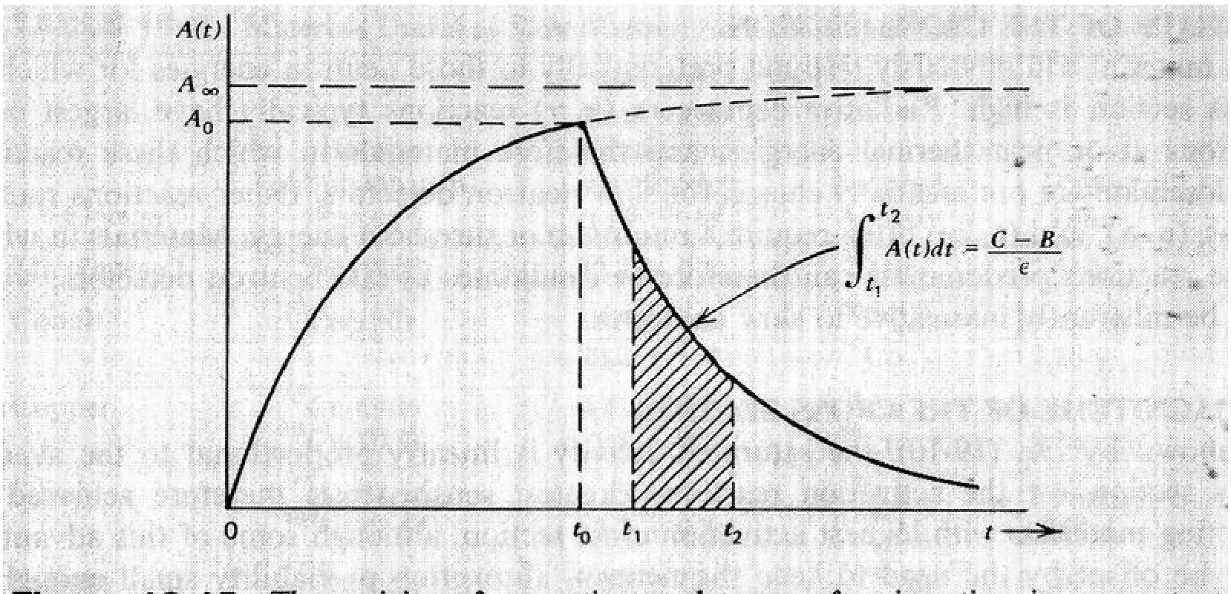

Figure 19-15 The activity of an activator detector after insertion in a constant neutron flux at time = 0 and removal at time = t_0. The measured number of counts is proportional to the area under the decay curve between t_1 and t_2.

Bonner spheres with TLDs and silver activation detectors PF1000 in Warsaw

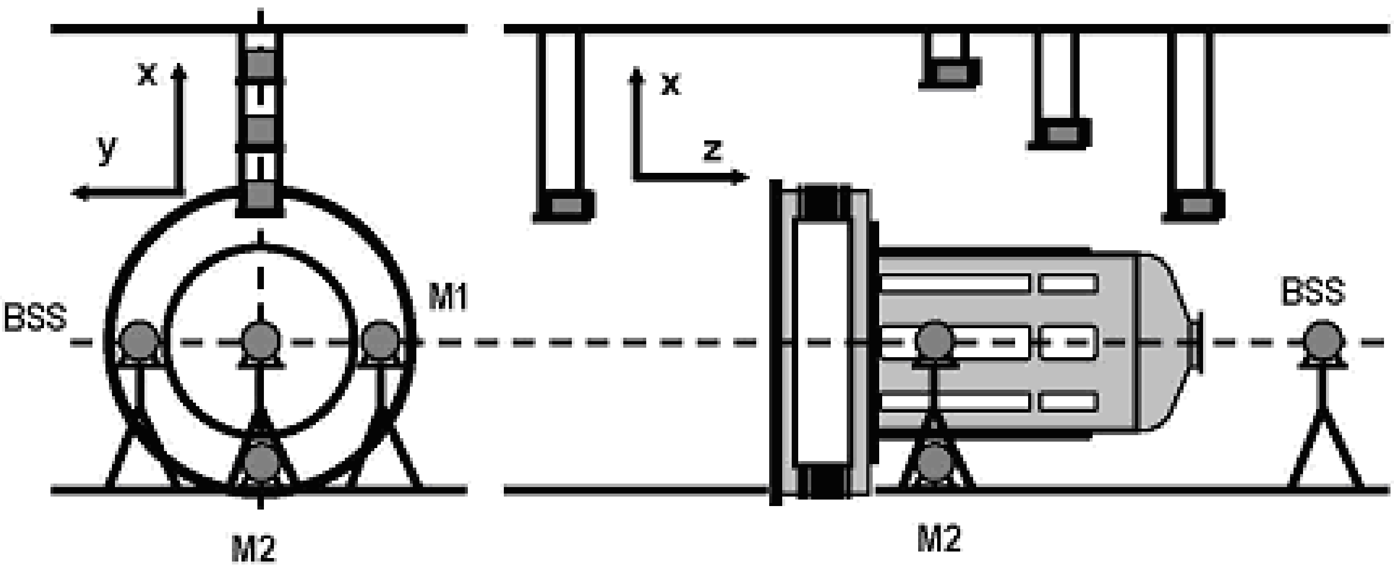

Scintillation Detectors

- Scintillators connected to PM-Tubes
- Time resolution in the ns range

Bubble detectors

They integrate the neutron yield

Bubbles have to be counted

Calibration necessary

Neutron Diagnostics

Beam Target Processes and their verification

Ion Trajectories in the Azimuthal Magnetic Field of the Pinch Current

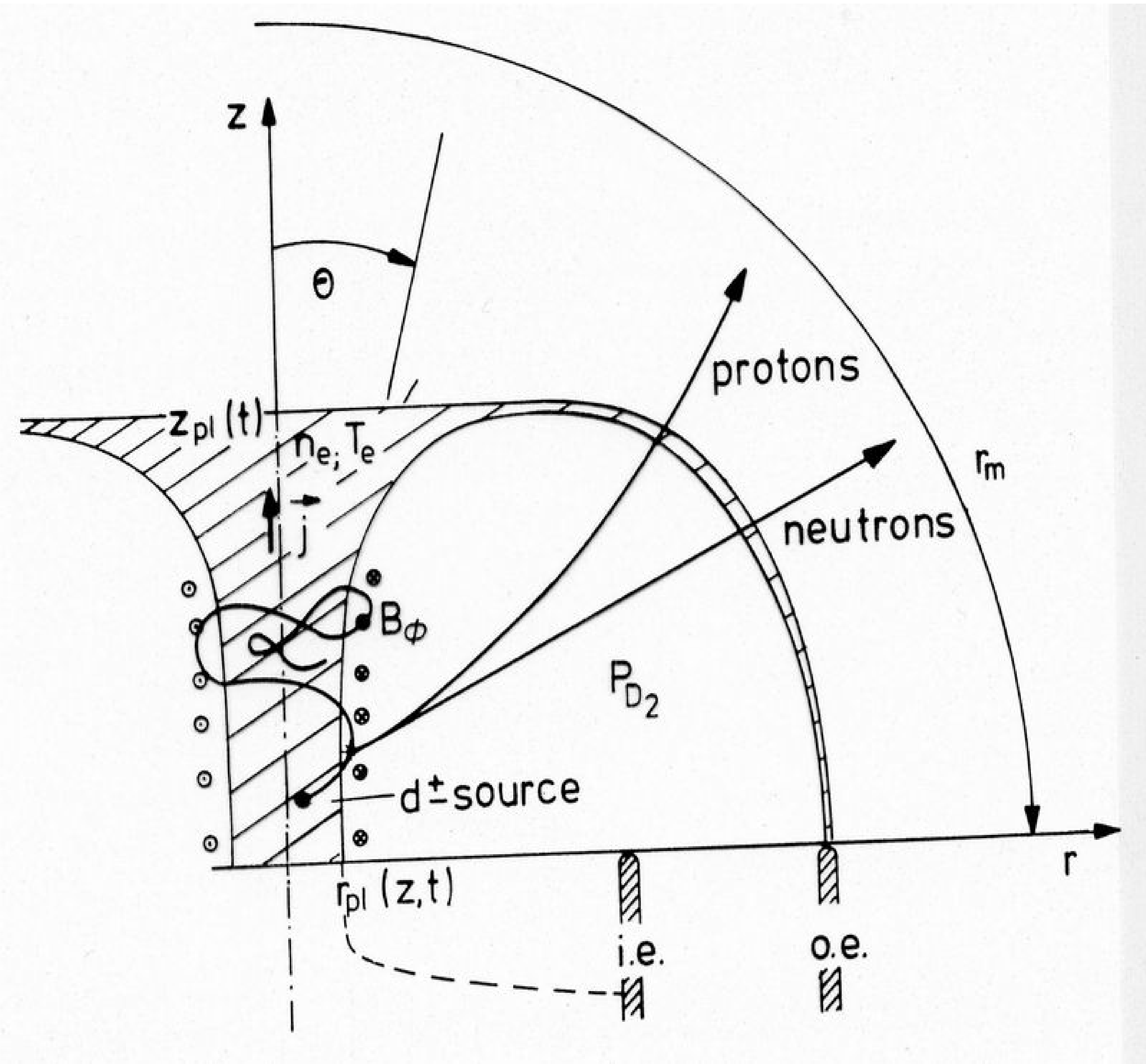

Beam-Target neutron production ! ?

statement to be verified:

deuterons of mean energy (50 - 100 keV) contribute mainly and essentially to fusion yield

the following processes take place:

- acceleration of deuterons by high transient electromagnetic fields
- absorption of those deuterons in the pinch
- atomic processes in the surrounding gas/plasma
  - charge exchange
  - scattering

⇒ no direct observation of deuteron distribution (which is responsible for fusion reactions)

→ indirect methods

- neutron spectroscopy (time-of-flight, nuclear emulsions)
- neutron flux anisotropy
- neutron source location and intensity distribution

(integral and/or time-resolved measurements)

Two Neutron emitting Phases Correlated to Plasma Dynamics

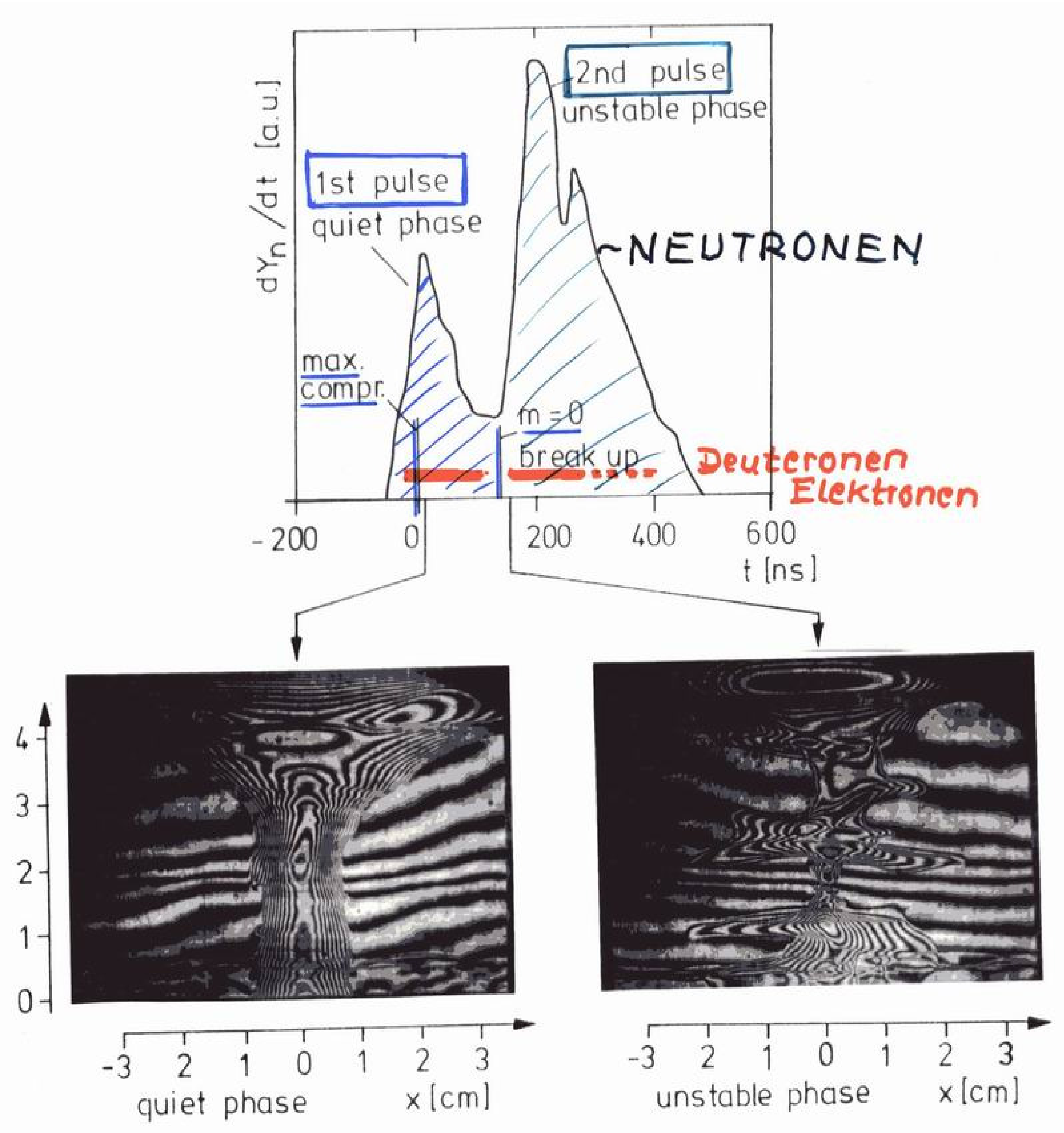

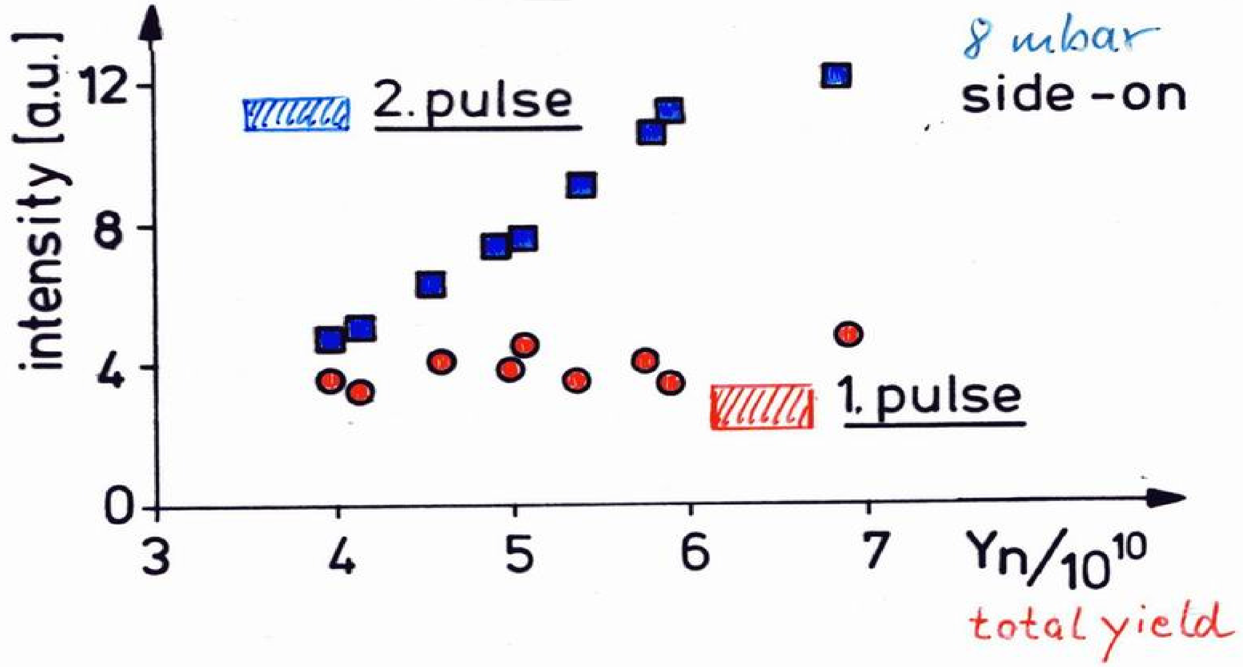

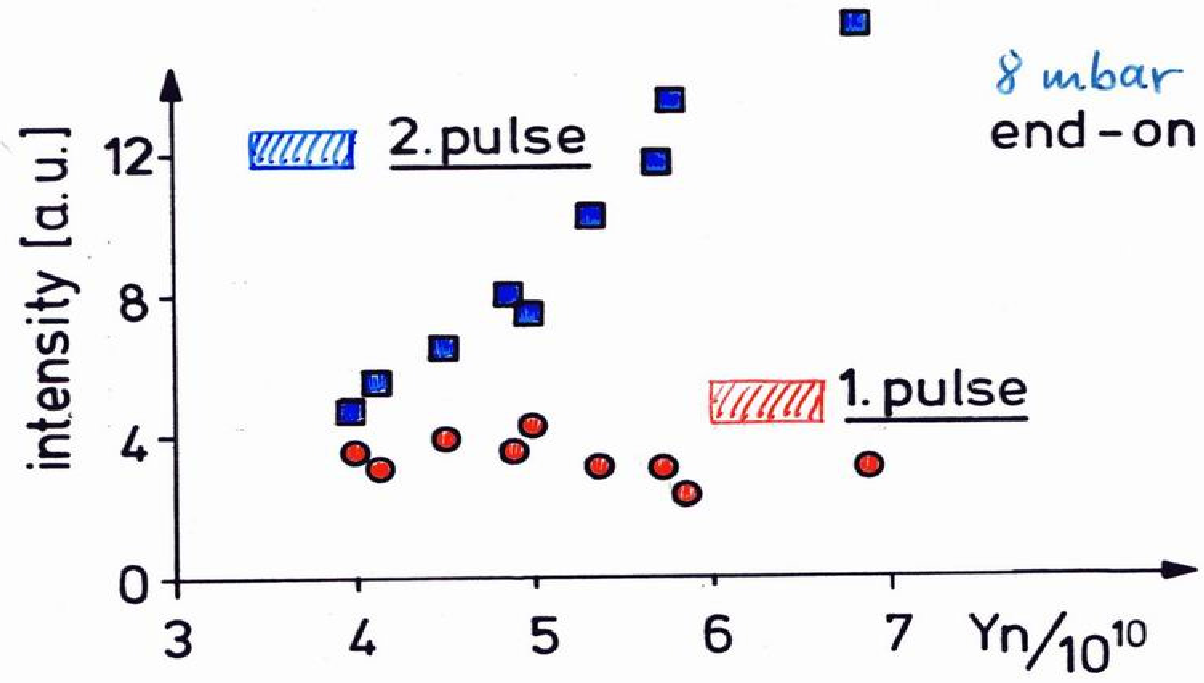

neutron yield of the two phases

8 mbar

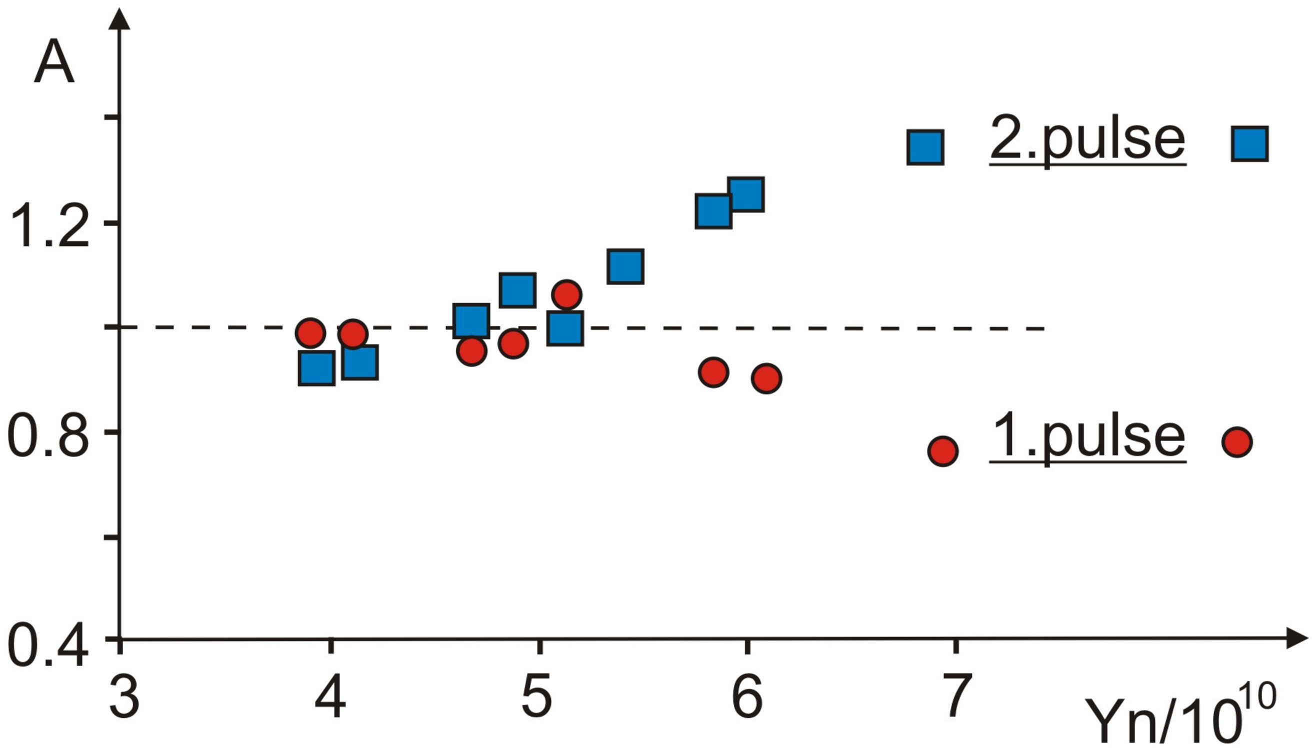

anisotropy factor of the two phases

$$A = \frac{\text{neutron flux end-on}}{\text{neutron flux side-on}}$$

Neutron Anisotropic factor of 1. and 2. Neutron Pulse

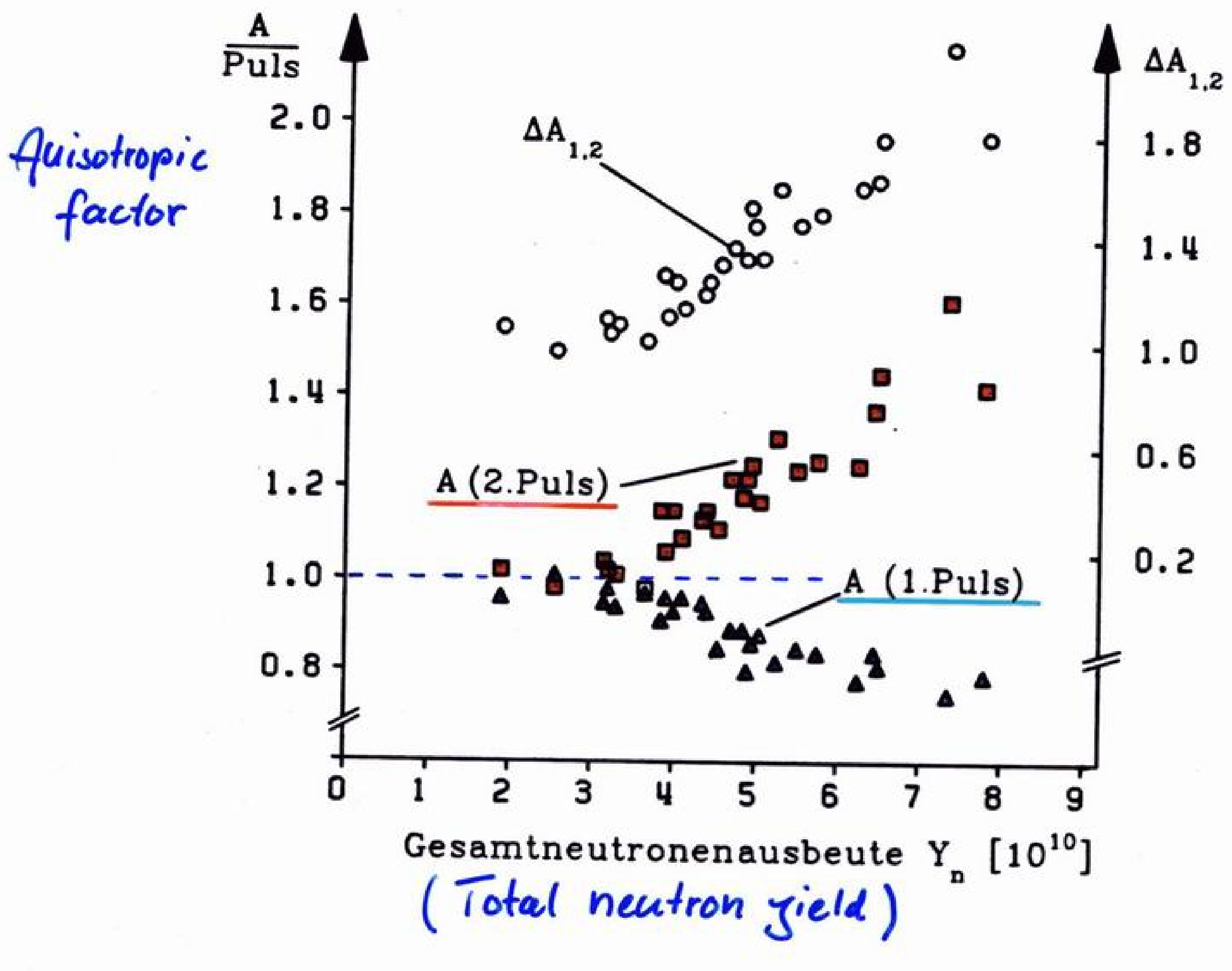

Anisotropic factor $A = \frac{Y(\text{"end-on"})}{Y(\text{"side-on"})}$

Neutron pinhole measurements

Pinhole Measurements Setup for Neutrons

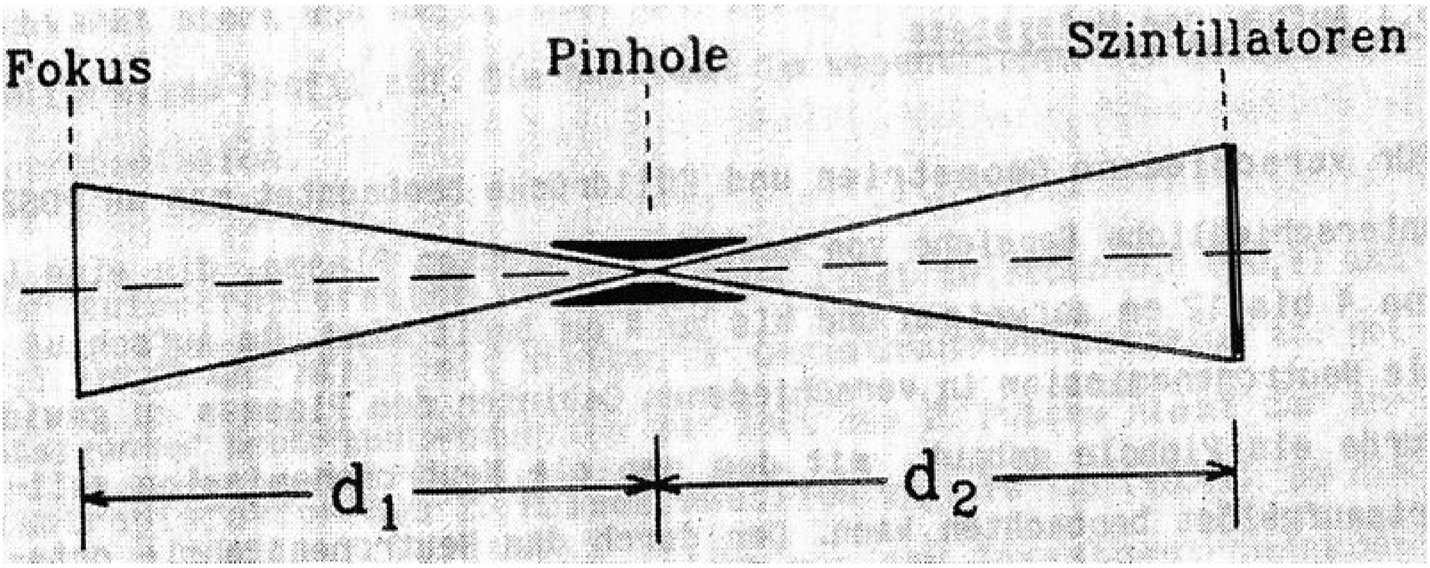

Pinhole for Neutrons

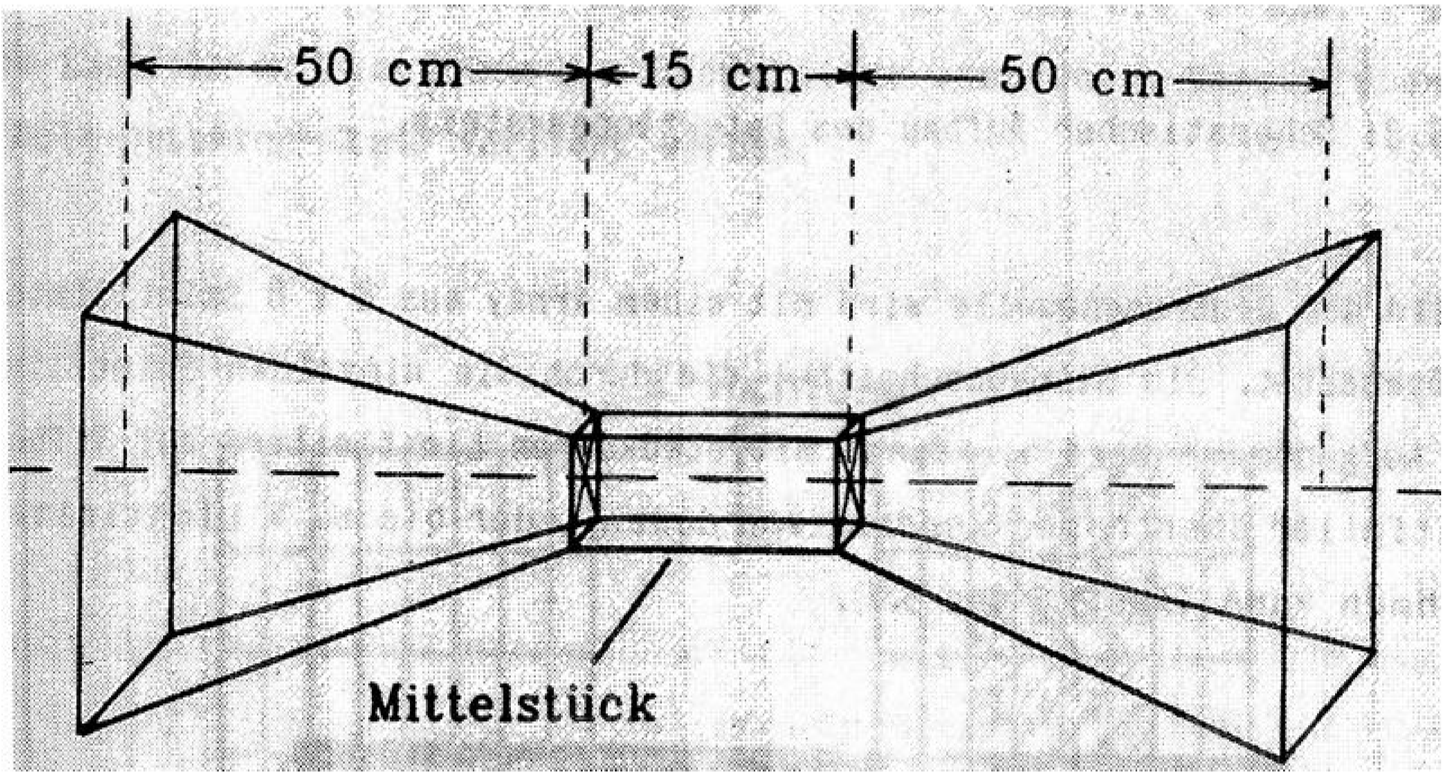

Array of Scintillators Connected via Light Fibres To Photomultipliers

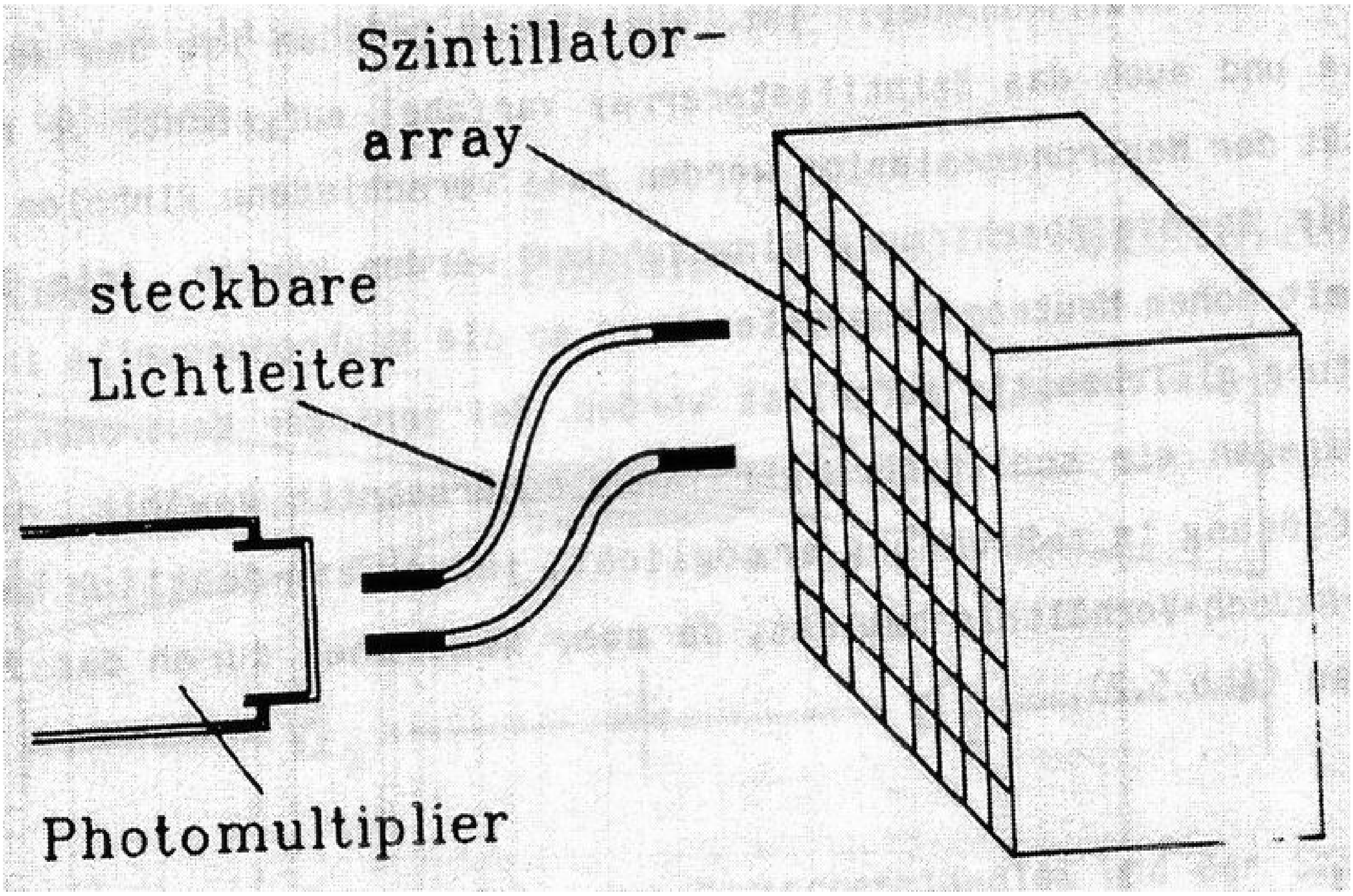

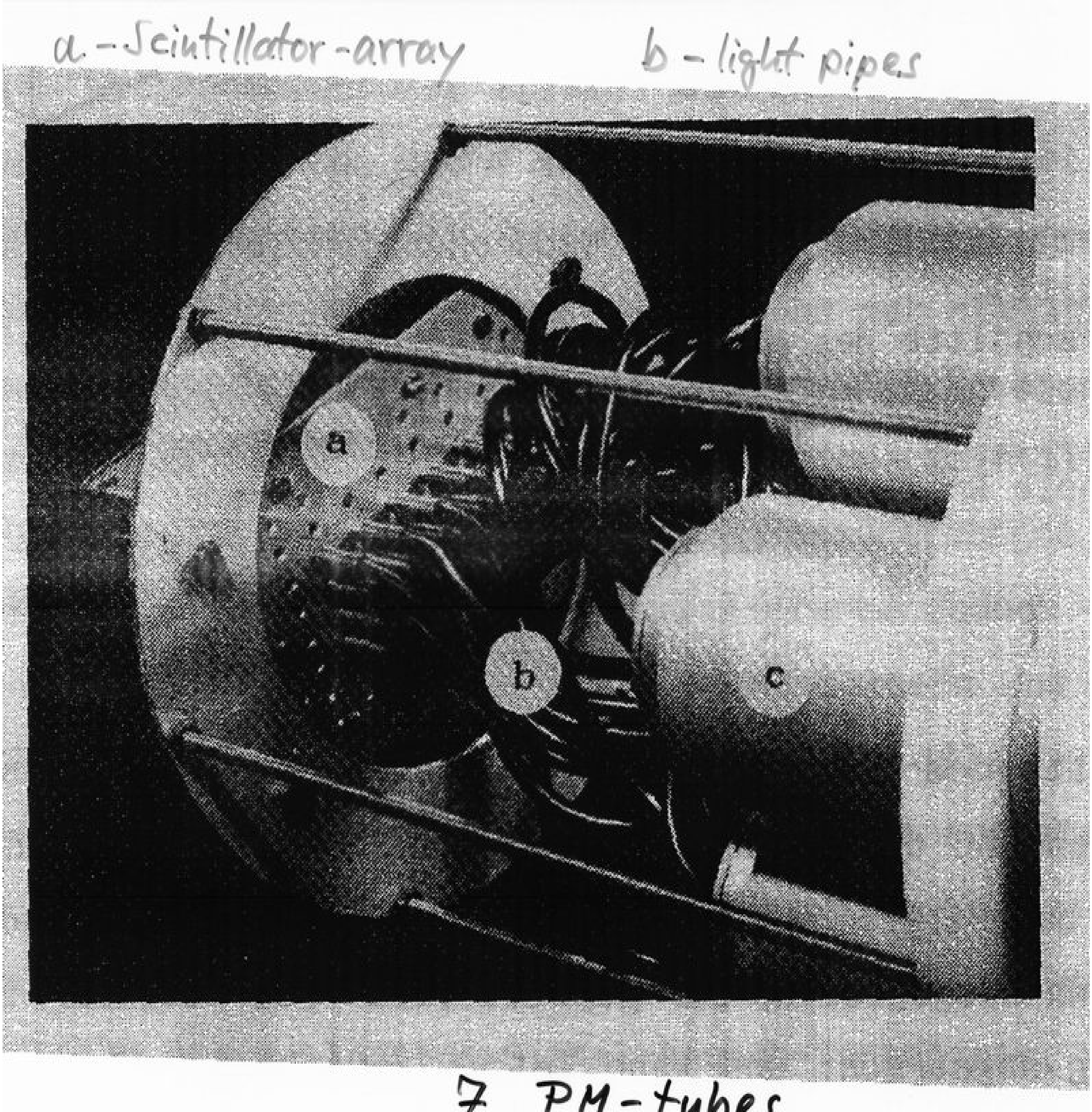
a - Scintillator - array
b - light pipes
a
b
c
7 PM-tubes

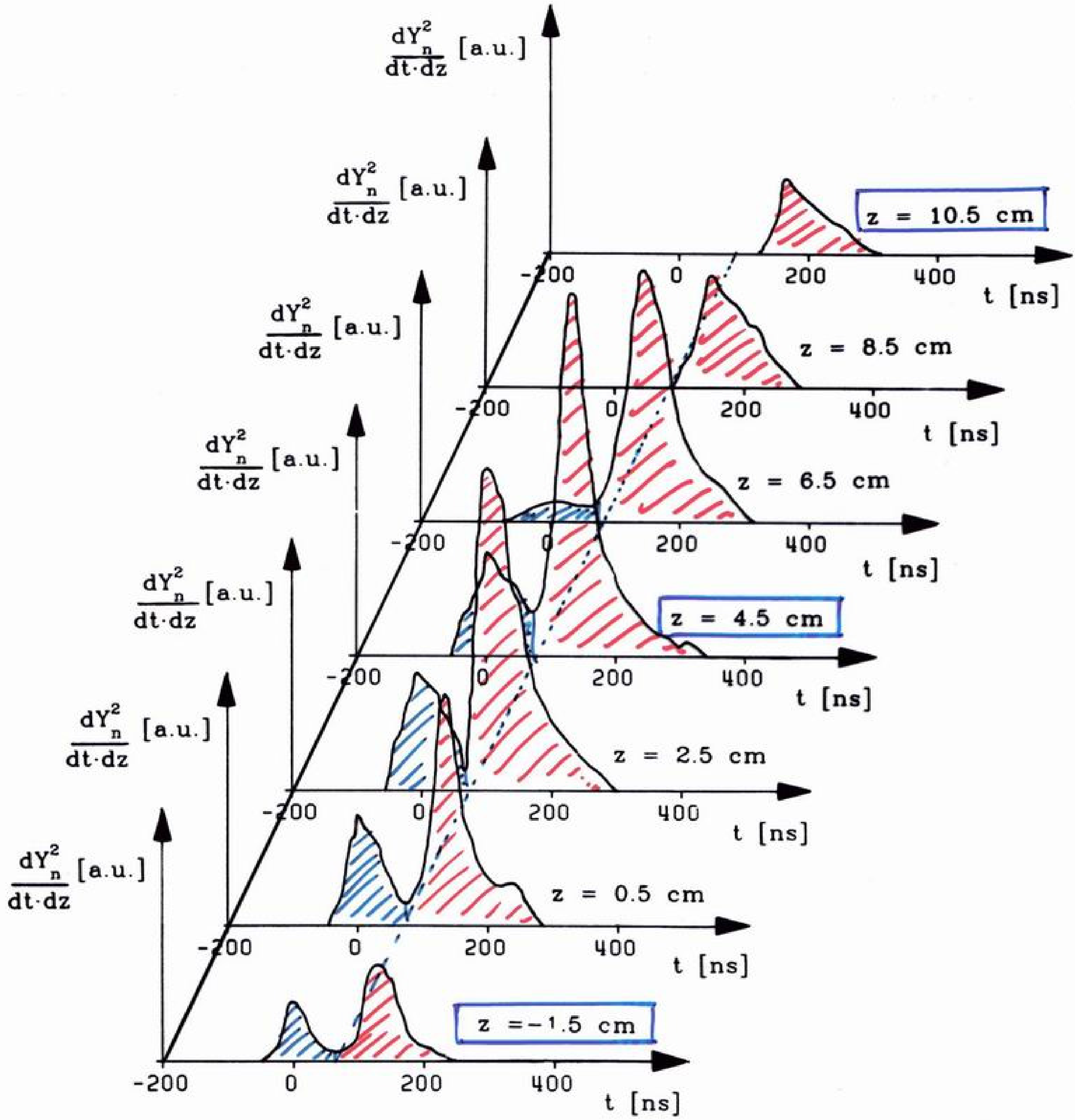

Fig. 9: Result of neutron pinhole measurements. Neutron emission spatially resolved in axial direction (resolution $\Delta z \leq 2$ cm, $\Delta t \leq 20$ ns) on POSEIDON (280 kJ, 60 kV, 500 Pa D_2, $Y_n = 6.6 \cdot 10^{10}$, hollow inner electrode, 131 mm diameter).

Neutron

Time of Flight

Measurements

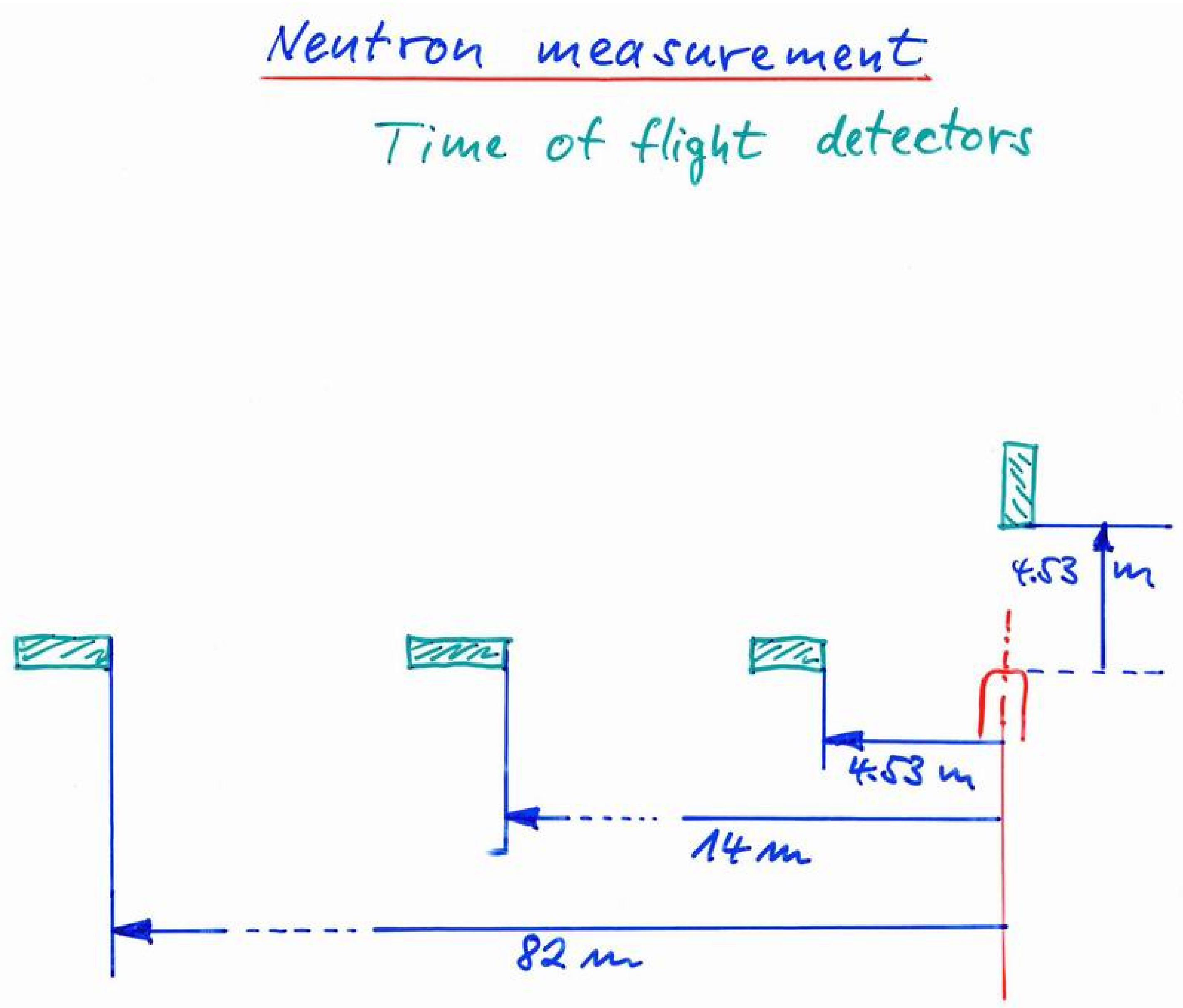

Neutron measurement
Time of flight detectors
4.53 m
4.53 m
14 m
82 m

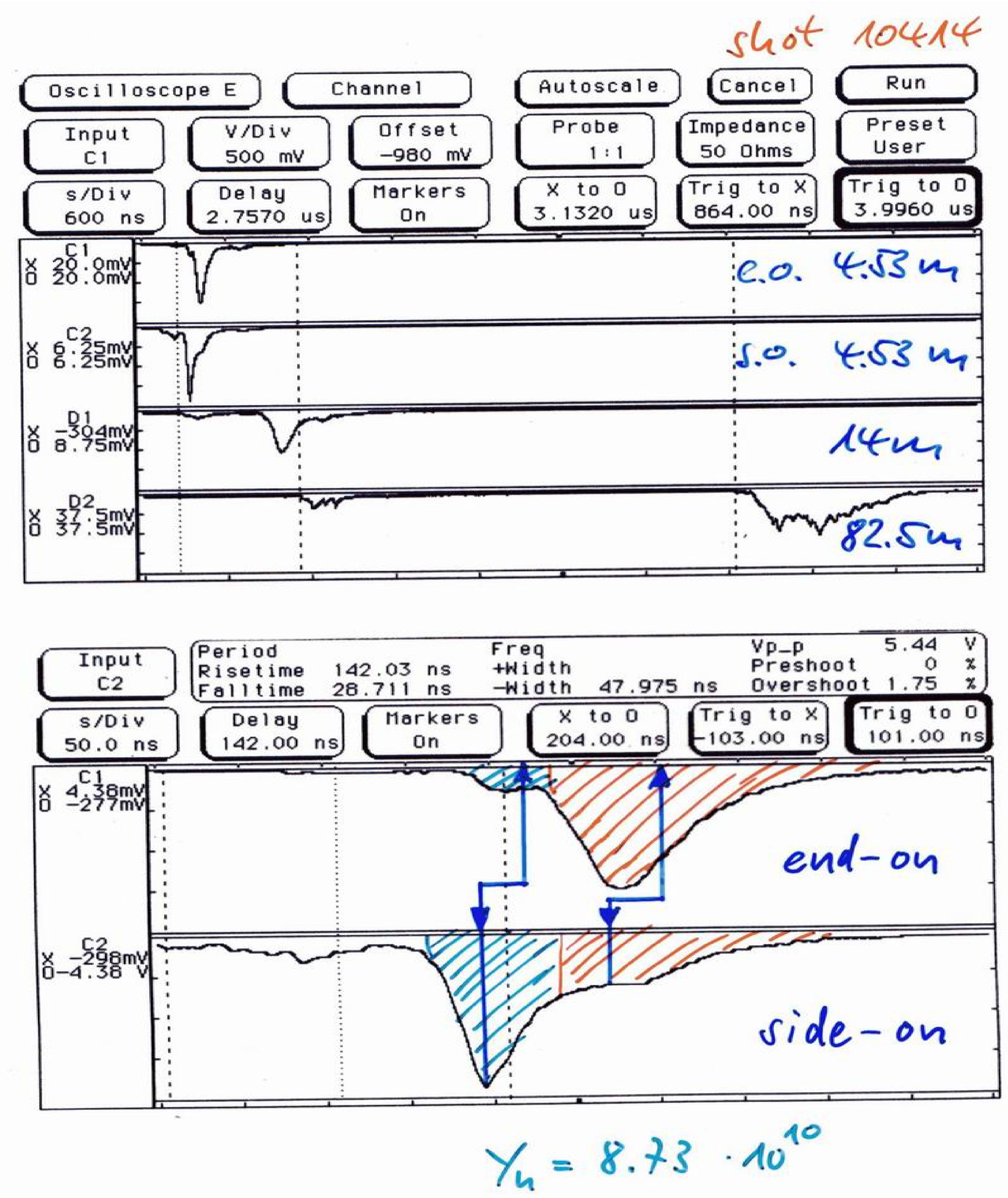
shot 10414
Oscilloscope E
Channel
Autoscale
Cancel
Run
Input C1
V/Div 500 mV
Offset −980 mV
Probe 1:1
Impedance 50 Ohms
Preset User
s/Div 600 ns
Delay 2.7570 us
Markers On
X to O 3.1320 us
Trig to X 864.00 ns
Trig to O 3.9960 us
C1 X 20.0mV O 20.0mV
C2 X 6.25mV O 6.25mV
D1 X −304mV O 8.75mV
D2 X 37.5mV O 37.5mV
e.o. 4.53 m
s.o. 4.53 m
14 m
82.5 m
Input C2
Period
Risetime 142.03 ns
Falltime 28.711 ns
Freq
+Width
−Width 47.975 ns
Vp_p 5.44 V
Preshoot 0 %
Overshoot 1.75 %
s/Div 50.0 ns
Delay 142.00 ns
Markers On
X to O 204.00 ns
Trig to X −103.00 ns
Trig to O 101.00 ns
C1 X 4.38mV O −277mV
C2 X −298mV O −4.38 V
end-on
side-on
$Y_n = 8.73 \cdot 10^{10}$

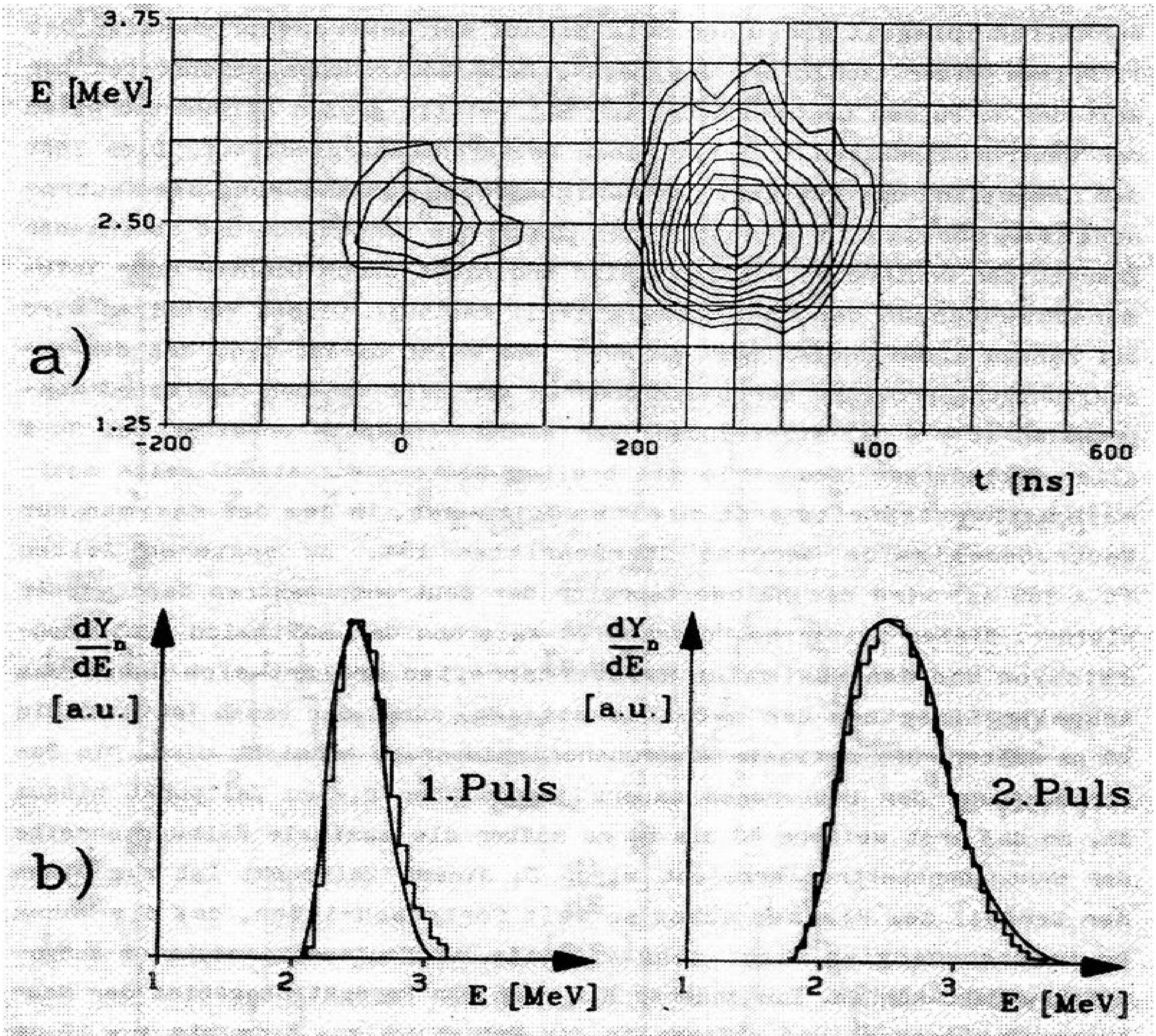

Abb. 6.14: Rekonstruktion einer typischen POSEIDON-Entladung, Schuß Nr. 7522, breiter Elektrodenabstand, Ladespannung 70 kV, Fülldruck 8 mbar.
a) Höhenlinienbild.
b) Neutronenspektren der Einzelpulse (zeitintegriert): ermittelt aus der rekonstruierten Quellfunktion (Stufenfunktion) und berechnet nach dem verallgemeinerten "Beam-Target"-Modell (glatte Kurve).

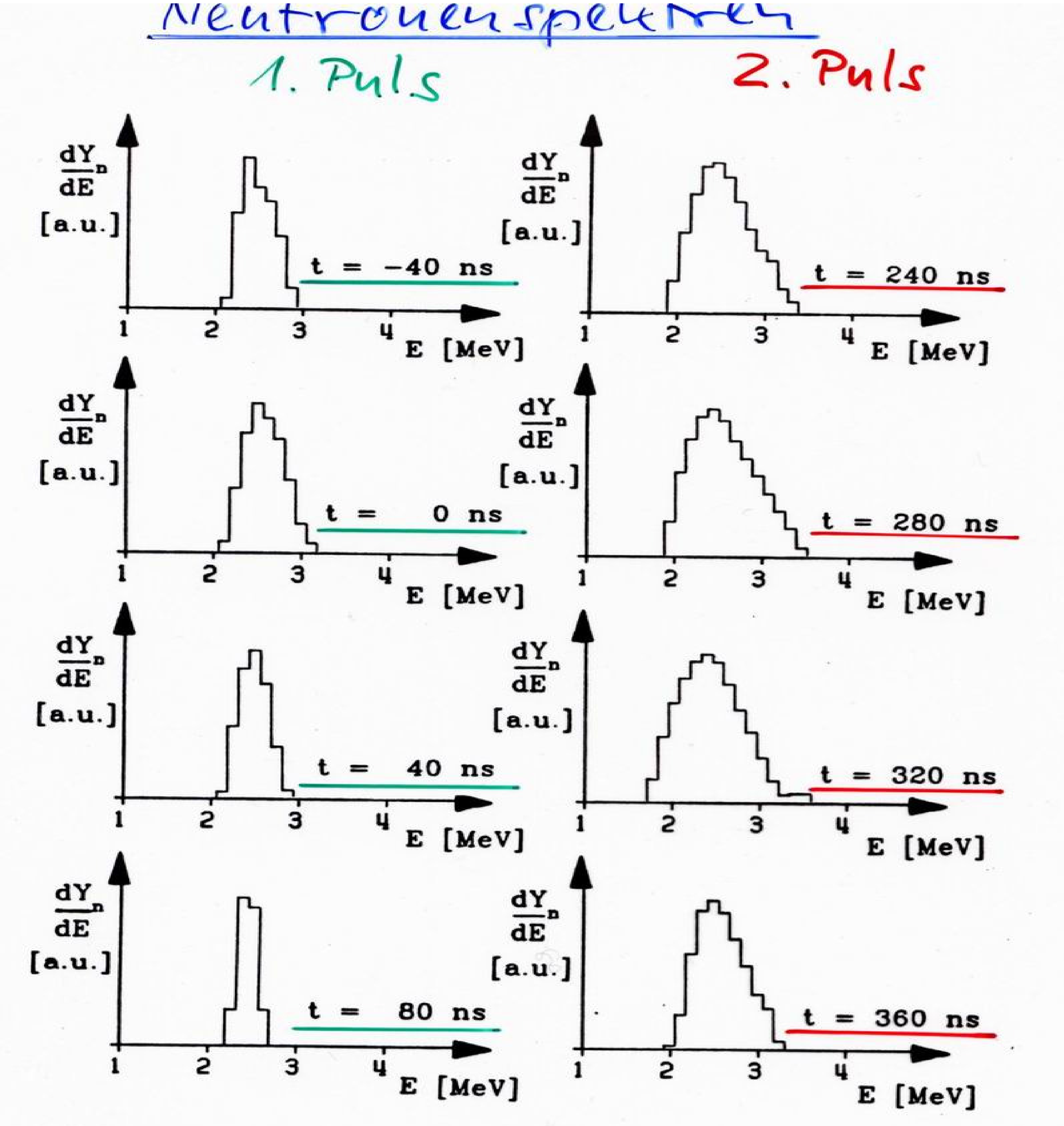

Abb. 6.15: Neutronenspektren einer typischen POSEIDON-Entladung zu verschiedenen Zeiten, Schuß Nr. 7522 (vgl. Abb.6.14a).

Neutronenspektren

Spalt 36 mm

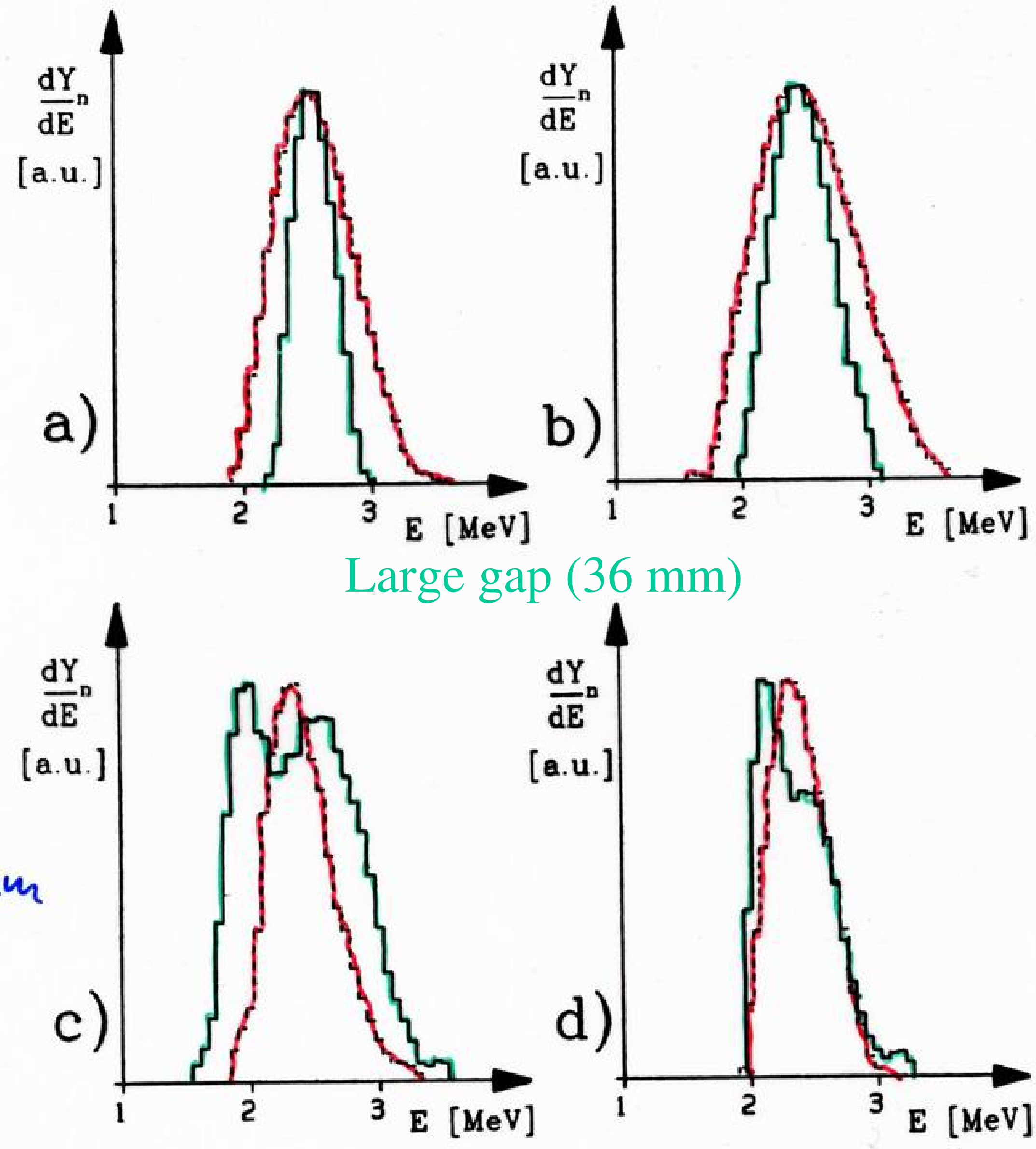

28,5 mm

Small gap (28.5 mm)

Abb. 6.19: Typische Neutronenspektren des 1. Pulses (——) und des 2. Pulses (– – –) mit breitem (a,b) und engem (c,d) Elektrodenabstand.

$Y_n/10^{10}$			Y_2/Y_1
1.6	a) Y_n(1.Puls) = $0{,}3\cdot10^{10}$,	Y_n(2.Puls) = $1{,}3\cdot10^{10}$.	4.3
6.2	b) Y_n(1.Puls) = $0{,}6\cdot10^{10}$,	Y_n(2.Puls) = $5{,}6\cdot10^{10}$.	9.3
2.7	c) Y_n(1.Puls) = $1{,}9\cdot10^{10}$,	Y_n(2.Puls) = $0{,}8\cdot10^{10}$.	0.4
1.3	d) Y_n(1.Puls) = $0{,}5\cdot10^{10}$,	Y_n(2.Puls) = $0{,}8\cdot10^{10}$.	1.6

Neutron Yield and

FWHM of Neutron Spectra
as a function of time

-> relaxation of deuterons

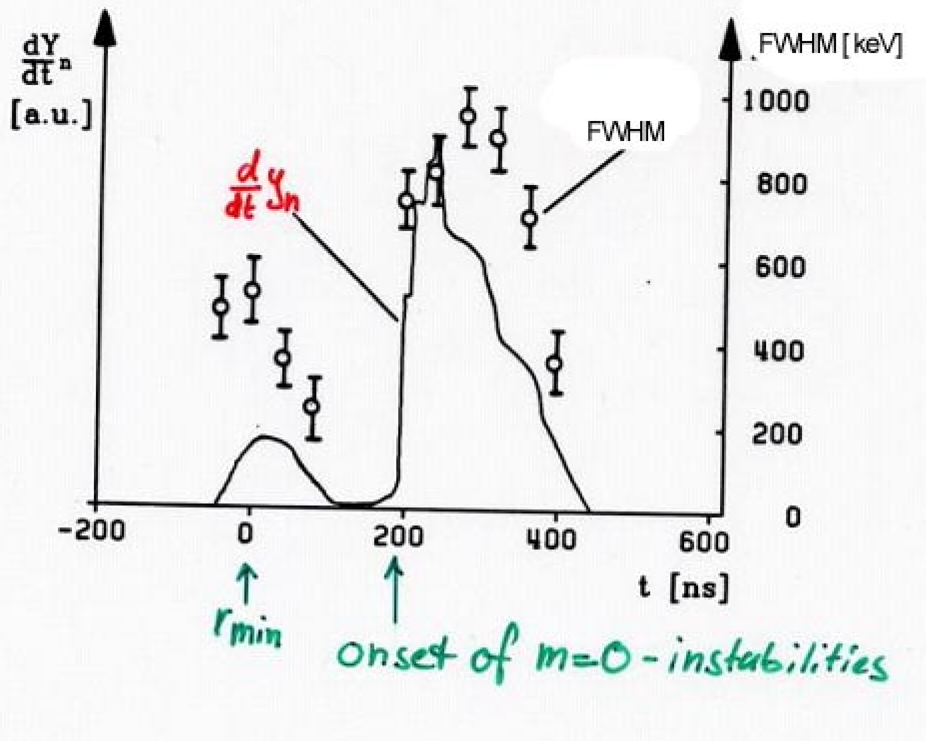

Typical POSEIDON shot, voltage 70 kV, filling pressure 8 mbar.

Y_n (1. pulse) $= 0.6 \cdot 10^{10}$

Y_n (2. pulse) $= 4.1 \cdot 10^{10}$

Why

Reaction Proton

Diagnostics?

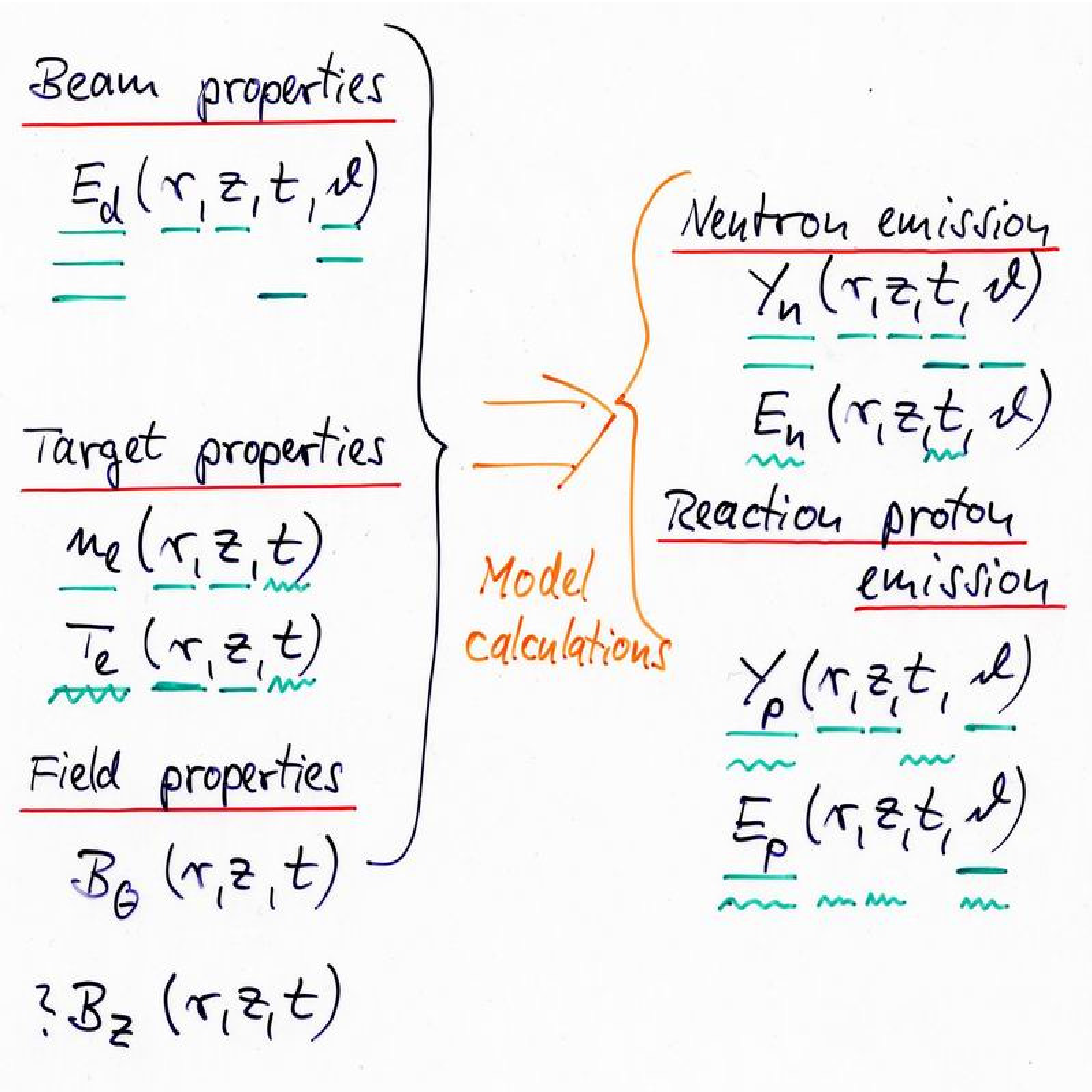
Beam properties
$E_d(r, z, t, \vartheta)$
Target properties
$n_e(r, z, t)$
$T_e(r, z, t)$
Field properties
$B_\Theta(r, z, t)$
? $B_z(r, z, t)$
Model calculations
Neutron emission
$Y_n(r, z, t, \vartheta)$
$E_n(r, z, t, \vartheta)$
Reaction proton emission
$Y_p(r, z, t, \vartheta)$
$E_p(r, z, t, \vartheta)$

Proton Diagnostics

Solid state nuclear track detectors are used for the registration of protons

Individual particles can be registered using an etching process.

Small craters are visible under the Microscope

Spectral information can be obtained using absorbing metal foils

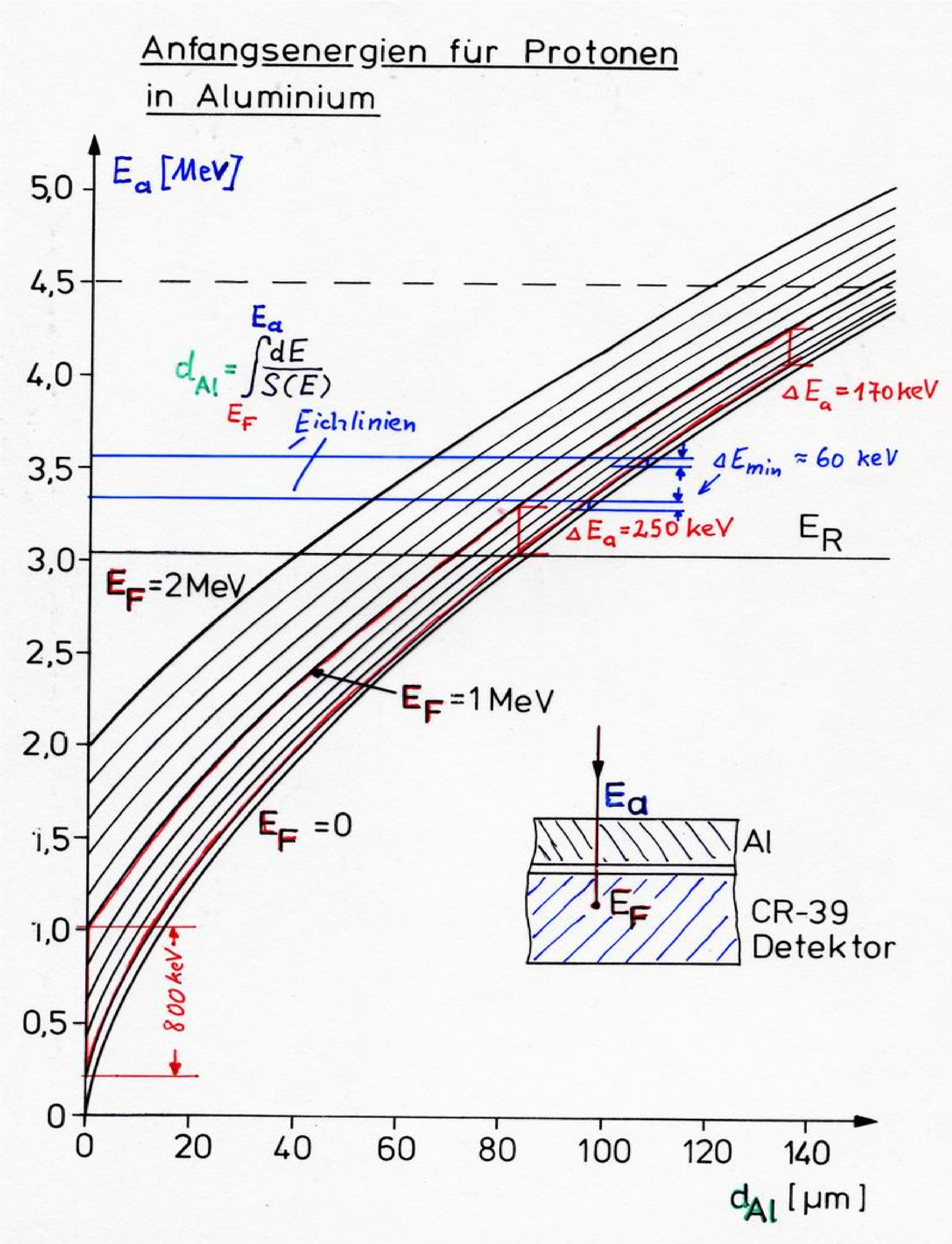
Anfangsenergien für Protonen
in Aluminium
E_a [MeV]
5,0
4,5
4,0
3,5
3,0
2,5
2,0
1,5
1,0
0,5
0
d_Al = ∫ dE/S(E) (E_F bis E_a)
Eichlinien
ΔE_a = 170 keV
ΔE_min ≈ 60 keV
ΔE_a = 250 keV
E_R
E_F = 2MeV
E_F = 1 MeV
E_F = 0
800 keV
E_a
Al
E_F
CR-39
Detektor
20
40
60
80
100
120
140
d_Al [µm]

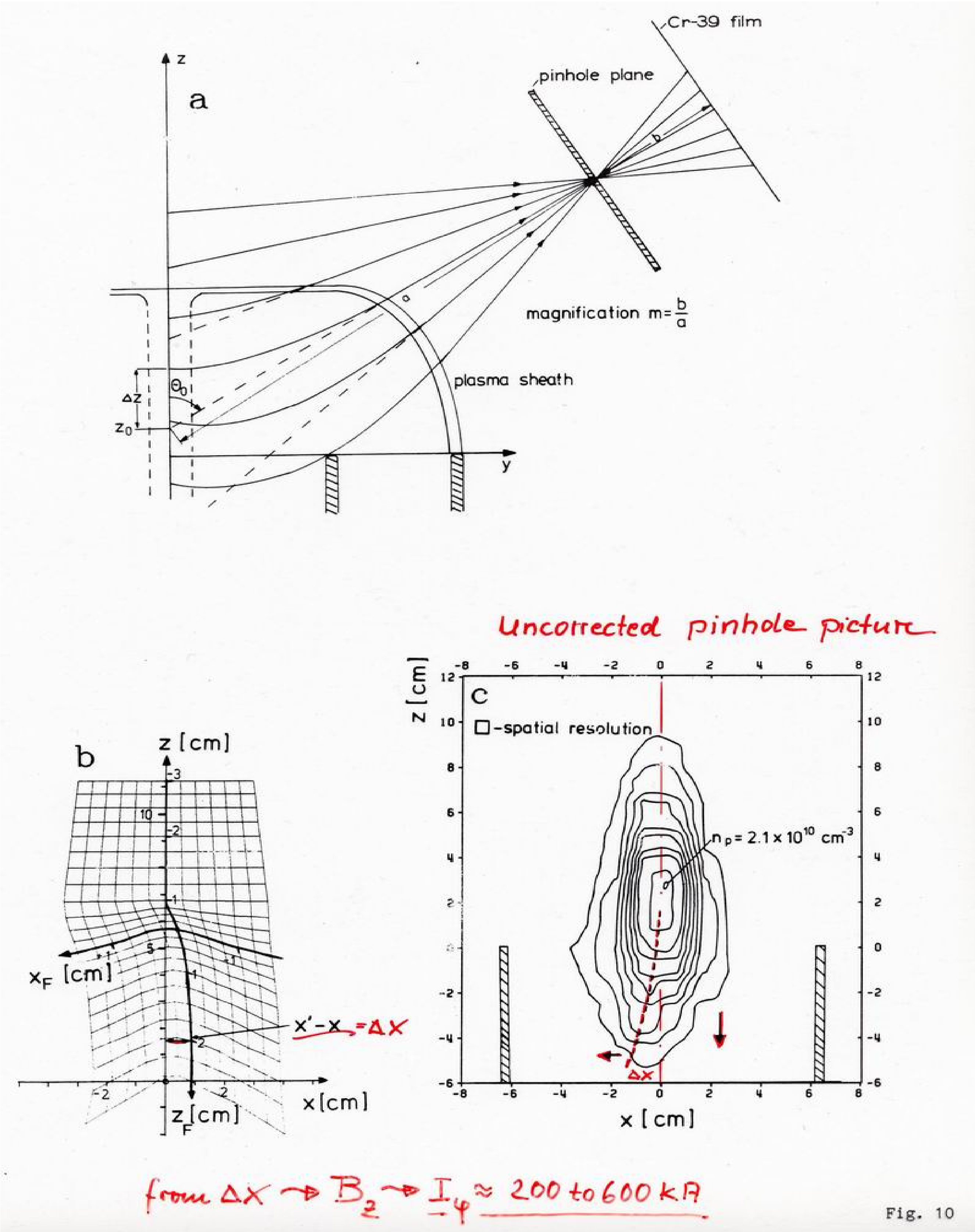

Cr-39 film
pinhole plane
a
z
magnification m= b/a
plasma sheath
Θ0
Δz
z0
y
Uncorrected pinhole picture
b
z [cm]
x_F [cm]
x'-x =ΔX
x [cm]
z_F [cm]
c
z [cm]
□-spatial resolution
n_p = 2.1 x 10^10 cm^-3
ΔX
x [cm]
from ΔX → B_z → I_φ ≈ 200 to 600 kA

Fig. 10

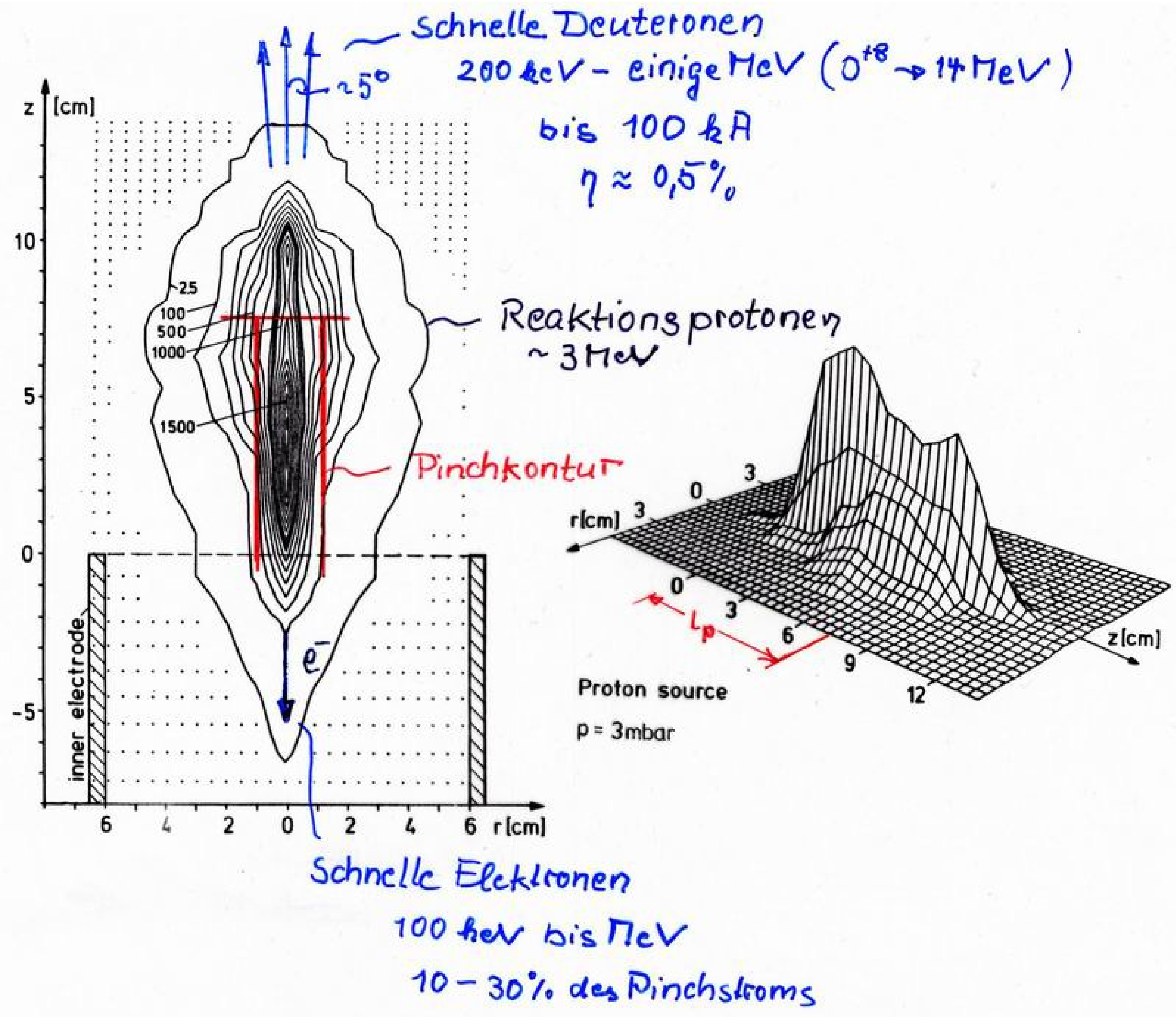

Bild der Reaktionsprotonen (Neutronen) Quelle
(Äqui-Dichte Linien, entabelt)

Pinhole picture of

Pinhole pictur

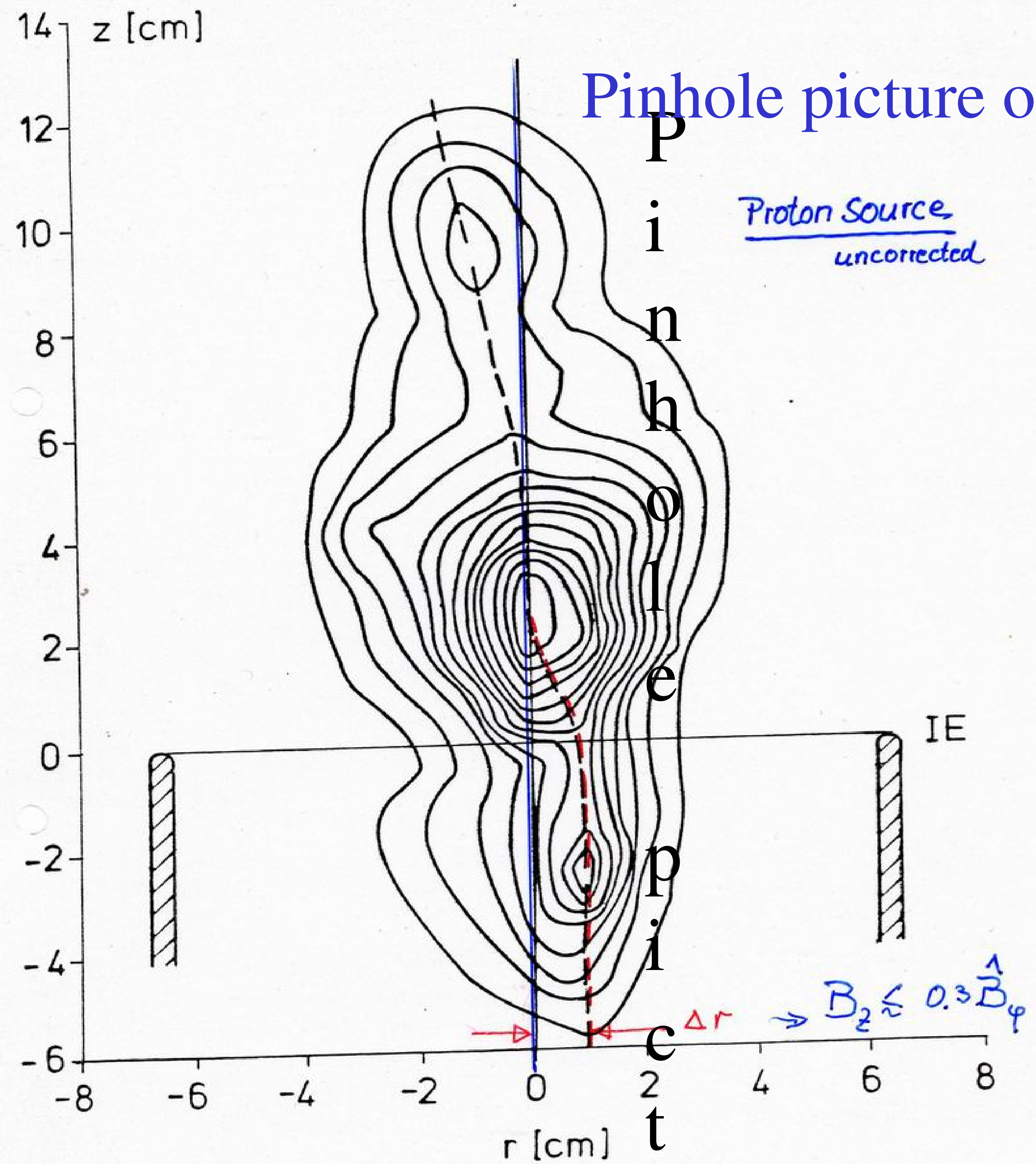

Fig. 7: Pinhole picture of the reaction proton source, uncorrected for beam deviation by focus magnetic fields. The contours are lines of constant proton density on the film. IE = inner electrode. W_o = 280 kJ; p_o = 5 mbar D_2.

Proton spectra

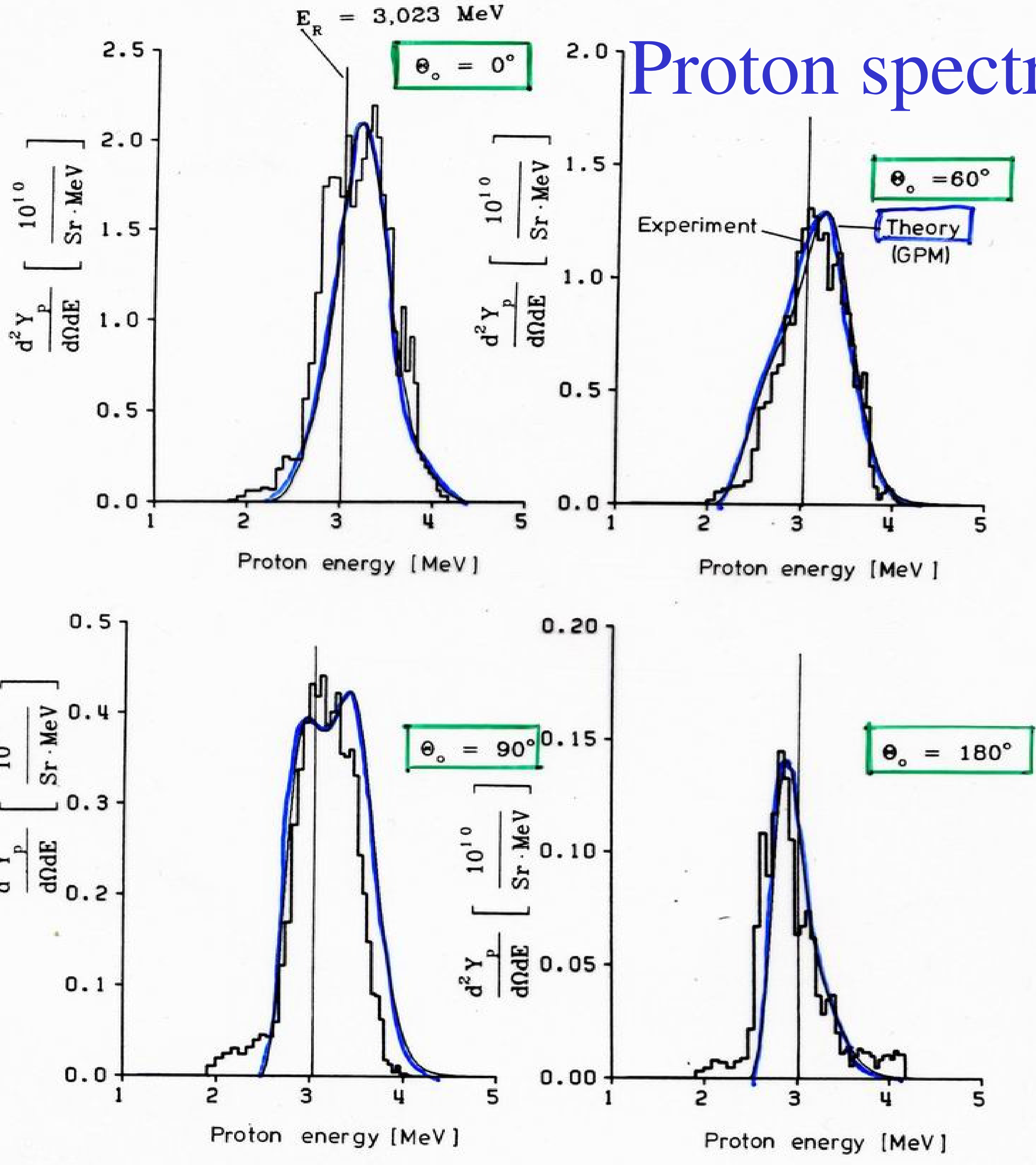

Fig. 14: Reaction proton spectra on POSEIDON (280 kJ, 60 kV, 500 Pa D_2), proton yield Y_p = $5.7 \cdot 10^{10}$, contribution of the first pulse 34%. For the GPM-calculations [30] of the curves the following parameters were taken: T_{i1}^* = 75 keV, N_{b1} = $5 \cdot 10^{16}$, T_{i2}^* = 200 keV, N_{b2} = $3 \cdot 10^{14}$, A_d = 3, I_{pl} = 790 kA.

Calculated Spectra

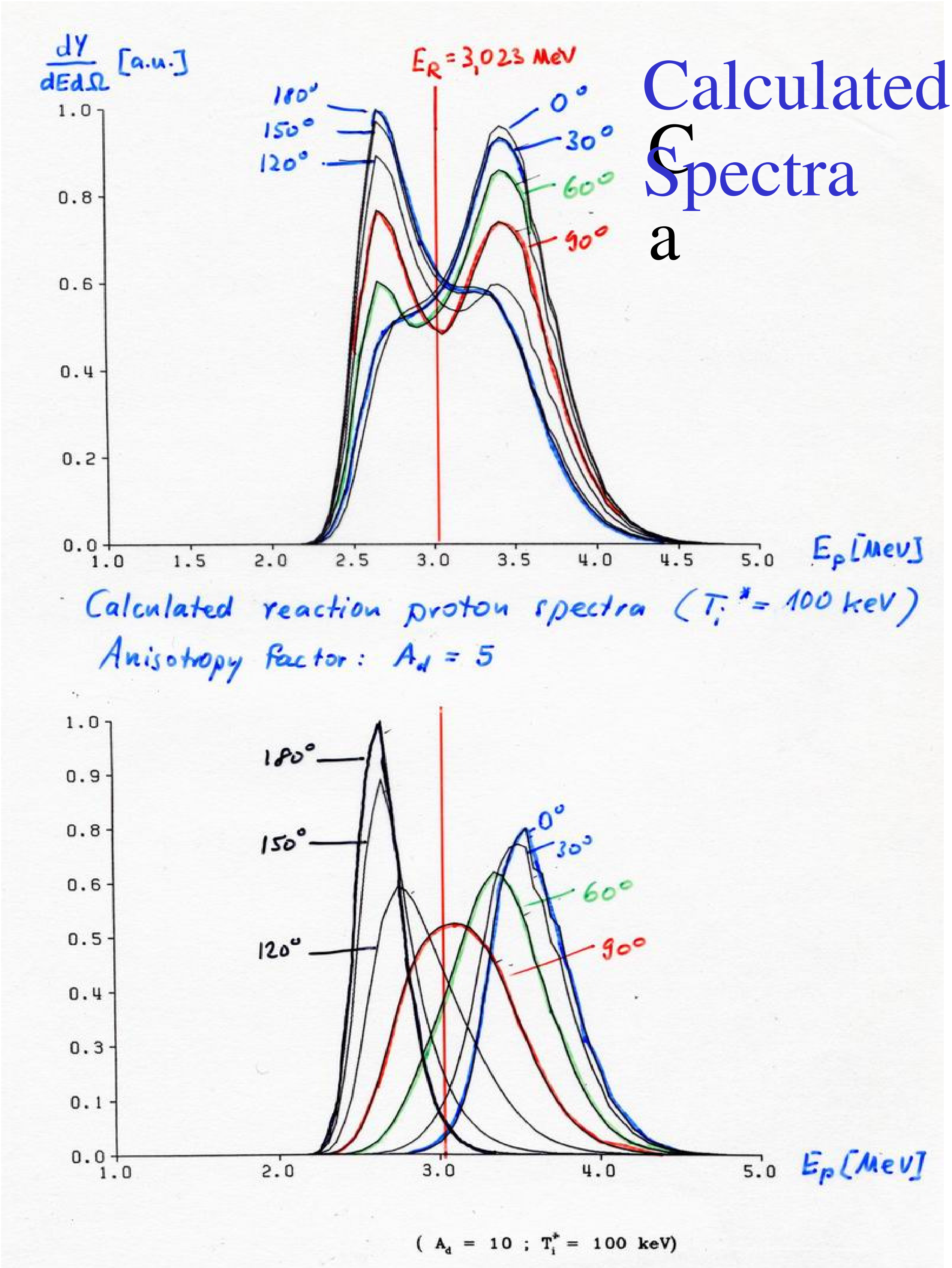

Neutron diagnostics deliver valuable information on various processes which occur in the plasma, such as:

Pinch dynamics

fast ion beams interacting with a target

fast ion energy distributions

Fusion neutron measurements should be complemented by Fusion proton measurements.

NEUTRONS

angular resolution

---> anisotropy
beam target processes

temporal resolution

---> two (three) pulses
various pinch phases

spatial resolution

---> dimensions of source
(better using proton measurements)

axial propagation of source

spectral resolution

---> energy of deuterons

relaxation of deuterons

Gyrating Particle Model

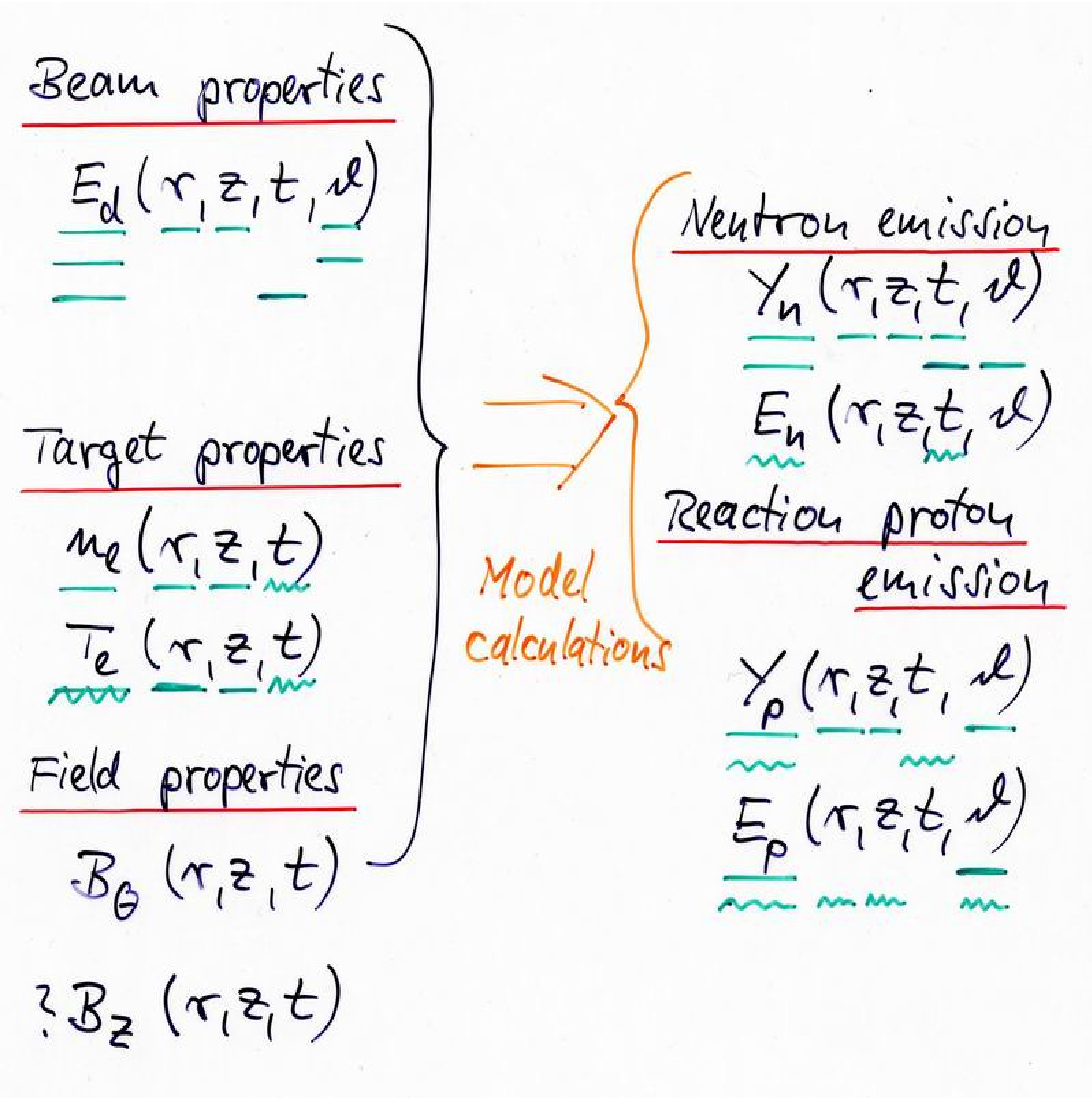
Beam properties
$E_d(r, z, t, \vartheta)$
Target properties
$n_e(r, z, t)$
$T_e(r, z, t)$
Field properties
$B_\Theta(r, z, t)$
? $B_z(r, z, t)$
Model calculations
Neutron emission
$Y_n(r, z, t, \vartheta)$
$E_n(r, z, t, \vartheta)$
Reaction proton emission
$Y_p(r, z, t, \vartheta)$
$E_p(r, z, t, \vartheta)$

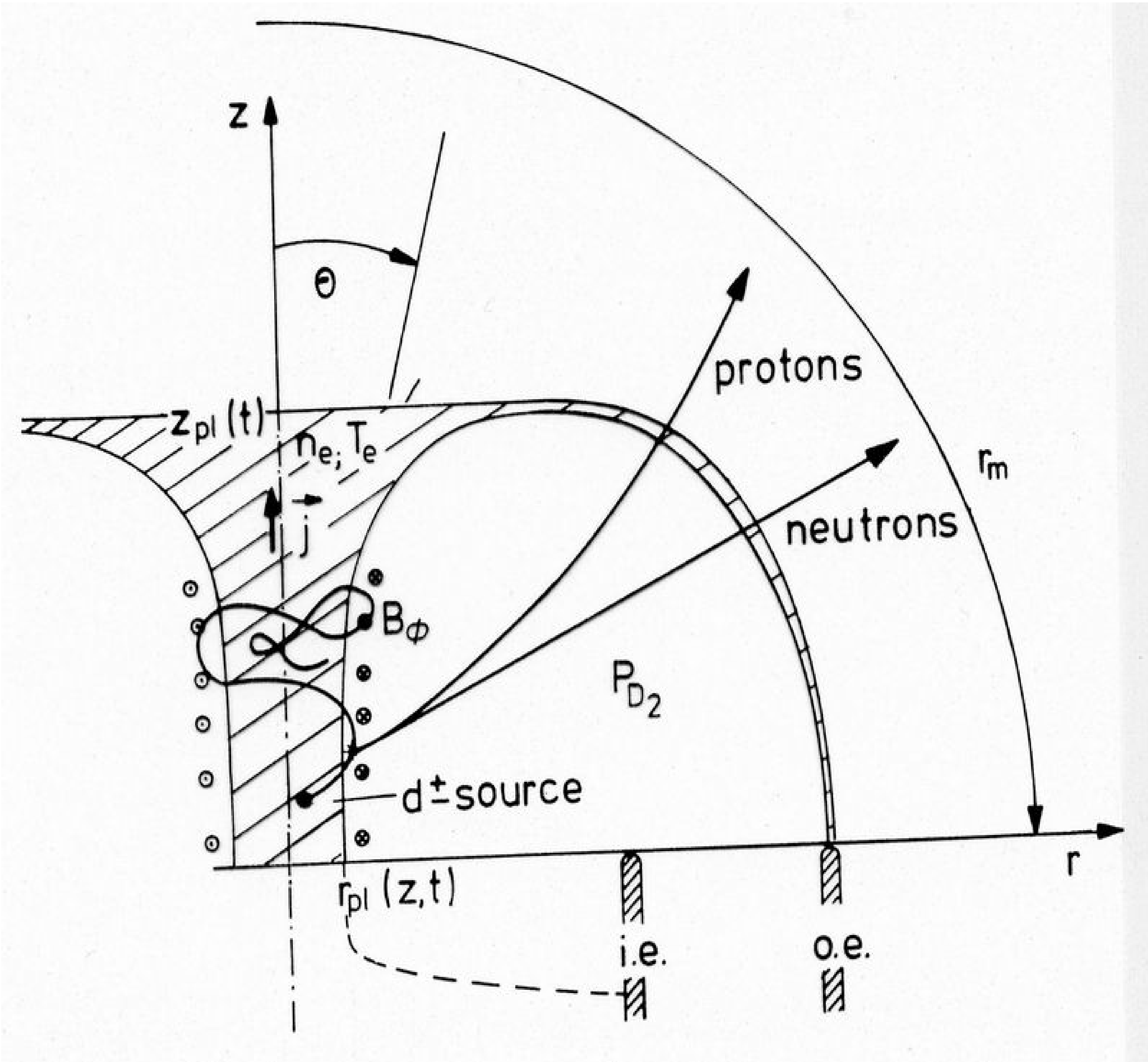
z
Θ
protons
$z_{pl}(t)$
$n_e; T_e$
r_m
$\vec{j}$
neutrons
B_ϕ
p_{D_2}
$d^\pm$ source
r
$r_{pl}(z,t)$
i.e.
o.e.

Temperatur-Verteilung für Deuteronen (aus Maxwellverteilung):

$$\frac{dN_d}{dE_d} = \frac{2}{\sqrt{\pi}} \cdot N_b \cdot \sqrt{\frac{E_d}{T_i^3}} \cdot e^{-E_d/T_i^3} \left[\frac{1}{keV} \right]$$

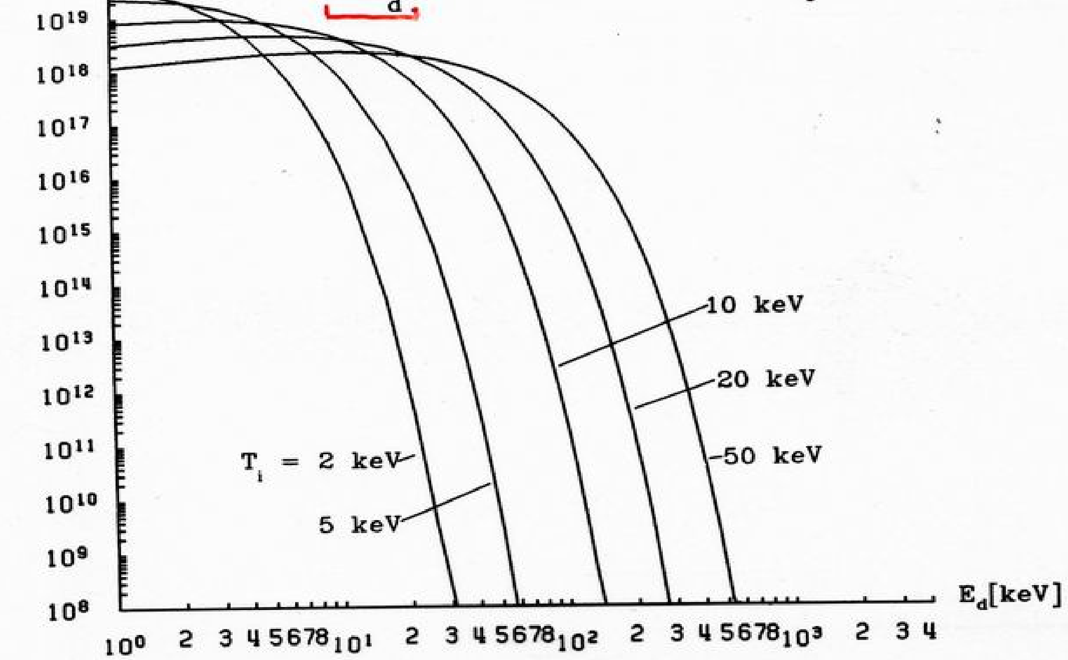

Verteilungsfunktion für eine Temperatur ($N = 10^{20}$)

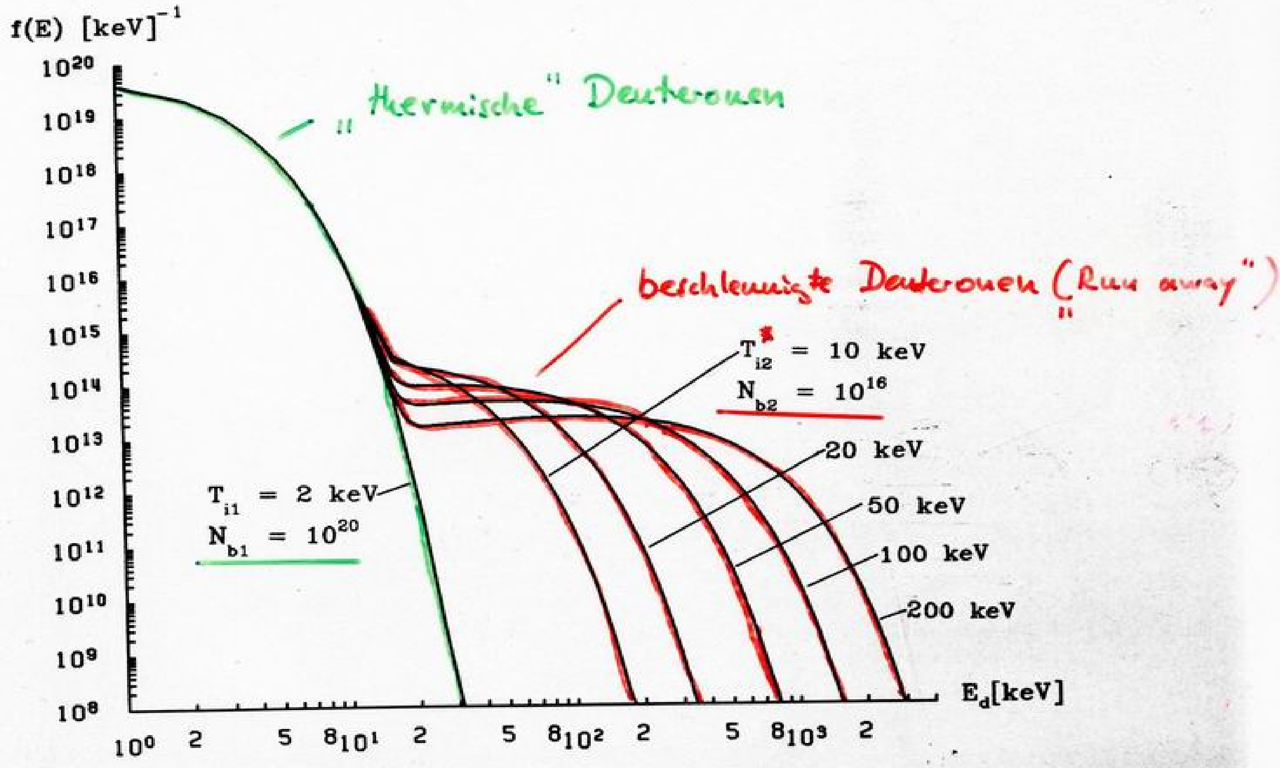

Verteilungsfunktionen für 2 Temperaturen

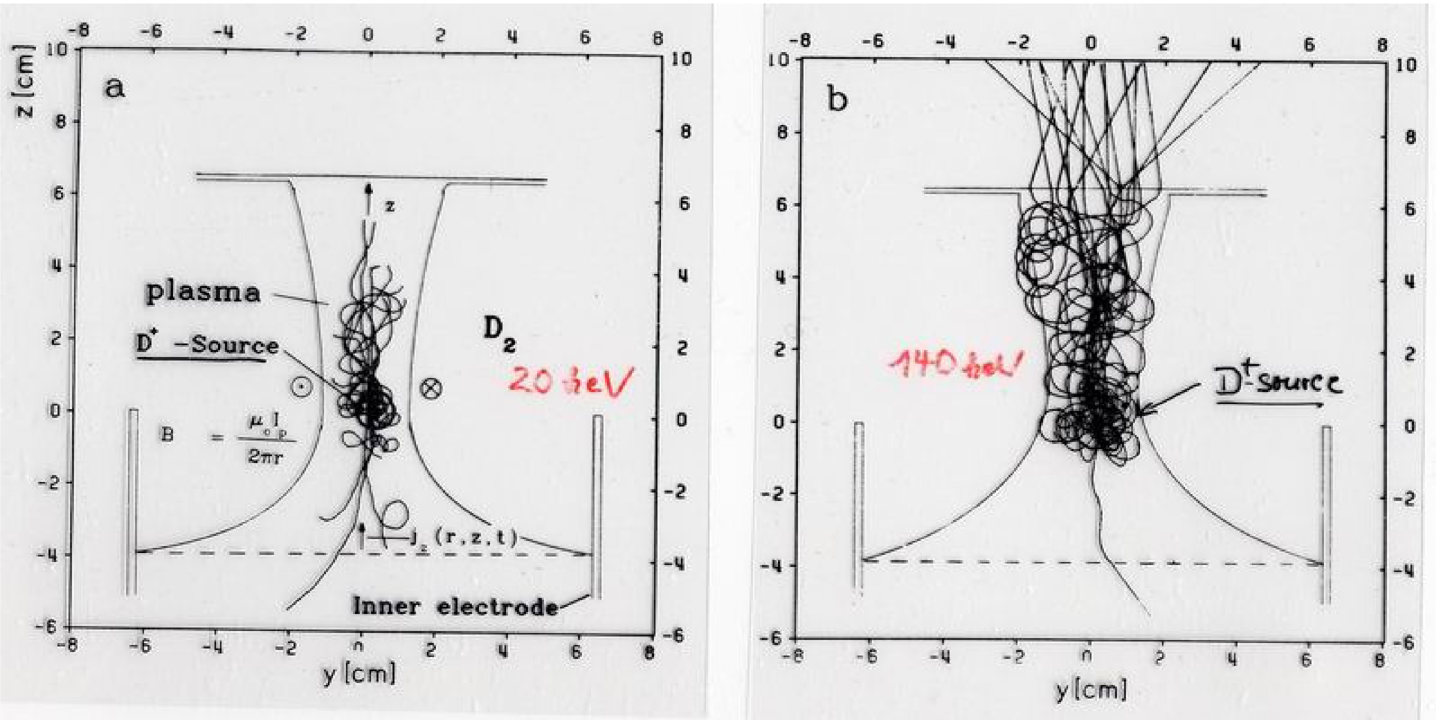
a
z [cm]
plasma
D⁺ -Source
D₂
20 keV
B = μ₀I_p / 2πr
z
j_z (r,z,t)
Inner electrode
y [cm]
b
140 keV
D⁺-source
y [cm]

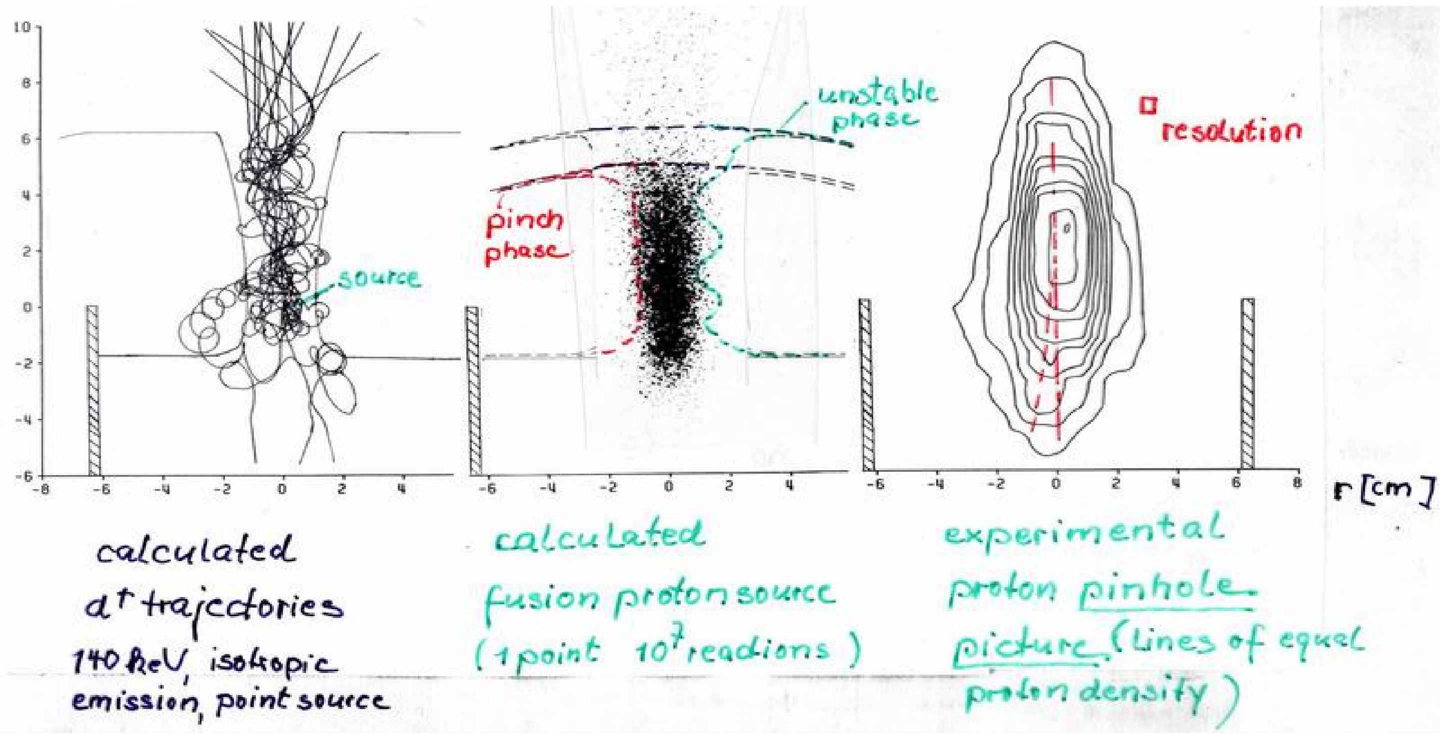
unstable phase
pinch phase
source
resolution
r [cm]
calculated
d+ trajectories
140 keV, isotopic emission, point source
calculated
fusion proton source
(1 point 10^7 reactions)
experimental
proton pinhole
picture (Lines of equal
proton density)

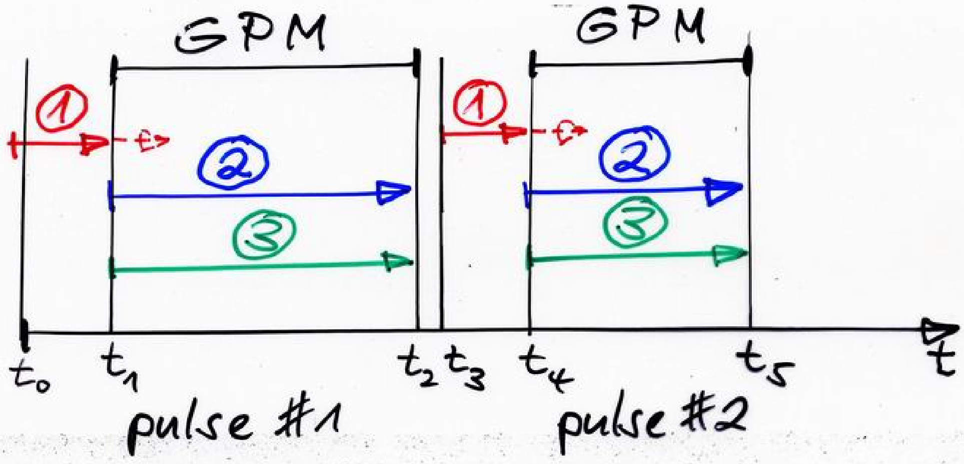

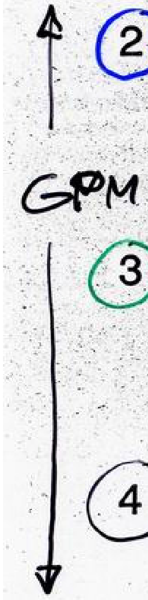

(1) ion acceleration in time- and space-dependent electromagnetic fields
---> deuteron distribution f_{D1} (E,**r**,t,Θ)

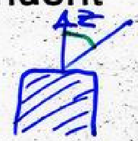

(2) ion relaxation
predominantly by Coulomb collisions with electrons T_e, n_e(**r**,t), **B** (**r**,t)
---> deuteron distribution f_{D2} (E,**r**,t)

(3) fusion reactions of the fast deuterons with the target $n_{i,o}$(**r**,t)

measured quantities

(4) fusion products n(E,t) and p(E,t) pass through the plasma/gas up to the detectors.
protons experience deviations in B(**r**,t)

POSEIDON diagnostics:

neutrons n(E,t) in one direction (side on)

protons p(E) in 8 directions

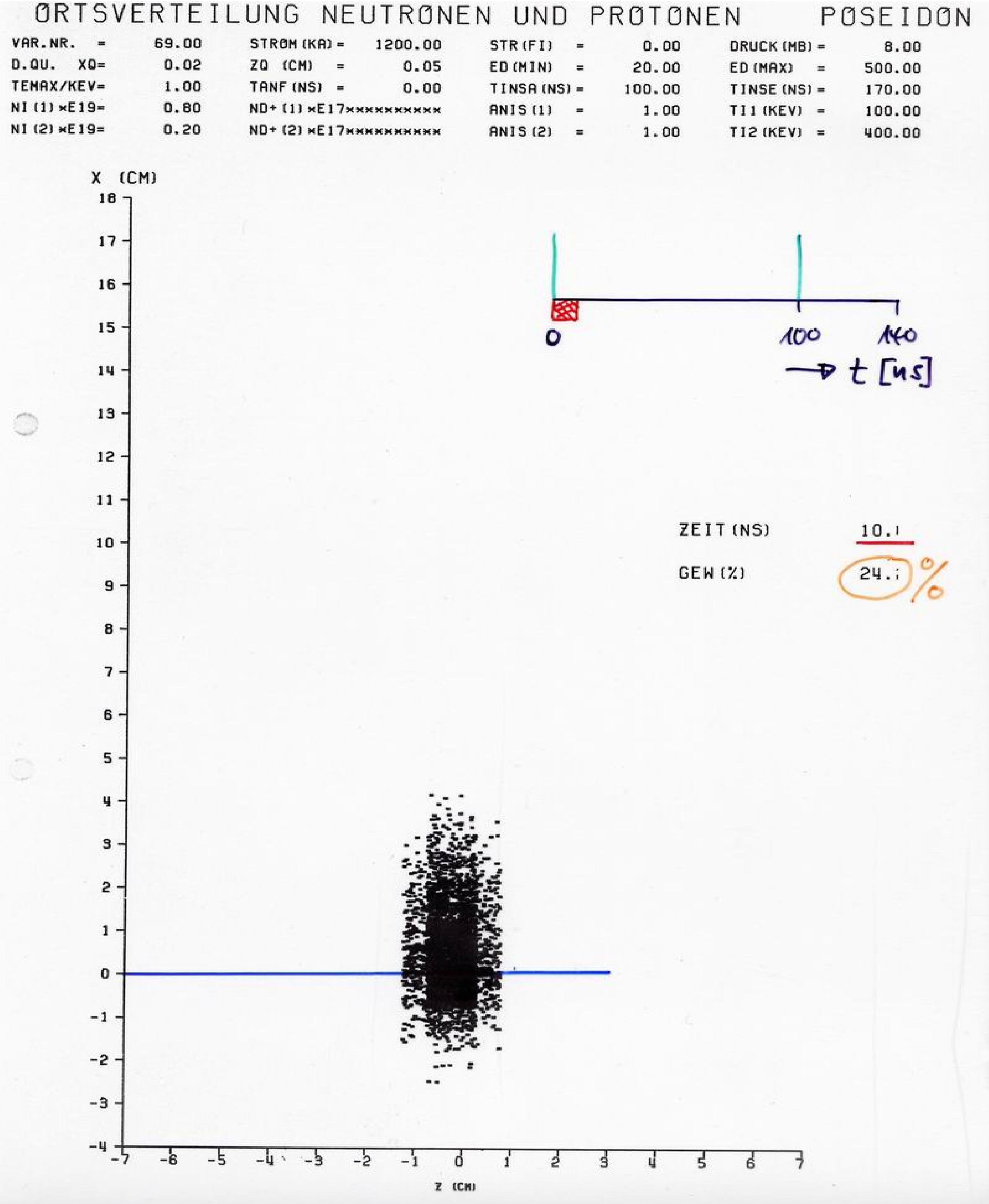
ØRTSVERTEILUNG NEUTRØNEN UND PRØTØNEN POSEIDØN
VAR.NR. = 69.00
D.QU. XQ= 0.02
TEMAX/KEV= 1.00
NI (1) *E19= 0.80
NI (2) *E19= 0.20
STRØM (KA) = 1200.00
ZQ (CM) = 0.05
TANF (NS) = 0.00
ND+ (1) *E17**********
ND+ (2) *E17**********
STR (FI) = 0.00
ED (MIN) = 20.00
TINSA (NS) = 100.00
ANIS (1) = 1.00
ANIS (2) = 1.00
DRUCK (MB) = 8.00
ED (MAX) = 500.00
TINSE (NS) = 170.00
TI1 (KEV) = 100.00
TI2 (KEV) = 400.00
X (CM)
Z (CM)
0
100
140
t [ns]
ZEIT (NS) 10.1
GEW (%) 24.7 %

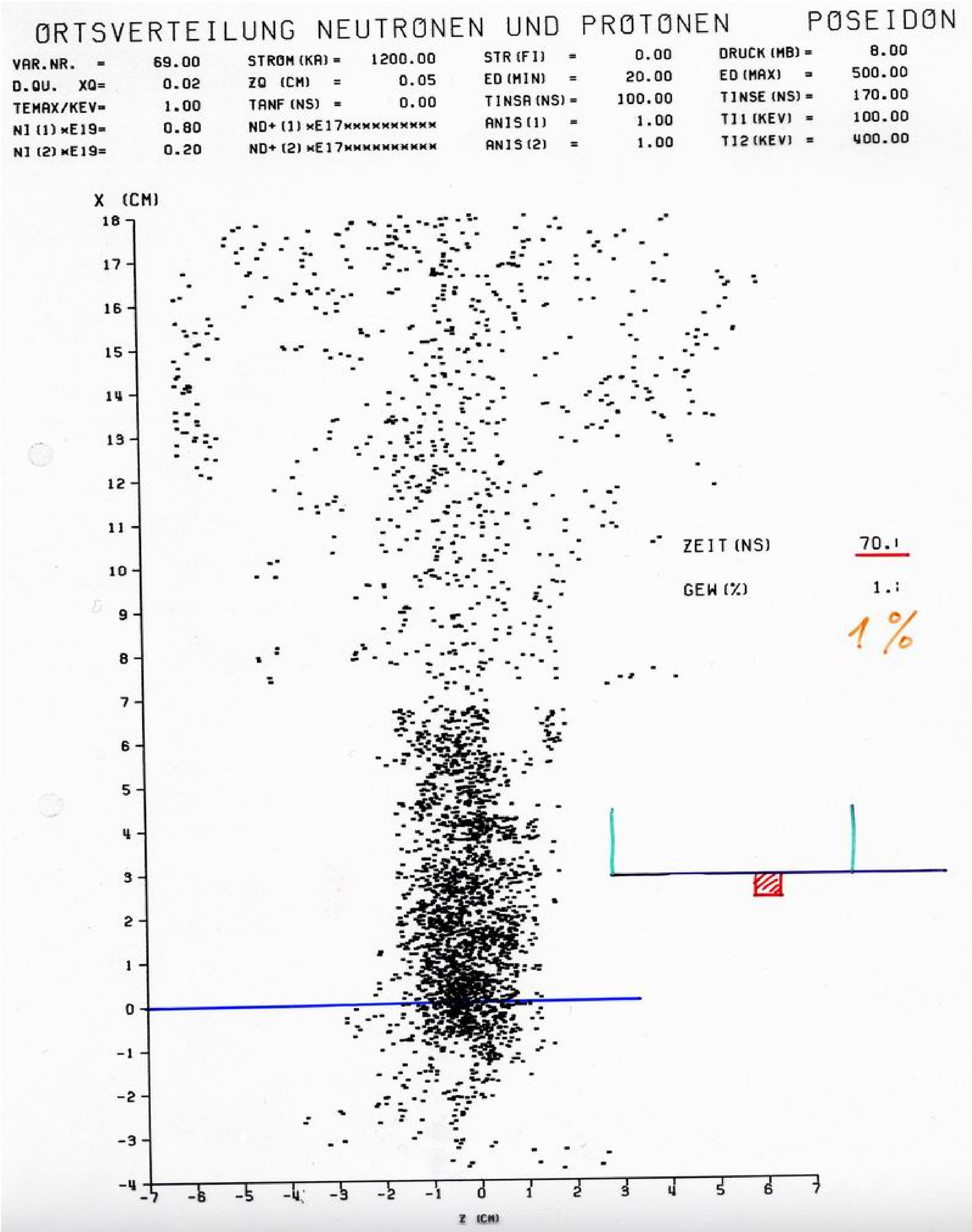
ØRTSVERTEILUNG NEUTRØNEN UND PRØTØNEN
PØSEIDØN
VAR.NR. = 69.00
D.QU. XQ= 0.02
TEMAX/KEV= 1.00
NI (1) *E19= 0.80
NI (2) *E19= 0.20
STROM (KA) = 1200.00
ZQ (CM) = 0.05
TANF (NS) = 0.00
ND+ (1) *E17**********
ND+ (2) *E17**********
STR (FI) = 0.00
ED (MIN) = 20.00
TINSA (NS) = 100.00
ANIS (1) = 1.00
ANIS (2) = 1.00
DRUCK (MB) = 8.00
ED (MAX) = 500.00
TINSE (NS) = 170.00
TI1 (KEV) = 100.00
TI2 (KEV) = 400.00
X (CM)
ZEIT (NS) 70.1
GEW (%) 1.:
1 %
Z (CM)

ØRTSVERTEILUNG NEUTRØNEN UND PRØTØNEN POSEIDØN

VAR.NR. =	69.00	STRØM (KA) =	1200.00	STR (FI) =	0.00	DRUCK (MB) =	8.00
D.QU. XQ=	0.02	ZQ (CM) =	0.05	ED (MIN) =	20.00	ED (MAX) =	500.00
TEMAX/KEV=	1.00	TANF (NS) =	0.00	TINSA (NS) =	100.00	TINSE (NS) =	170.00
NI (1) *E19=	0.80	ND+ (1) *E17**********		ANIS (1) =	1.00	TI1 (KEV) =	100.00
NI (2) *E19=	0.20	ND+ (2) *E17**********		ANIS (2) =	1.00	TI2 (KEV) =	400.00

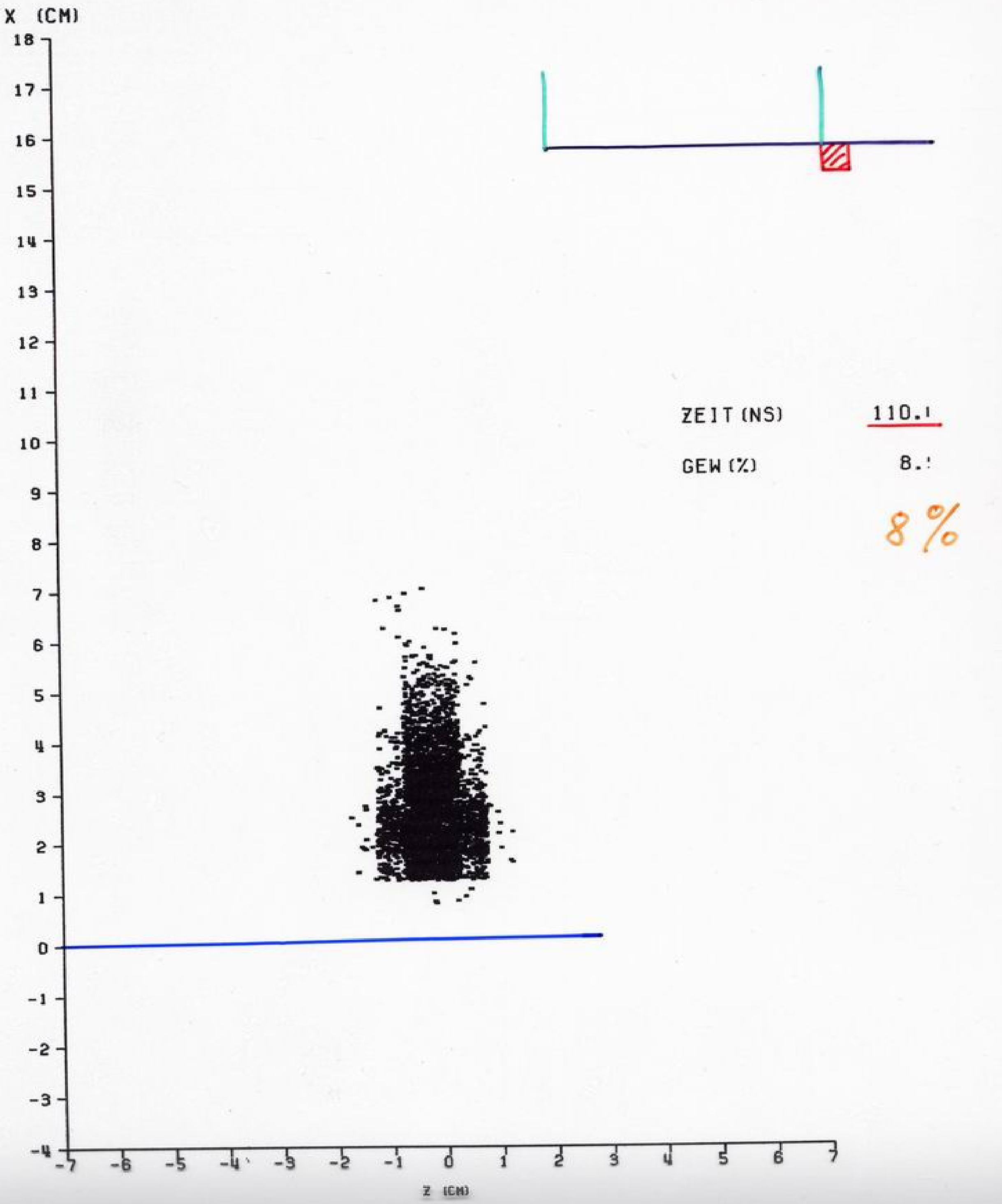

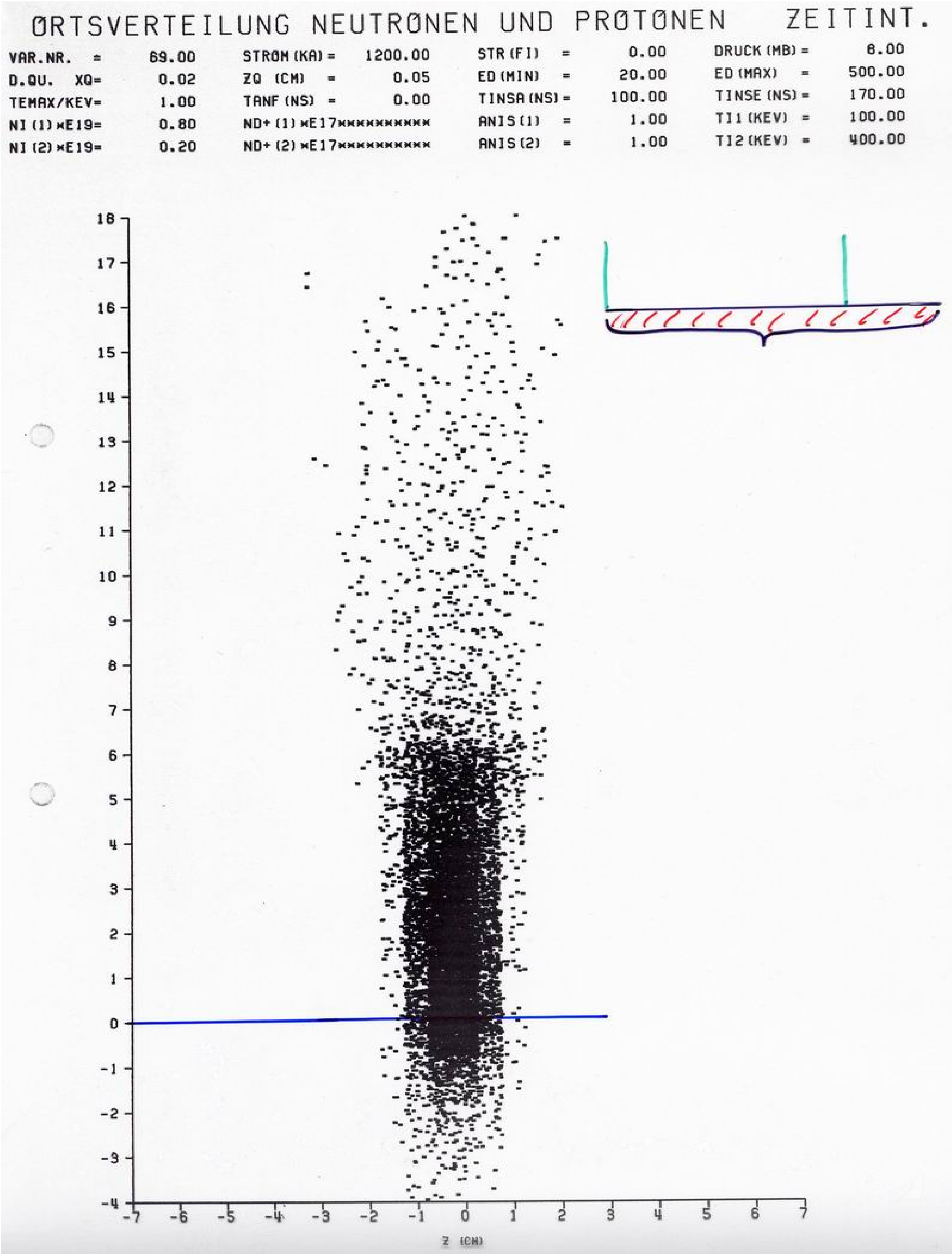
ØRTSVERTEILUNG NEUTRØNEN UND PRØTØNEN ZEITINT.
VAR.NR. = 69.00
D.QU. XQ= 0.02
TEMAX/KEV= 1.00
NI (1) *E19= 0.80
NI (2) *E19= 0.20
STRØM (KA) = 1200.00
ZQ (CM) = 0.05
TANF (NS) = 0.00
ND+ (1) *E17**********
ND+ (2) *E17**********
STR (FI) = 0.00
ED (MIN) = 20.00
TINSA (NS) = 100.00
ANIS (1) = 1.00
ANIS (2) = 1.00
DRUCK (MB) = 6.00
ED (MAX) = 500.00
TINSE (NS) = 170.00
TI1 (KEV) = 100.00
TI2 (KEV) = 400.00
Z (CM)

Scaling

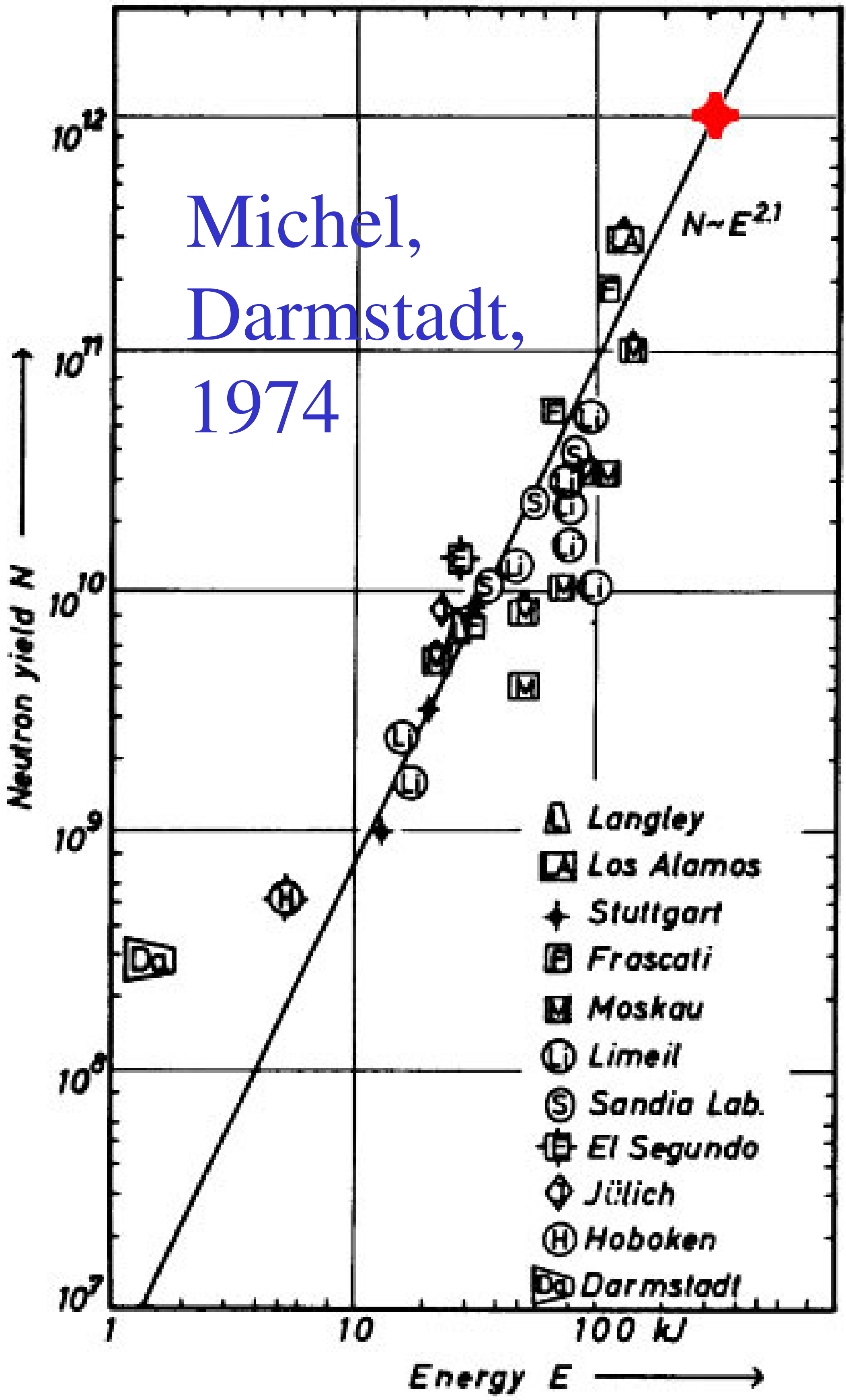

Michel, Darmstadt, 1974
$N \sim E^{2.1}$
Neutron yield N
10^{12}
10^{11}
10^{10}
10^{9}
10^{8}
10^{7}
1
10
100 kJ
Energy E
Langley
Los Alamos
Stuttgart
Frascati
Moskau
Limeil
Sandia Lab.
El Segundo
Jülich
Hoboken
Darmstadt

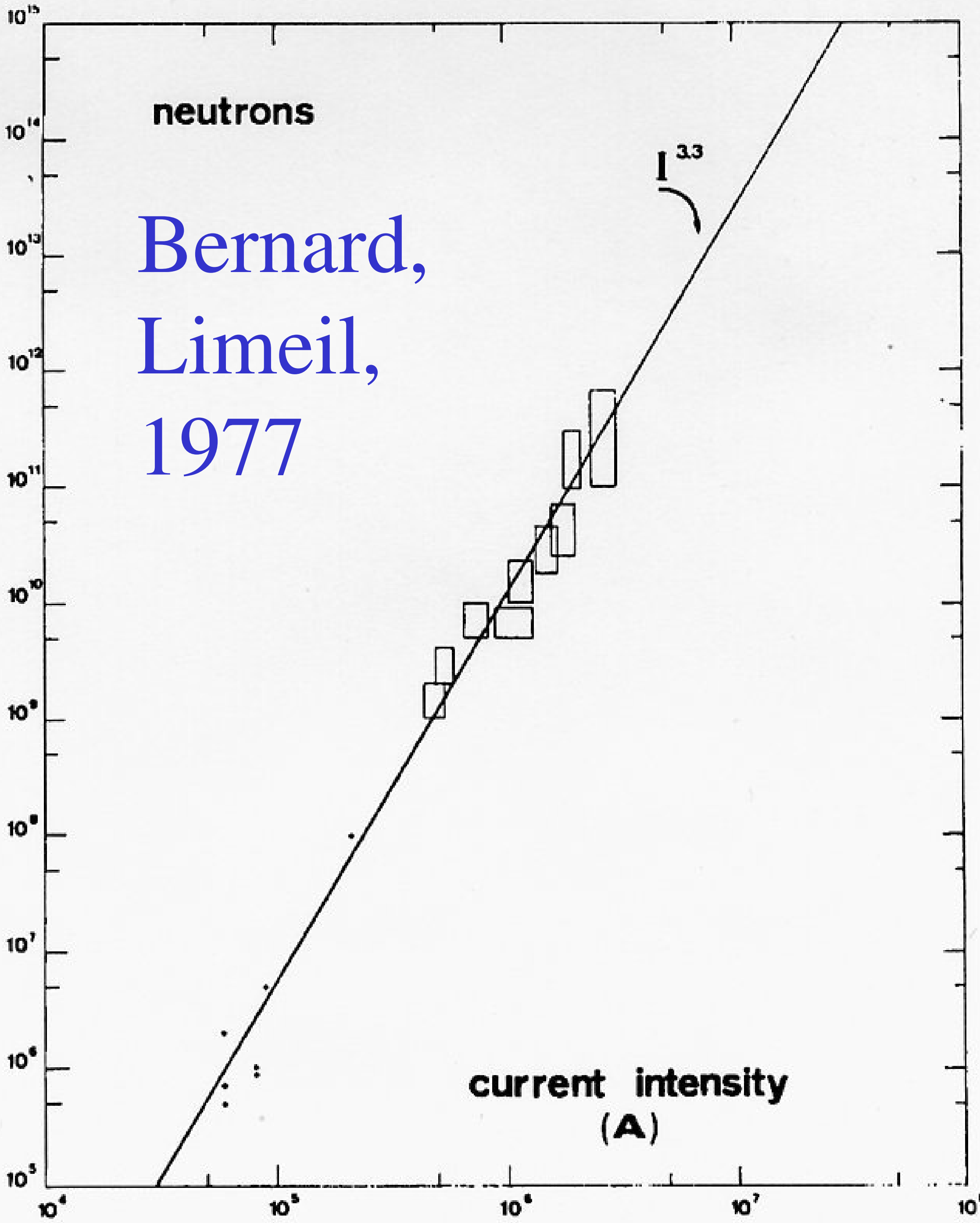

Fig. 15. Neutron scaling with current intensity of various focus and Z-pinch experiments.

Krompholz / Herold
1981 /1991

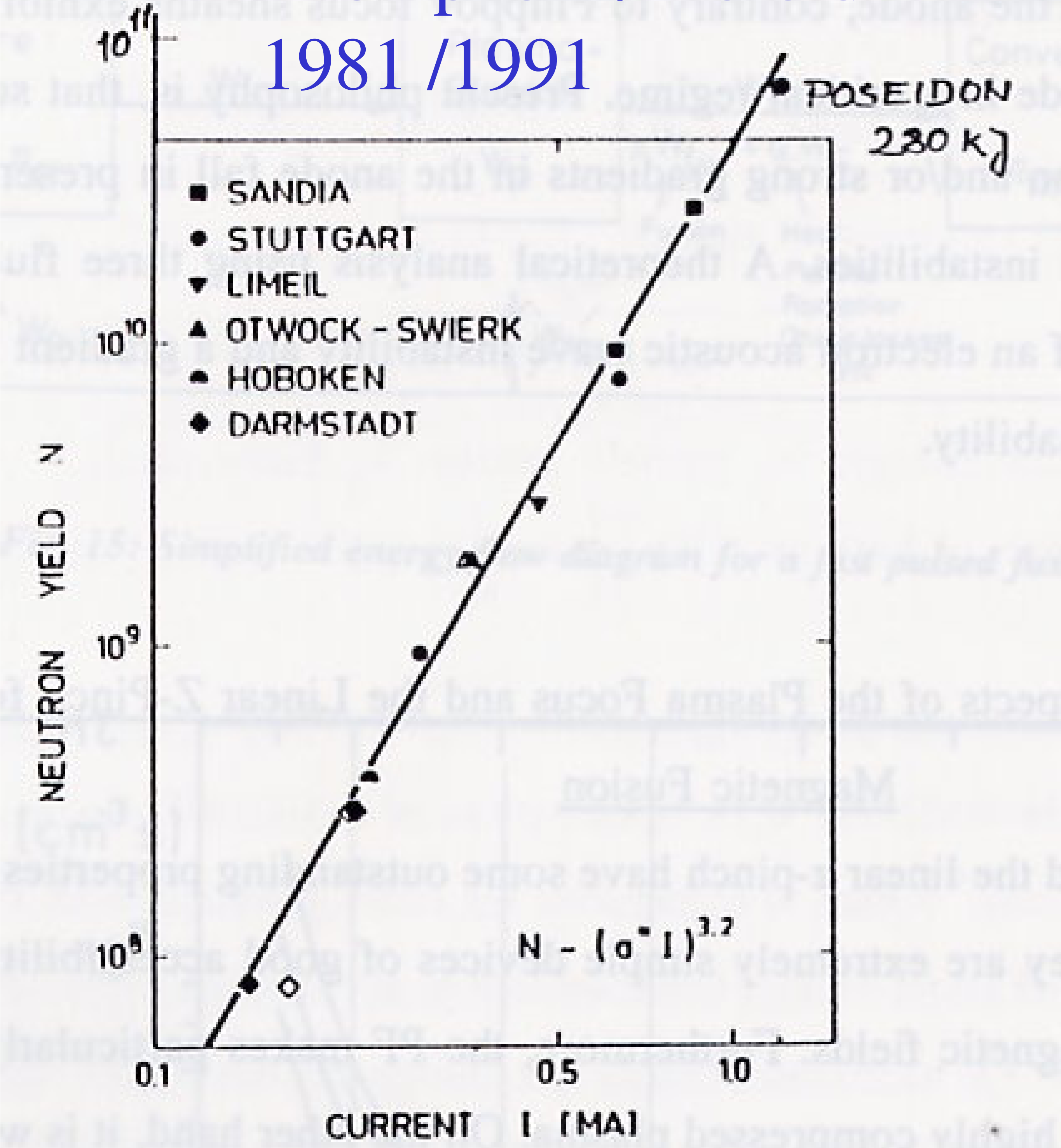

Herold 1989

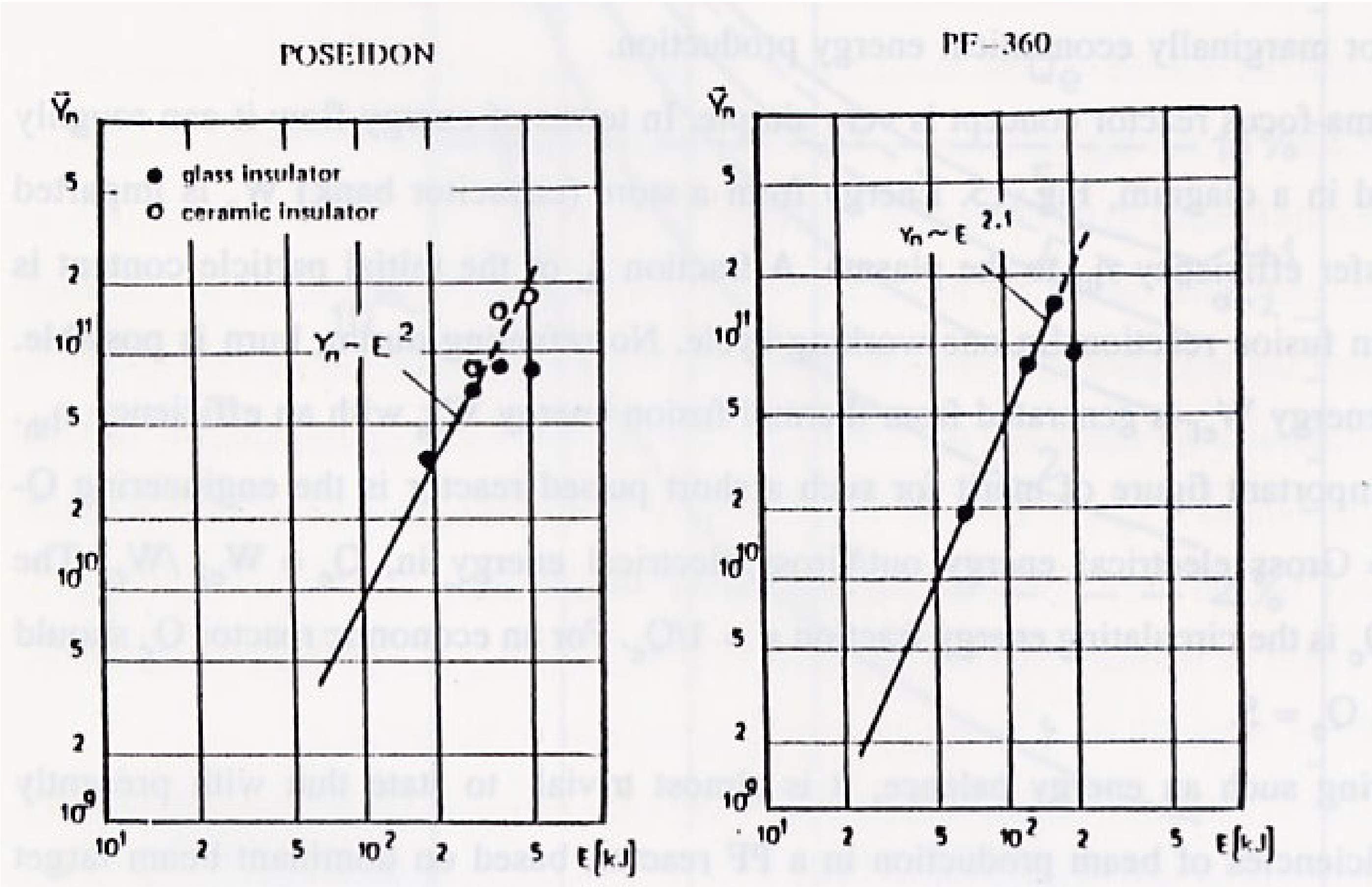

Influence of insulator material!

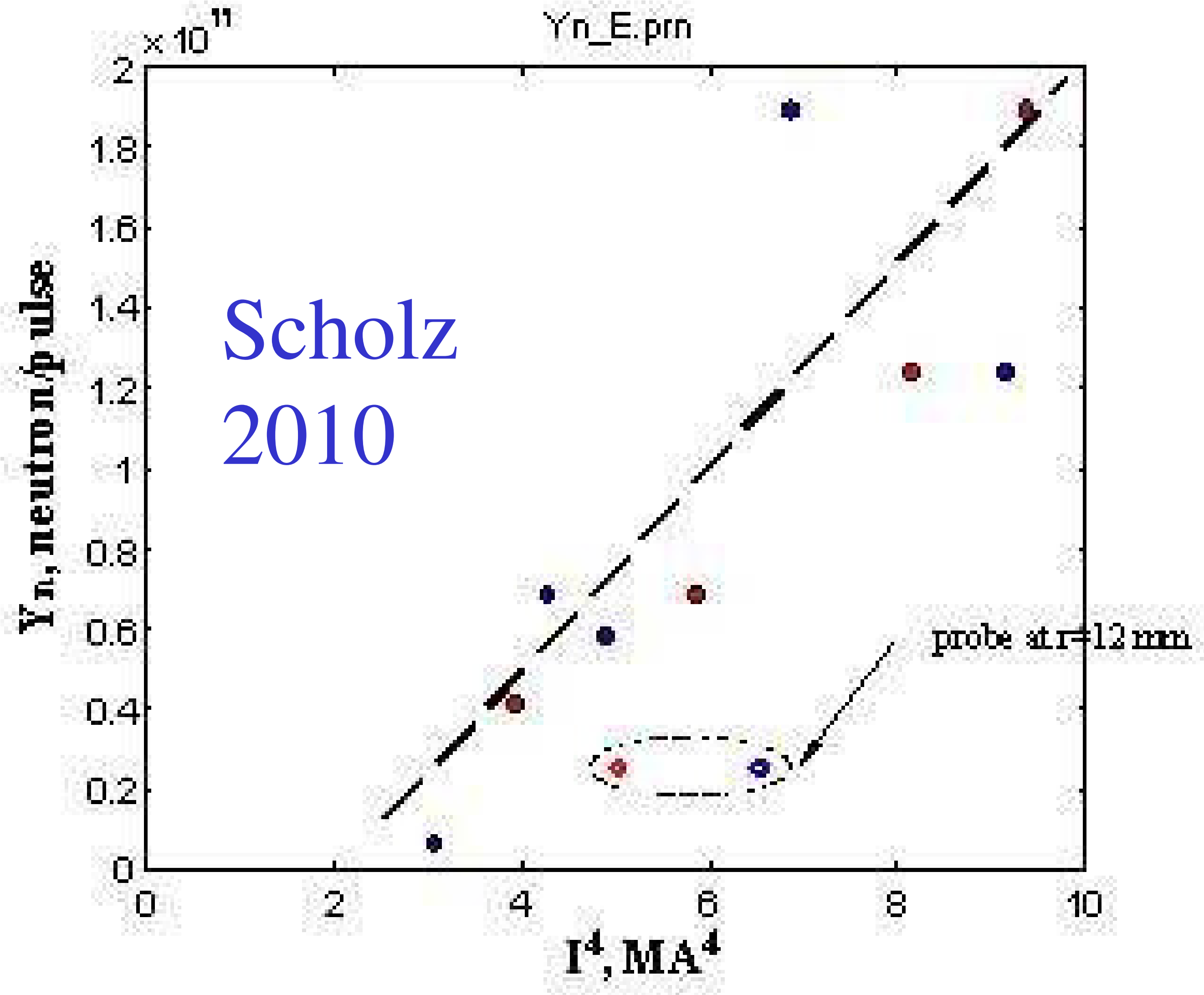

Ic- Current on collector probe, at the max current on ACMP

Ip - Max current on ACMP, measured at 40/12 mm

Scholz 2010

Results for probe position at r = 40 mm

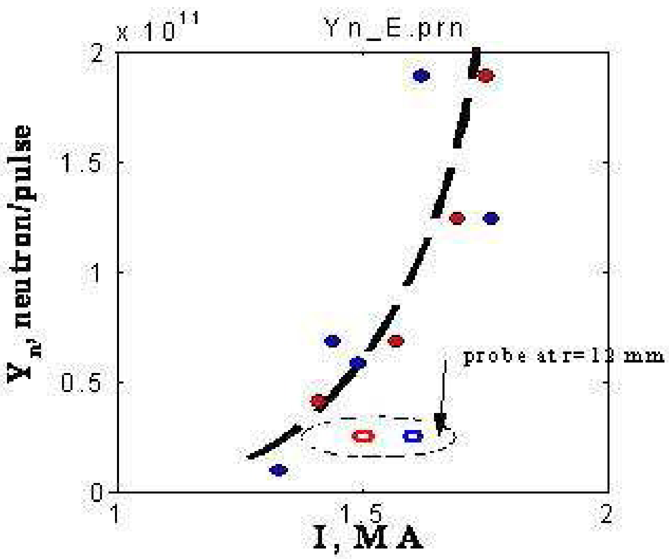

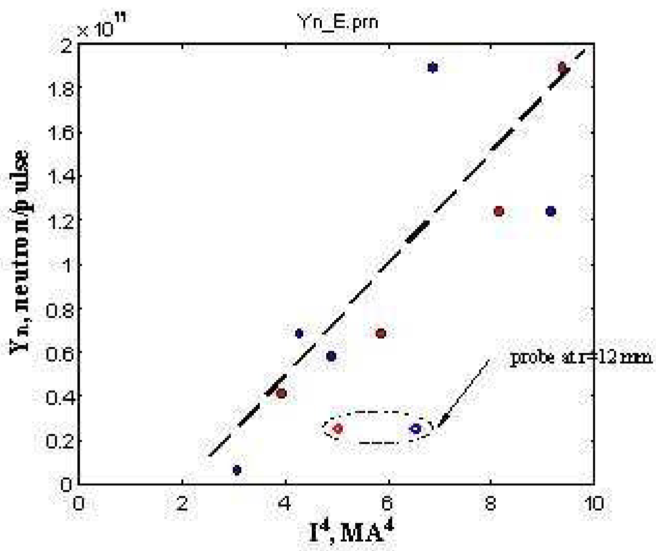

Ic- Current on collector probe, at the max current on ACMP

Ip - Max current on ACMP, measured at 40/12 mm

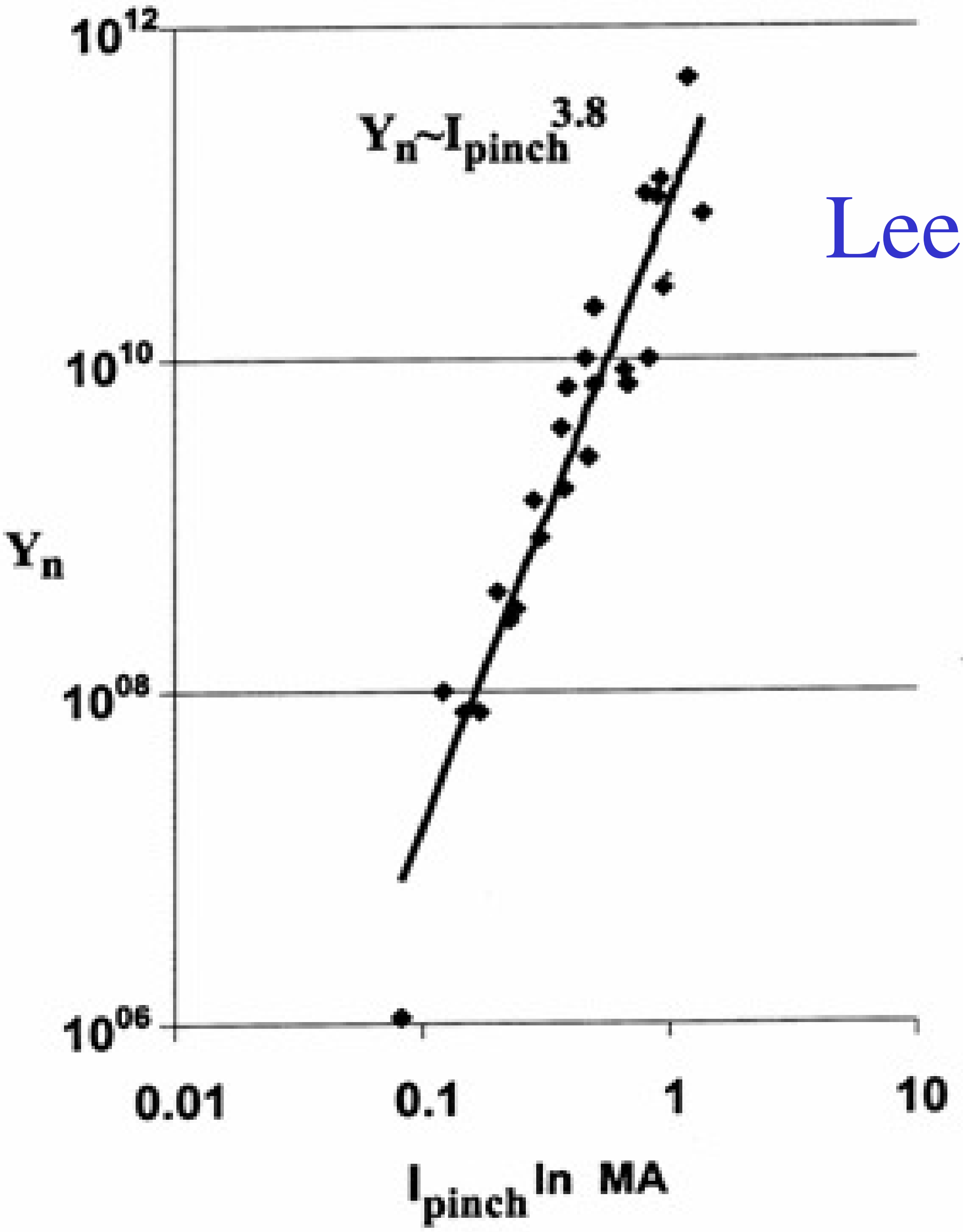

Lee 2009

Figure 4. Assembly of experimental data to obtain Yn scaling with current; loosely termed as the current or pinch current in the literature. This is the experimental curve from which a calibration point is obtained, at 0.5 MA, to calibrate the neutron yield equation (3) for the Lee model code.

Lee, 2009

L
e
e

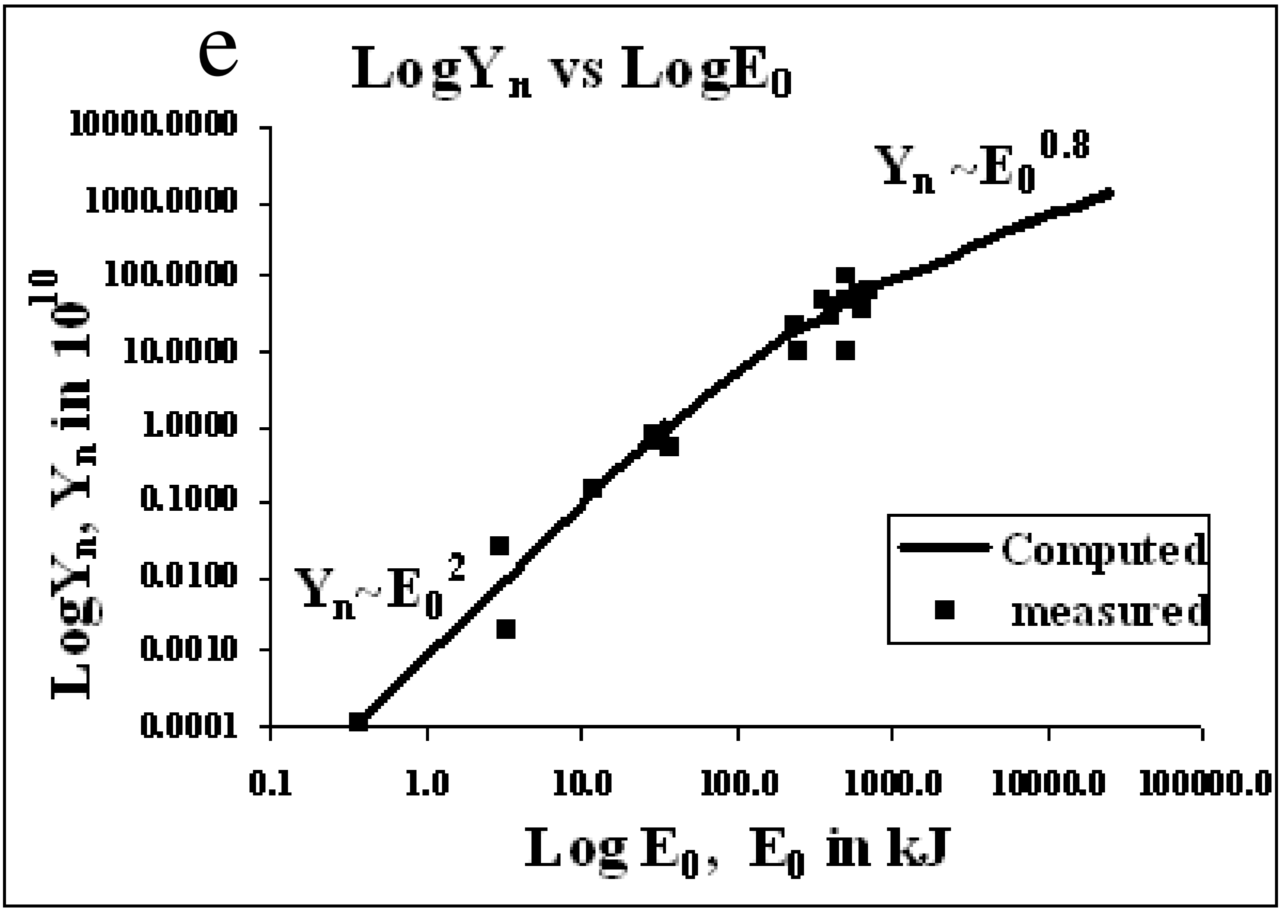

LogYn vs LogE0
Yn ~E0 0.8
Yn~E0 2
LogYn, Yn in 10^10
10000.0000
1000.0000
100.0000
10.0000
1.0000
0.1000
0.0100
0.0010
0.0001
0.1
1.0
10.0
100.0
1000.0
10000.0
100000.0
Log E0, E0 in kJ
Computed
measured

Geometry for Lee-Model

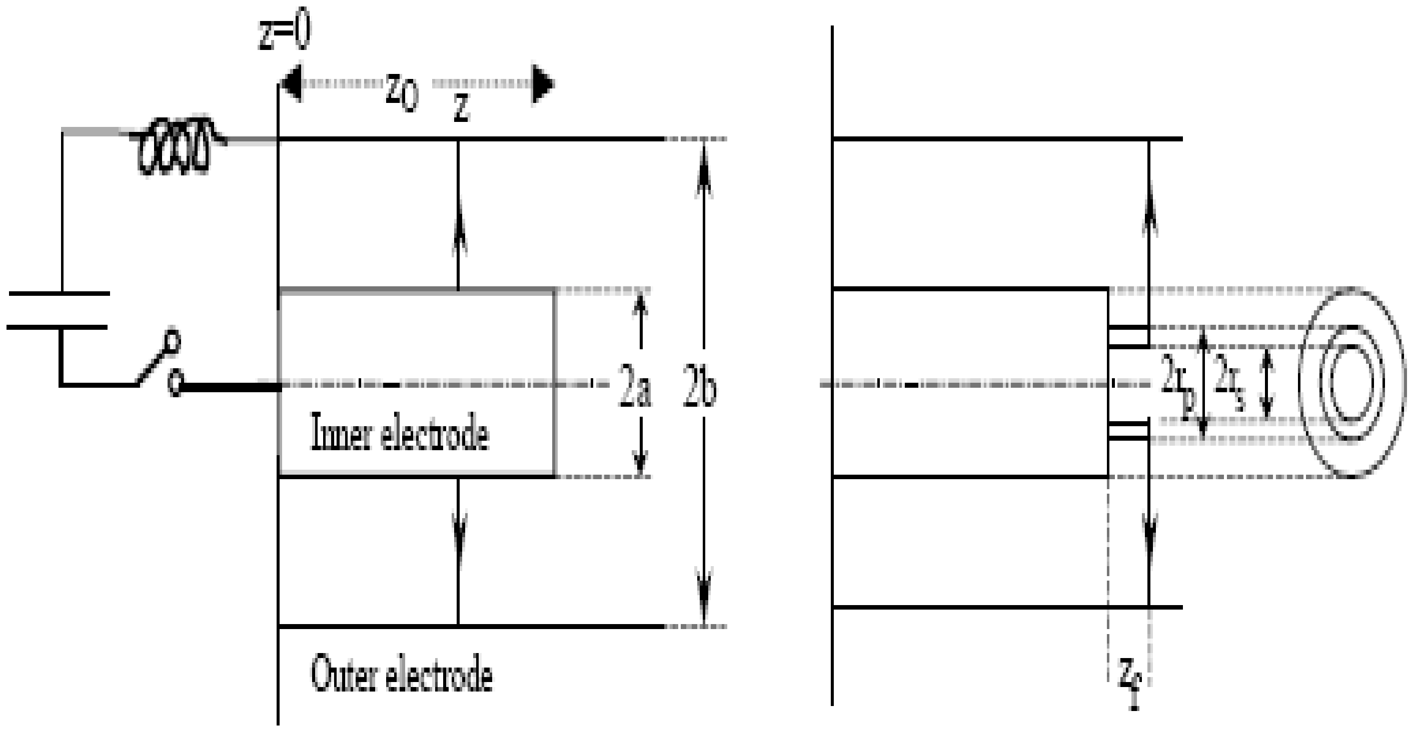

Spherical Geometry – Different results for scaling expected

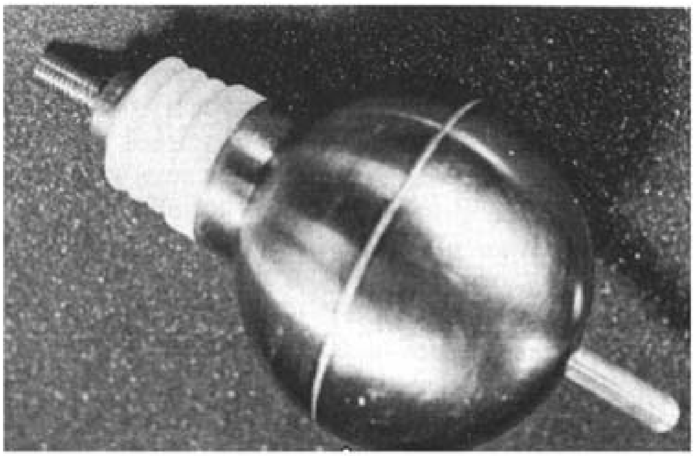

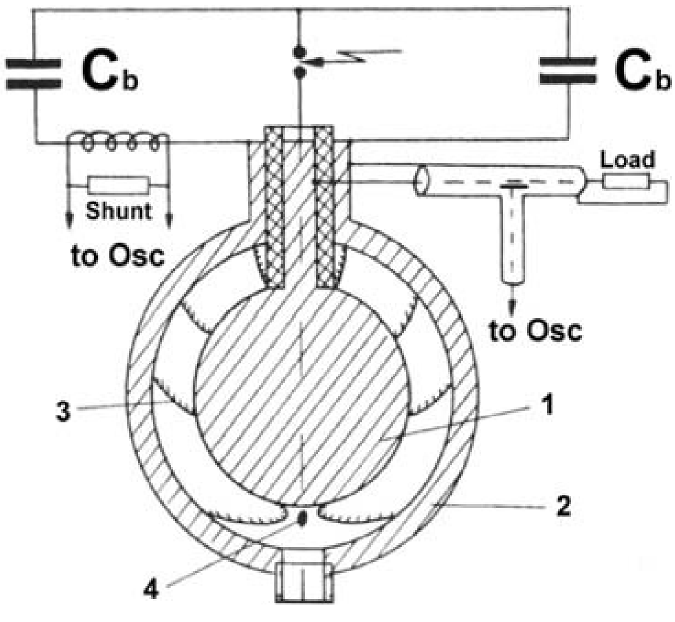

Mather type

Kdw

Example: DPF-6-1/2 Peak Current (720 kJ Capacitor Bank at 60 kV)

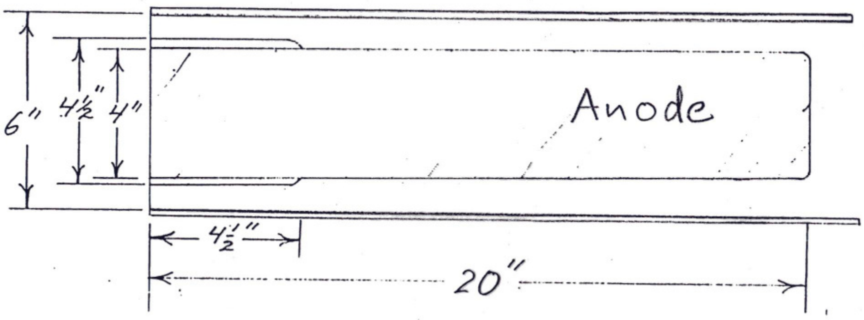

$Y_n \approx 2 \cdot 10^{12}$

$C_0 = 400\,\mu F$, $L_0 = 17.8\,nH$, $R_0 = 0.78\,m\Omega$

$$I_{pk}(MA) = \frac{1}{8.75} P_0(\text{TORR } D_2)^{1/8} V_0(kV)^{3/4}$$

MEASURED : 3.12 MA AT 50 kV, 20 TORR D_2

CALCULATED, $L(t)$ = 3.34 MA

CONST-$\dot{L}$ = 3.02 MA

c:\aware\briefing\acal-dpf.ppt 9/16/97 7

ICDMP Visit to Shiva Star Phillips Lab 30.3.1992

Conclusions

- Neutrons from a plasma focus, measured as a function of time, location and direction of emission reveal quite a number of important parameters on fusion reactions occurring in the dense high current phase of the experiment. In addition determination of the energy spectra of the emitted neutrons are important for understanding of the mechanisms taking place for the neutron production. The two main reasons for neutron diagnostics are 1) to determine the fusion yield, i.e. the efficiency of a device and its scaling; and 2) to learn the characteristics of the fusion reactions.
- Correlations of the neutron emission to other properties of a plasma focus such as pinch current, plasma density and temperature as well as electron beam and ion beam emission are of importance as well.
- Methods and results of neutron diagnostics for large experiments such as the former experiment Poseidon in Stuttgart and PF 1000 in Warsaw were presented and discussed.
- Neutron diagnostics presented include nuclear track detectors, plastic scintillators coupled to photomultipliers, activation measurements, time-of-flight methods as well as pinholes for spatial resolution of the neutron source.
- The well known scaling law according to which neutron yield scales roughly with the square of the energy input and the fourth power of the current was commented. Reasons for strong deviations from this law for high energy – know as saturation – are still a subject of debate.

References:

Liberman, A.M., De Groot, J.S., Toor, A., Spielman, R.
Physics of High-Density Z-Pinch Plasmas
Springer, 1998

Schmidt, H.
Plasma focus and z-pinch
Proceedings of the II Latin-American Workshop on Plasma Physics and Controlled Thermonuclear Fusion, CIF Series, Vol. 12, pp. 1-30
Medellin, Colombia, 16-28 Feb. 1987
Editor: R. Krikorian

Schmidt, H.
Neutron Yield Optimization of Plasma Focus Devices
J. Tech. Phys. **41**, 2, Special Issue, 93-108 (2000)

Knoll, Glenn F.
Radiation Detection and Measurement, Second Edition
John Wiley & Sons, 1989

Vikhrev, V.V. and Korolev, V.D.
Neutron Generation from Z-Pinches
Plasma Phys. Rep. **33**, 356-380 (2007)

Velikovich, A.L.et al.
Z-pinch plasma neutron sources
Phys. of Plasmas **14**, 022701 (2007)

Schmidt, R. and Herold,H.
A method for time resolved neutron spectroscopy on short pulsed fusion neutron sources
Plasma Physics and Controlled Fusion. **29**, *523* – 534 (1987)